

NASA CR-132388

SLA-73-0714

(NASA-CR-132388) SONIC BOOM MEASUREMENTS  
FROM ACCELERATING SUPERSONIC TRACKED SLEDS  
(Sandia Labs.) -107 p HC \$8.50 CSCL 20D

N74-16725

Unlimited Release

(Sandia Labs.) ~~407~~ p HC \$8.50 : CSCL 20D

Unclas

G3/02 30456

# SONIC BOOM MEASUREMENTS FROM ACCELERATING SUPERSONIC TRACKED SLEDS



**J. W. Reed**

PRICES SUBJECT TO CHANGE

Prepared by Sandia Laboratories, Albuquerque, New Mexico 87115  
and Livermore, California 94550 for the United States Atomic Energy  
Commission under Contract AT (29-1)-789

Printed January 1974

Supported in Part by NASA Langley Research Center Order L-75,054.



# Sandia Laboratories

900 Q(7-73)

Reproduced by  
**NATIONAL TECHNICAL  
INFORMATION SERVICE**  
US Department of Commerce  
Springfield, VA. 22151

## N O T I C E

THIS DOCUMENT HAS BEEN REPRODUCED FROM THE BEST COPY FURNISHED US BY THE SPONSORING AGENCY. ALTHOUGH IT IS RECOGNIZED THAT CERTAIN PORTIONS ARE ILLEGIBLE, IT IS BEING RELEASED IN THE INTEREST OF MAKING AVAILABLE AS MUCH INFORMATION AS POSSIBLE.

SLA-73-0714

SONIC BOOM STUDIES ON AREA III SLED TESTS

Jack W. Reed  
Particulate Dynamics Division, 5644  
Sandia Laboratories, Albuquerque, New Mexico 87115

January 1974

ABSTRACT

Supersonic sled tests on the Sandia 1524-m (5000-ft) track generate sonic booms of sufficient intensity to allow some airblast measurements at distance scales not obtained from wind tunnel or flight tests. During acceleration, an emitted curved boom wave propagates to a caustic, or focus. Detailed measurements around these caustics may help to clarify the overpressure magnification which can occur from real aircraft operations. Six fixed pressure gages have been operated to document the general noise field, and a mobile array of twelve gages—obtained through NASA Langley—Research Center support have been used to record in the vicinity of caustics.

Results from the fifteen tests assembled to date have been only partially analyzed, but lead to the following conclusions.

- Although sonic boom overpressures appear to follow Whitham theory with respect to offset distance from the vehicle track trajectory, they are not in good agreement with the Mach number dependence of the theory.
- Nearly 3X magnification has been observed within  $\pm 8$  m (25 ft) of a calculated caustic at 900 m (3000 ft) off set distance.
- Compression rise times of 2 to 20 milliseconds have been observed, whereas viscous shock theory predicts only 1 microsecond (corresponding to 0.3-mm ( $10^{-3}$ -ft)) shock thickness.
- Vehicle impacts at the end of the track give explosion waves comparable to those from up to 90.7 kg (200 lb) of high explosives.

Supported in Part by NASA Order L-75, 054.

## TABLE OF CONTENTS

	<u>Page</u>
Foreword	5
Introduction	7
Background	7
Basic Sonic Boom Behavior	8
Acoustic Focusing	11
Experiment Plan	13
Calculations	19
Results	23
Off-Site Noise Nuisance	23
Impact Waves	25
Ignition and Rocket Engine Noise	28
Calibration Shots	30
Compression Rise Times	33
Summary and Conclusions	35
References	37
Appendix - Test Results and Discussions	39

## LIST OF TABLES

<u>Table</u>		
I	Stationary Pressure Gage Array	17
II	Caustic Location Parameter Test and Response Summary	22
III	Summary of Sled Boom Measurements	24
IV	Summary of Sled Test Impact Explosion Data	26
V	Rocket Engine Noise Extrapolations	29

**Preceding page blank**

## LIST OF ILLUSTRATIONS

<u>Figure</u>		<u>Page</u>
	Frontispiece - Sled Test	6
1	Sonic Boom Wave Geometry	9
2	Sonic Boom Formation From Accelerating Vehicles	9
3	Airblast Wave Pressure/Time Signatures	10
4	Shock Ray Tube Focusing	11
5	Shock Wave Divergence in Focus	12
6	Kirtland AFB East (Sandia Area) and Sled Track	13
7	Map of Area III Sled Track and Sonic Boom Project Facilities	14
8	Sled Impact Area, View Toward Southwest	14
9	Sled Launch Area, View Toward Northwest	15
10	Utility Sled With 25 HVAR Rockets, 425-m/s Maximum Speed	15
11	Utility Sled With Three Little John Rockets, 600-m/s Maximum Speed	16
12	Canister for Mobile Pressure Transducer	18
13	Sonic Boom Focusing From Accelerating Supersonic Sled	20
14	Geometry for Wave Source Solutions	21
15	Energy Comparisons Impact vs Pressure Waves	27
16	Comparison Curves for Impact Explosion Evaluation	28
17	Calibration High-Explosives Shot, View Toward Southeast	30
18	Calibration Shot Pressures	31
19	Calibration Shot Amplitudes and Corrections	32
20	Calibration Shot Positive-Phase Durations	32
21	Calibration Shot Negative-Phase Durations	33
22	Compression Rise Time Observations, Calibration Shots	33
23	Rise Times From Sonic Boom Signatures	34

## FOREWORD

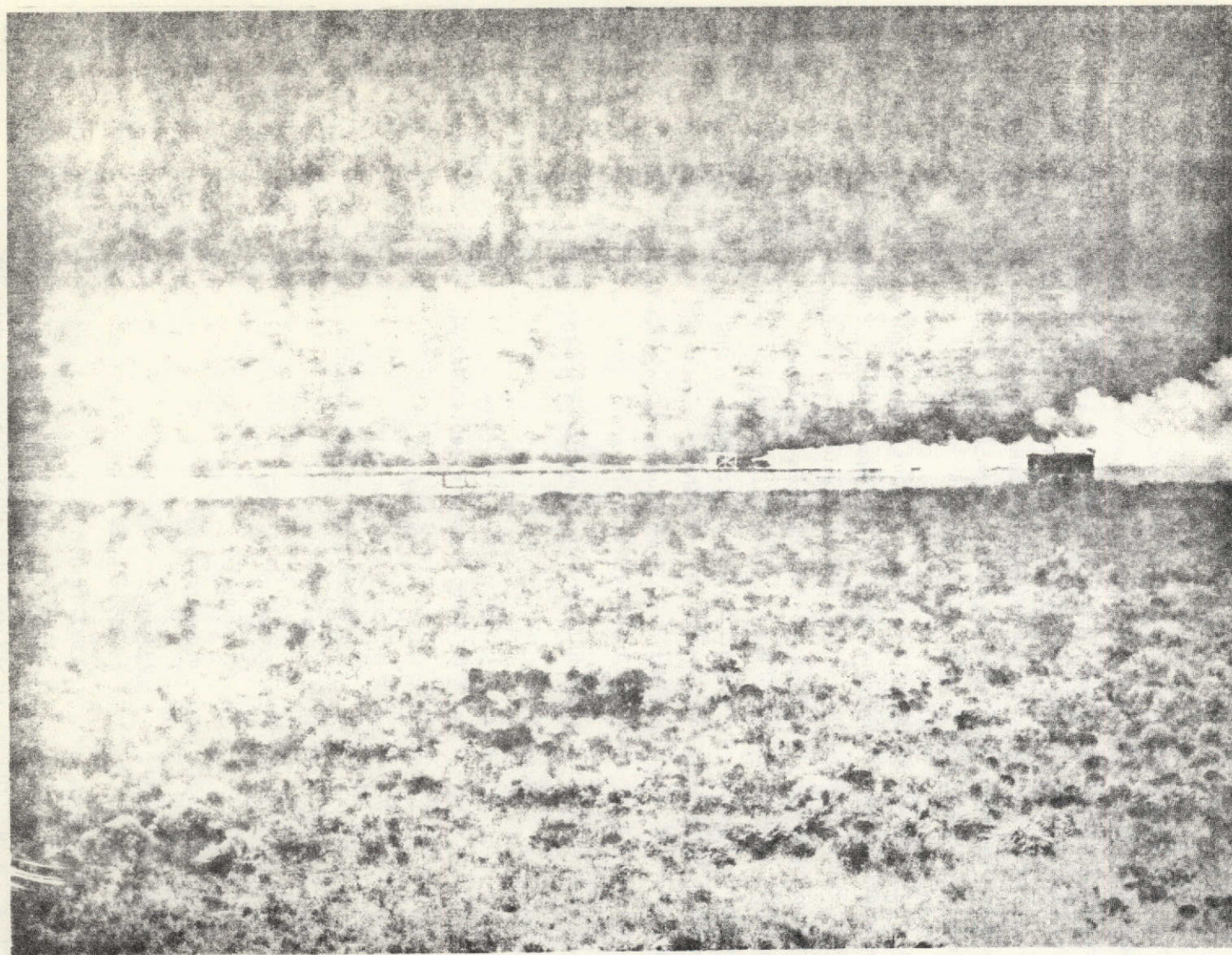
The use of a dual system of units in this report reflects an attempt to follow Sandia Laboratories guidelines during the period of transition from the English system to the metric system. In the body of this report distance units are primarily metric (SI, for Le Système International d'Unités), with traditional English units occasionally shown in parentheses. Figures usually show dual scales. In the appendix, however, the considerable volume of tabulated data dictates presentation in only the units obtained from the field or from programmed calculations. It does not appear that the cost of translating the listings into SI units is warranted.

Pressure units are particularly troublesome to present because of several of the units having been used previously in different specialized fields of application, and the entirely new unit, pascal, being prescribed in SI. Sonic booms are usually evaluated in psf (pounds per square foot), because of the small number size, to avoid many small fractions of psi (pounds per square inch). Inasmuch as the author is a meteorologist and has long used millibars for the small-amplitude waves at large distances from explosions, the measurements and calculations in this project are made in this cgs-related system. Conversion to SI mks pascals, therefore, is made only where convenient. There is no use of decibels, which were mixed into sonic boom problem usage by acousticians who were concerned more with psychoacoustic than physical responses.

In the hope of reducing reader difficulty, the conversions are listed below.

SI (mks):	1 pascal	= 1 Pa = 1 N/m <sup>2</sup> = 10 dynes/cm <sup>2</sup> = 10 <sup>-5</sup> bars = 0.02088551 psf = 0.0001450382 psi.
cgs:	1 millibar	= 1 mb = 10 <sup>3</sup> dynes/cm <sup>2</sup> ≈ 10 <sup>-3</sup> atmospheres (STP) = 0.01450382 psi = 2.088551 psf ≈ 2 psf = 0.1 kPa.
Sonic Booms:	1 psf	= 0.4788009 mb ≈ 1/2 mb = 47.88009 Pa = 0.006944444 psi.
English:	1 psi	= 144 psf = 68.94733 mb ≈ 69 mb = 6.894733 kPa.

Although the acoustic decibel is supposedly defined as an SPL (sound pressure level) usually referenced to "2 x 10<sup>-4</sup> μb," where SPL should be the RMS half-amplitude of a sine wave of specified frequency, these details are usually overlooked. It was generally impossible to find out exactly what was meant when an N-wave peak overpressure was reported in decibels. Therefore, this author finds no justification for perpetuating any use of this ambiguous notation.



Frontispiece - Sled Test

## Introduction

### Background

Track Guns and Hydrodynamics Division of Sandia Laboratories operates a sled test facility in Area III, about 8 km south of Area I, the main base (now called Kirtland Air Force Base East). Tests run here (e.g. see Frontispiece) have caused several off-site noise nuisance complaints. In 1970 the noise nuisance became serious in the Four Hills residential area 10 km northeast of the track. To establish what noise sources were created by these supersonic rocket-driven test sleds and to predict and control their impact on neighboring communities, six blast pressure gages were installed at various locations to help quantify the three expected noise sources:

1. Rocket motor noise
2. Sonic boom
3. Impact explosion

Since an average of one test per week was being run, it appeared that this facility could provide valuable information, otherwise not easily obtainable, about the generation and propagation of aircraft sonic booms.

Supersonic wind tunnel tests have long furnished sonic boom near-field source data. Very small models, sometimes of jewelry scale, are needed to allow measurements at significant scaled distances from a source,<sup>1</sup> and it has, so far, been impossible to simulate real atmospheric parameters of thermal stability, attenuation, and turbulence in these wind tunnel tests. Far-field measurements have been obtained by aircraft flight tests, but there have often been severe performance limitations, to prevent data collections with desirable combinations of altitude and Mach number, as well as tracking and control problems. In certain cases where adequate parametric variations could not be obtained, agreement between aircraft data and predictions based on wind tunnel sources and theoretical propagation laws has sometimes been questionable. It would be useful to have measurements of boom wave signatures at several points along their path and extending to distances comparable to realistic supersonic flight altitudes. This should allow a more detailed check of theoretical models for propagation mechanics, particularly in the controversial region of quasi-nonlinear acoustics.

A major sonic boom problem which could also be studied at reduced scale is the boom wave focus, or caustic, generated by an accelerating or maneuvering supersonic vehicle. Caustic loci computed for various sled test vehicle accelerations were found to fall in a reasonably confined area, generally east-southeast (and west-southwest) from the track. With additional, and movable, pressure gages it appeared that considerable data could be obtained about boom waves in and near caustics.



The problem of amplitude prediction in caustics has never been satisfactorily solved by either theoretical or experimental methods.<sup>2</sup> Linear acoustic theory yields infinite shock strength at a caustic, or focus. One simplified shock theory was used by Myers and Friedman<sup>3</sup> to predict an actual maximum of about 3.5X amplitude magnification above the amplitude expected for conical wave expansion. Seebass<sup>4</sup> indicated that amplification factors should be less than 5X. Recent calculations by Parker and Zalosh,<sup>5</sup> however, indicate that 4.4-20X magnifications are possible over a distance scale of about one wavelength. French trials with sonic booms, when preparing for the Concorde SST, showed up to 9X magnification.<sup>6</sup> Original results from NASA-USAF flight tests, with measurements on the 465-m (1527-ft) BREN<sup>6</sup> tower at the AEC Nevada Test Site<sup>7</sup> have shown only 3X magnification.

A joint NASA Langley Research Center/Sandia project was developed to make detailed measurements near these caustics caused by accelerating supersonic rocket sleds. The first phase - design, procurement, assembly, calibration, and testing of a mobile gage array - will be reported here, along with the first data collections. A second phase - more or less routine data collection - is continuing and will be described in later reports.

#### Basic Sonic Boom Behavior

Supersonic vehicles generate a bow shock wave that radiates from a vehicle (as shown in Figure 1) at Mach angle,  $\beta$ , where

$$\sin \beta = \frac{c}{A} = \frac{1}{M} \quad (1)$$

and  $c$  is ambient sound speed,  $A$  is vehicle airspeed, and  $M$  is Mach number. At higher speed, or Mach number, smaller Mach angles are formed. During acceleration (as shown in Figure 2a), diminishing Mach angles thus result in a curved bow wave at fixed time (as shown in Figure 2b). A caustic is formed at the focus of the wave curvature along a line which depends on the vehicle trajectory parameters. Theoretically, two booms, or wave front passages, would be heard to the right of the caustic line and no geometric/acoustic boom would enter the "silent" zone to the left of the caustic line. In reality, however, some sound is scattered into this silent zone.

Similarly, caustics are formed by vehicle turns. Atmospheric variations of wind and temperature across the propagation field can also cause refractive ray bending, wave front curvature, and focusing.

---

\* Bare Reactor Experiment, Nuclear.

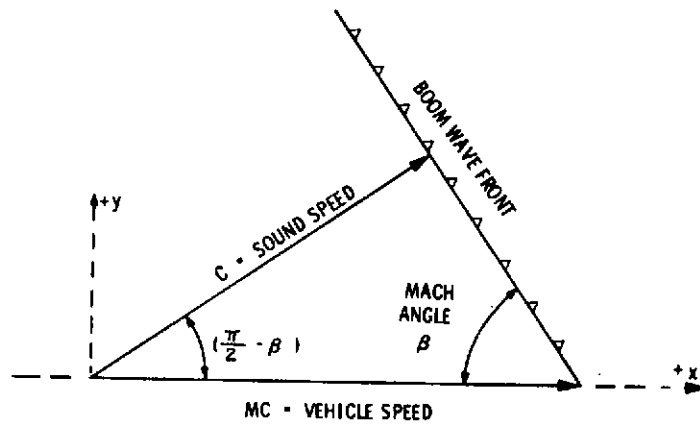
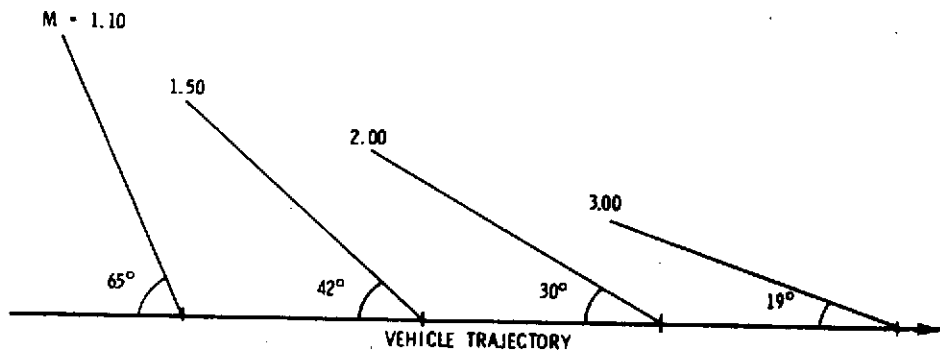
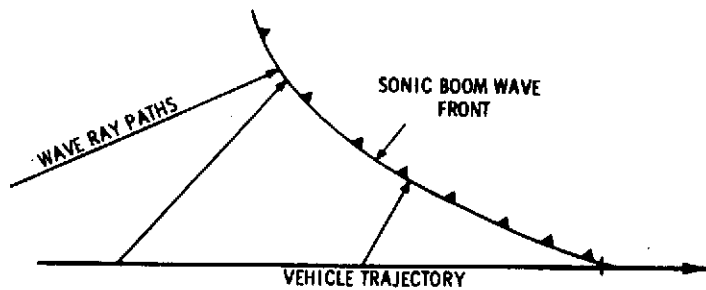


Figure 1. Sonic Boom Wave Geometry



a. Bow Wave Emission Angles



b. Instantaneous Bow Wave Section

Figure 2. Sonic Boom Formation From Accelerating Vehicles

Pressure/time signatures of sonic booms and explosions are compared in Figure 3. Overpressures,  $\Delta p$ , in supersonic bow waves from straight and level flight may be predicted from an equation derived by Whitham<sup>8</sup> that

$$\Delta p = K_r (p_h p_o)^{1/2} (M^2 - 1)^{1/8} h^{-3/4} \left[ K_v d_b L_b^{-1/4} \right], \quad (2)$$

depending on ambient pressure,  $p$ , at subscripted altitudes of flight,  $h$ , and measurement,  $o$ , and ground reflectivity,  $K_r \approx 2$ . Bracketed terms describe the source in terms of aerodynamic volume shape factor,  $K_v$ , maximum body diameter,  $d_b$ , and body length,  $L_b$ . There are questions<sup>9</sup> based on explosion wave scaling and propagation laws, about the functional form for dependence on  $p_h$  and  $h$ . However, extensive data collections now available show that  $h^{-3/4}$  appears to be empirically correct, thus corroborating the findings of DuMond, Cohen, Panofsky, and Deeds.<sup>10</sup>

One difficulty arises, however, with the DuMond *et al.* model, which depends on pulse length of the pressure signature,  $2T$ , as well as compression rise time,  $\tau$ , of the shock front. Behavior of neither of these times in far-field "asymptotic" acoustic regions is well predicted by the theory. Furthermore, transformation to the geometry of spherical explosion wave propagation, with the same theoretical mechanisms, yields  $\Delta p \approx (R \ln k R)^{-1}$ , where  $k$  is a constant, for dependence on distance,  $R$ . This does not agree with an established empirical expression for long ranges that  $\Delta p \approx R^{-1.2}$ <sup>11</sup> or with accepted models at intermediate scaled ranges.<sup>12</sup>

Another difficulty is that explosion overpressures depend only on ambient pressure at the gage,  $p_o$ ,<sup>12</sup> and not (as shown by Equation (2)) on source pressure altitude,  $p_h$ . It is thus not yet clear why this equation appears to work as well as it does.

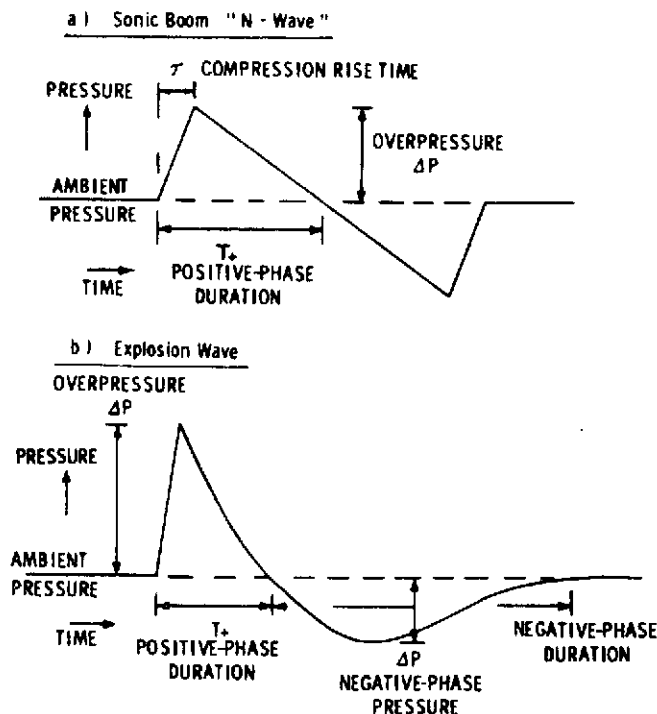


Figure 3. Airblast Wave Pressure/Time Signatures

Atmospheric turbulence interacts with weak shock waves to cause variable outputs which have been subject to much theoretical discussion and experimental research. Measurements by Maglieri<sup>13</sup> and Herbert *et al.*<sup>14</sup> have led to various attempts at explanation by Pierce,<sup>15</sup> Crow,<sup>16</sup> Lee and Ribner,<sup>17</sup> George and Plotkin,<sup>18</sup> Plotkin and George,<sup>19</sup> and most recently by Williams and Howe.<sup>20</sup> It had seemed that slow observed compressions could be attributed to turbulence until Williams and Howe<sup>20</sup> showed that this is questionable and that they are probably caused by non-equilibrium gas relaxation effects as advocated by Hodgson.<sup>21</sup> Experiments on a ballistic range by Bauer<sup>22</sup> also do not agree well with turbulence theory predictions. It is not yet clear why this should be limited, as it is, to occurrence in the atmospheric boundary layer<sup>13, 14</sup> during gusty winds and turbulent conditions. Hopefully, some intermediate range measurements from sled tests can also shed light on this subject. From an operating turbulence measuring program by Sandia about 3 km southeast of its sled track, records of three-dimensional wind components plus the temperature gradient to 30 m above ground could be used to compare actual with theoretical turbulence interaction phenomena.

A study of pressure wave signatures—to include spikes on waves, shock front thicknesses and their relations to shock strength, distances traveled, turbulence, and waveforms and magnifications near caustics—may allow significant refinement of sonic boom prediction theory.

#### Acoustic Focusing

"Acoustic" as used here refers to propagation of a pressure wave with conservation of energy and phase length. The overpressure in a small area of a wave front, traveling down a "ray tube" (see Figure 4) of varying diameter, changes in inverse proportion to the square root of the cross-section area of the tube. This area dependence results from shock energy being proportional to overpressure squared. Thus, as the tube area converges to zero, the resultant overpressure grows to infinity. This is an impossibility with real shock waves because, although contrary to the acoustic model, overpressure in the narrowed ray tube causes the shock front to accelerate (see Figure 5). It forms a bulge on the front, and thus diverges the rays and tube areas. To date, no adequate mathematical definition of this physical limitation<sup>2</sup> exists.

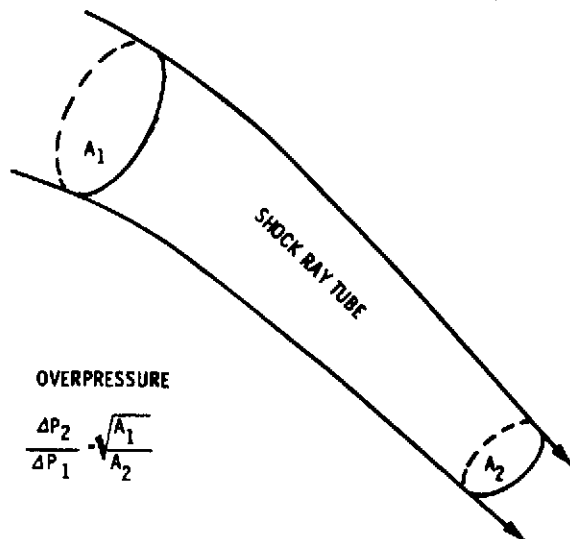


Figure 4. Shock Ray Tube Focusing

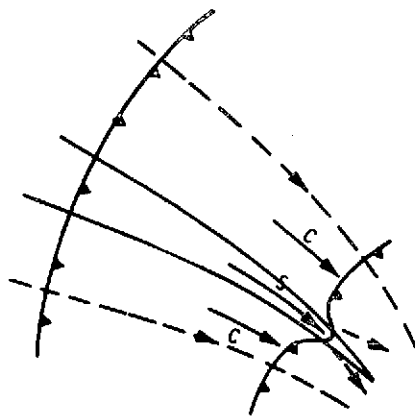


Figure 5. Shock Wave Divergence in Focus

SOUND SPEED  $C$

$$\text{SHOCK SPEED } S = C \sqrt{1 + \frac{\gamma + 1}{2\gamma} \frac{\Delta P}{P}}$$

There have been numerous attempts to make experimental determinations of the magnitudes and distributions of the focus factor, or the ratio between focused and unfocused overpressures at specified distances from an impulsive source. Perkins *et al.*<sup>23</sup> indicated that amplification factors of 100 could be caused by atmospheric refraction of explosion blast waves. Extensive observations by Reed<sup>24,25</sup> at various distances and from various explosion yields, however, have shown magnifications not nearly so large. From nearly 15,000 microbarograph recordings of explosions in various atmospheres, but often without ducting or focusing, the maximum observed magnification appeared to be just over 4X. An observed statistical distribution of focusing test data was extrapolated to estimate a 5-percent probability (per explosion) of about 7.5X magnification in a wavelength-wide belt around a caustic. The difficulty is, of course, in having an infinity of gages spaced at infinitesimal intervals as needed to observe an infinite magnification along a line.

This problem with caustics also plagues underwater sound specialists. Underwater explosion waves may be ducted and focused by stratifications of water temperature and salinity, which refract very similarly to atmospheric temperature and wind stratifications. Tests in flooded quarries and in the Sargasso Sea have given observations of a magnification<sup>26</sup> up to 10X.

Observers of sonic booms have reported 2-4,<sup>27</sup> 2.5,<sup>28</sup> 3,<sup>7</sup> and 4.75-5.78<sup>29</sup> from U. S. flight tests. The French, in preparing for Concorde SST operations,<sup>6</sup> have apparently accumulated the most detailed information and have found a maximum 9X from 90 flights.

The optimism of some theorists has not been verified, since several reports of magnifications greater than the 2X according to Wiggins,<sup>30</sup> 3.5X according to Friedman and Myers,<sup>3</sup> or even 5X according to Seebass,<sup>4</sup> now exist. It would seem that truncations and approximations needed for finite increment numerical evaluations, or even artificial viscosity as sometimes used to control calculation instabilities, have obscured the true physical limits.

## Experiment Plan

The supersonic sled test track in Area III, located with respect to Area I and Albuquerque as shown in Figure 6, is detailed at larger scale in Figure 7. This track is 1524 m (5000 ft) long and is oriented north-south; that is, sled vehicles are started at the north end and travel south. Views toward the ends of the track are shown as Figures 8 and 9. A frequent task of this track is to impact a stationary and heavily instrumented weapon system with a surface, such as a large block of concrete, to simulate the impact of a moving weapon on the ground. Two general-purpose sled vehicles are shown in Figures 10 and 11. Impact at the south end of the track often gives an impact explosion. There is a loud blast and roar at the north end when sled rockets are ignited. Finally, supersonic vehicles cause conical sonic boom wave emissions. By design, in some tests Mach 1 is not obtained; therefore, these do not cause sonic booms.

First studies, directed at defining the various noise outputs and explaining their noise nuisance at the Four Hills residential area, used an array of six blast pressure gages, situated as shown in Figure 7. A security fence around Area III limited gage positioning because it was inconvenient to place gages north and west of the track. Gage B was located to measure rocket ignition noise, but with the plan that, should it be found necessary, it could be moved outside and north of the fence to measure axial emissions. Gages C through G were placed to obtain general sonic boom characteristics as well as measurements of impact explosions in two general directions.

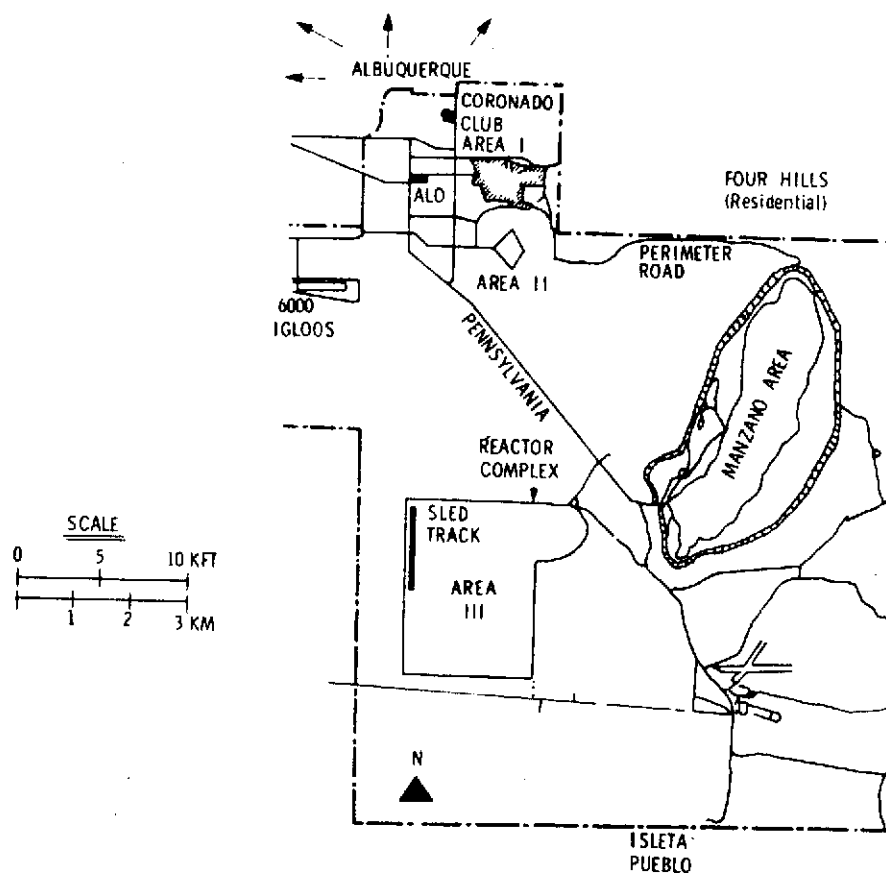


Figure 6. Kirtland AFB East (Sandia Area) and Sled Track

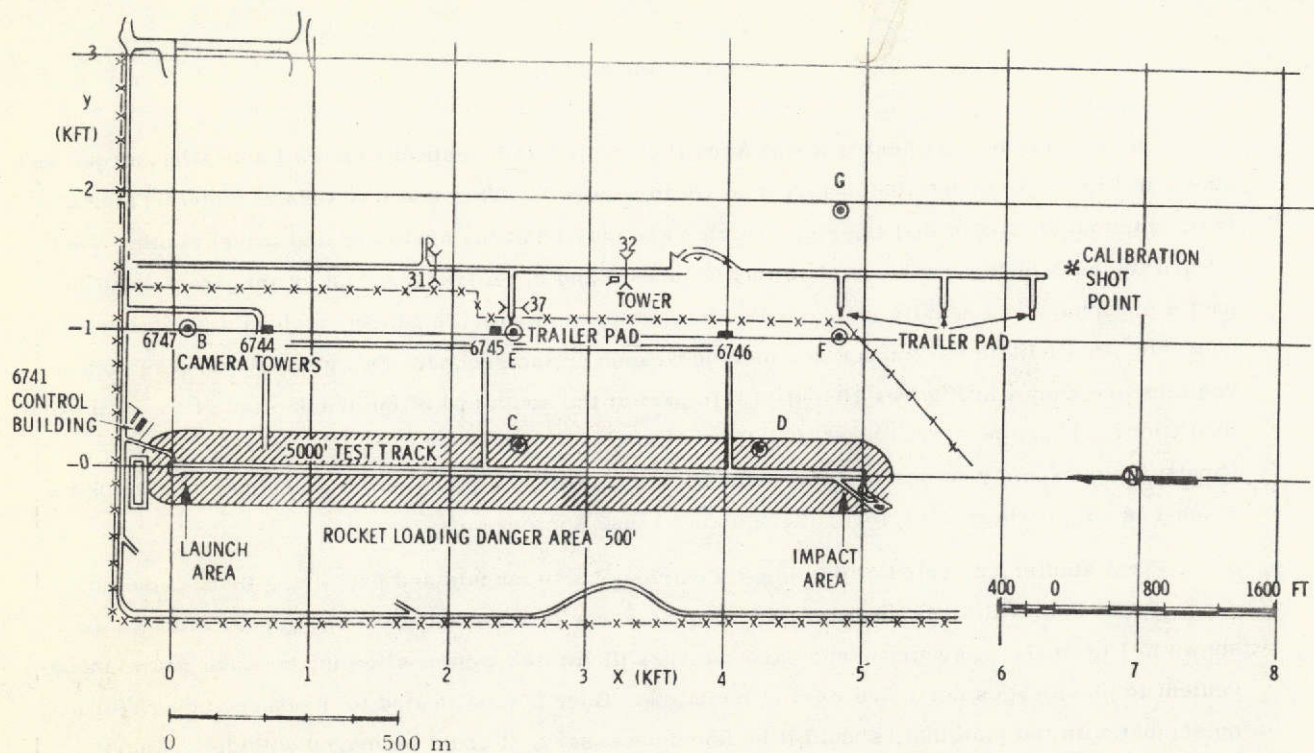


Figure 7. Map of Area III Sled Track and Sonic Boom Project Facilities

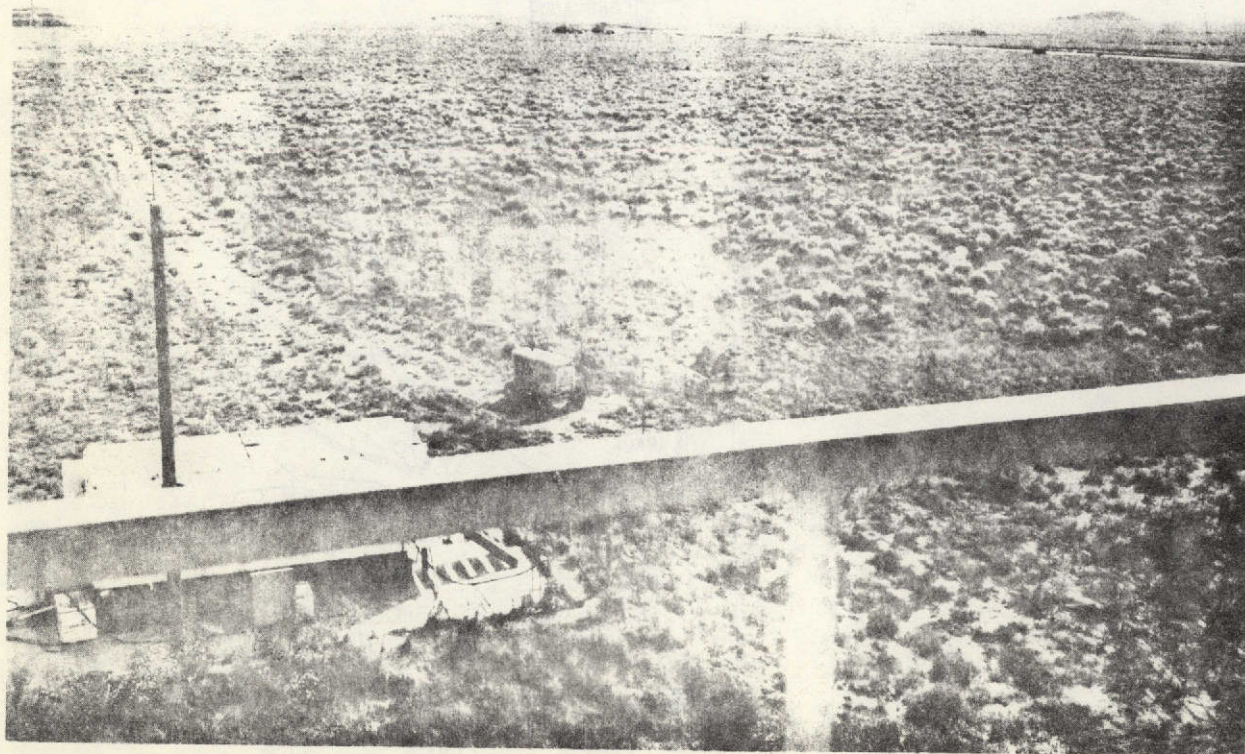


Figure 8. Sled Impact Area, View Toward Southwest





Figure 9. Sled Launch Area, View Toward Northwest

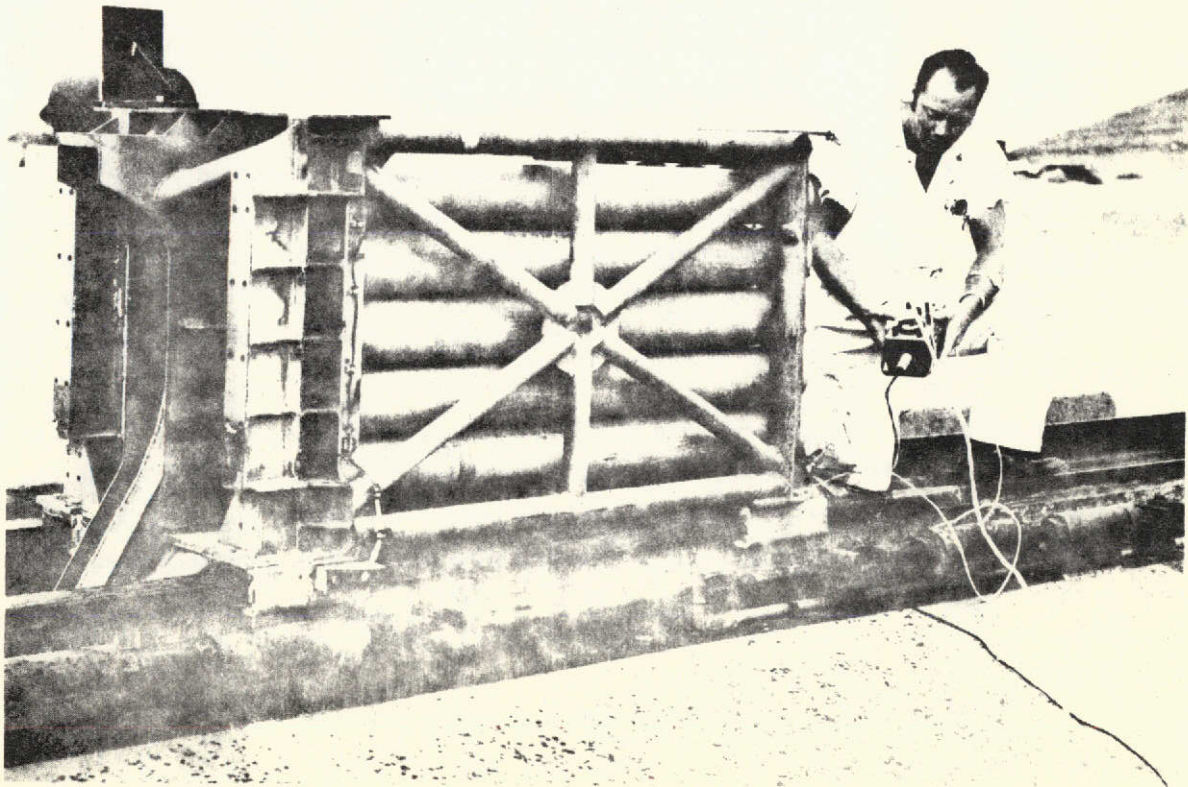


Figure 10. Utility Sled With 25 HVAR Rockets, 425-m/s Maximum Speed



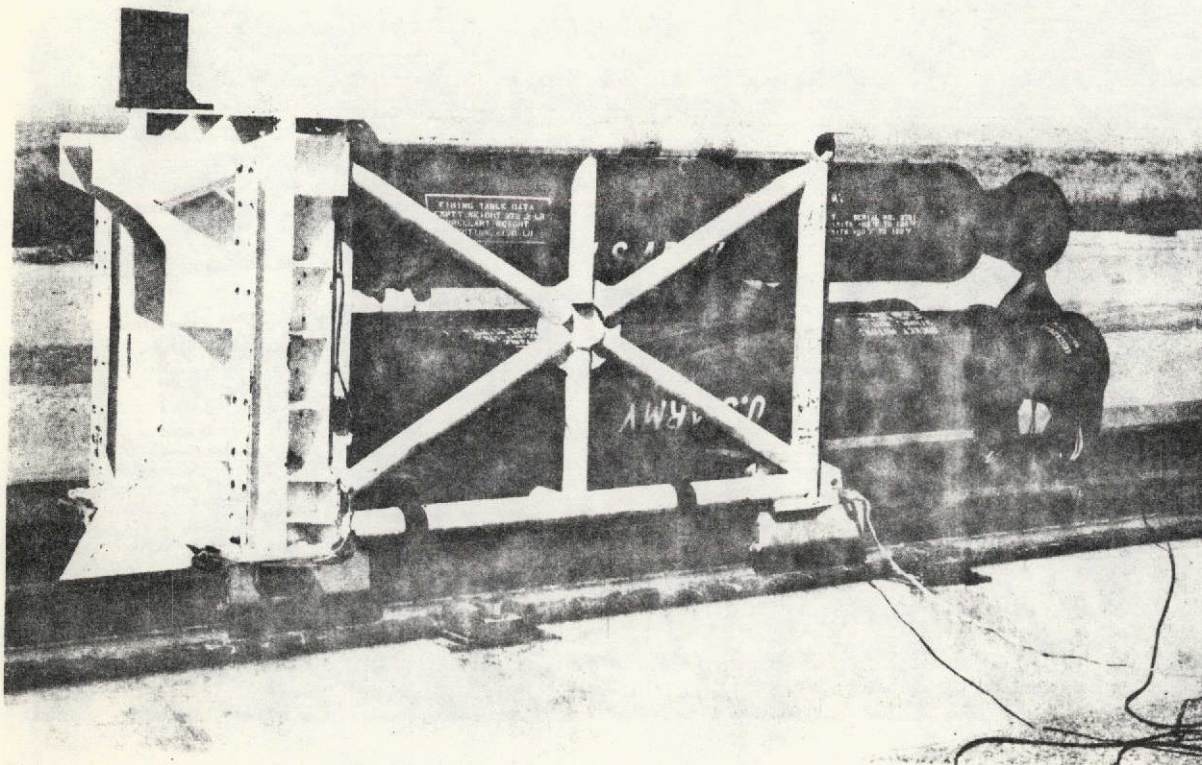


Figure 11. Utility Sled With Three Little John Rockets, 600-m/s Maximum Speed

Up to the time that these gages were installed, track activity averaged about one supersonic test per week. Requirements changed, however, and only eight tests were recorded during 1971 and 1972. There was, instead, a large program of subsonic sled testing, which did not offer useful information. Plans for one extensive supersonic test series, to begin in 1972, were canceled in general program cutbacks. From January through June 1973, there were only two supersonic impact tests, plus one demonstration and four runs to gather sonic boom data. Data from these 15 events will be presented in this report.

The stationary gage array, first operated on February 5, 1971, is described in Table I. For this project, track coordinates were adopted so that  $x$  increased southward from zero at the north end of the track and  $y$  increased eastward from zero on the track. The nose of the sled at ignition was usually about 8-15 m down from the north track end, and the impact at  $x > 1500$  m varied according to the particular experiment.

TABLE I  
Stationary Pressure Gage Array

Gage	Location			
	x		y	
	(m)	(ft)	(m)	(ft)
B	30.5	100	300.2	985
C	780.3	2560	61.0	200
D	1298.5	4260	61.0	200
E	778.5	2554	304.8	1000
F	1475.2	4840	304.8	1000
G	1475.2	4840	599.5	1967

Pressure gages at fixed locations, B-G, are Pace P7D variable-reluctance transducers, well known in airblast measurements. They are produced in  $\pm 0.7$  to 3.5 kPa ( $\pm 0.1$  to 500 psi) ranges by the Dynasciences Corp., a subsidiary of the Whittaker Corp. Transducers are undamped and have natural frequencies of 2 kHz and above. Response is linear below 1 kHz. The diaphragm is corrugated metal 2 cm in diameter and 2 mils in thickness for the 0.05-psi-rated gage. Sensors installed in canisters on tripod legs about 1 m high, with sensor ports opening downward, are subjected to horizontal blast wave motion.

Signal voltages are transmitted by underground cable, with a 6-kHz Natel Model 2088 carrier system, to a recording station in the Track Control building, 6741. This is a transistorized version, to Sandia specifications, of the older, well-known Consolidated System D. Outputs from carrier amplifiers, along with an IRIG coded time signal, are recorded by an Ampex CP-100 magnetic tape recorder. Track break-switch signals, which show sled arrivals at points along the track, are recorded on one tape track for synchronizing pressure wave arrivals with the time history of sled motion.

NASA Langley Research Center supported Sandia's Instrumentation Fielding Division in the design, procurement, assembly, and field testing of a mobile array of 12 gages for recording near caustics. This system consists of three L-band radio telemetry transmitters with an output of 4 VCO's, each driven by an amplified pressure transducer output, multiplexed into each transmitter. Power is provided by nicad batteries. These four transducer canisters, each driving 1 VCO, can be placed up to 150 m from their transmitter. A command receiver with each transmitter canister permits remote control of power (on/off) and calibration (on/off). A typical canister is shown in Figure 12.

Pressure transducers in this system are Statham Model PM 283 sensors, which are undamped and have natural frequencies above 2 kHz. They use a corrugated diaphragm about 4 cm in diameter. At the receiving station, these three L-band frequencies are preamplified and sent through a down-converter, into three P-band receivers, and onto the magnetic tape recorder.



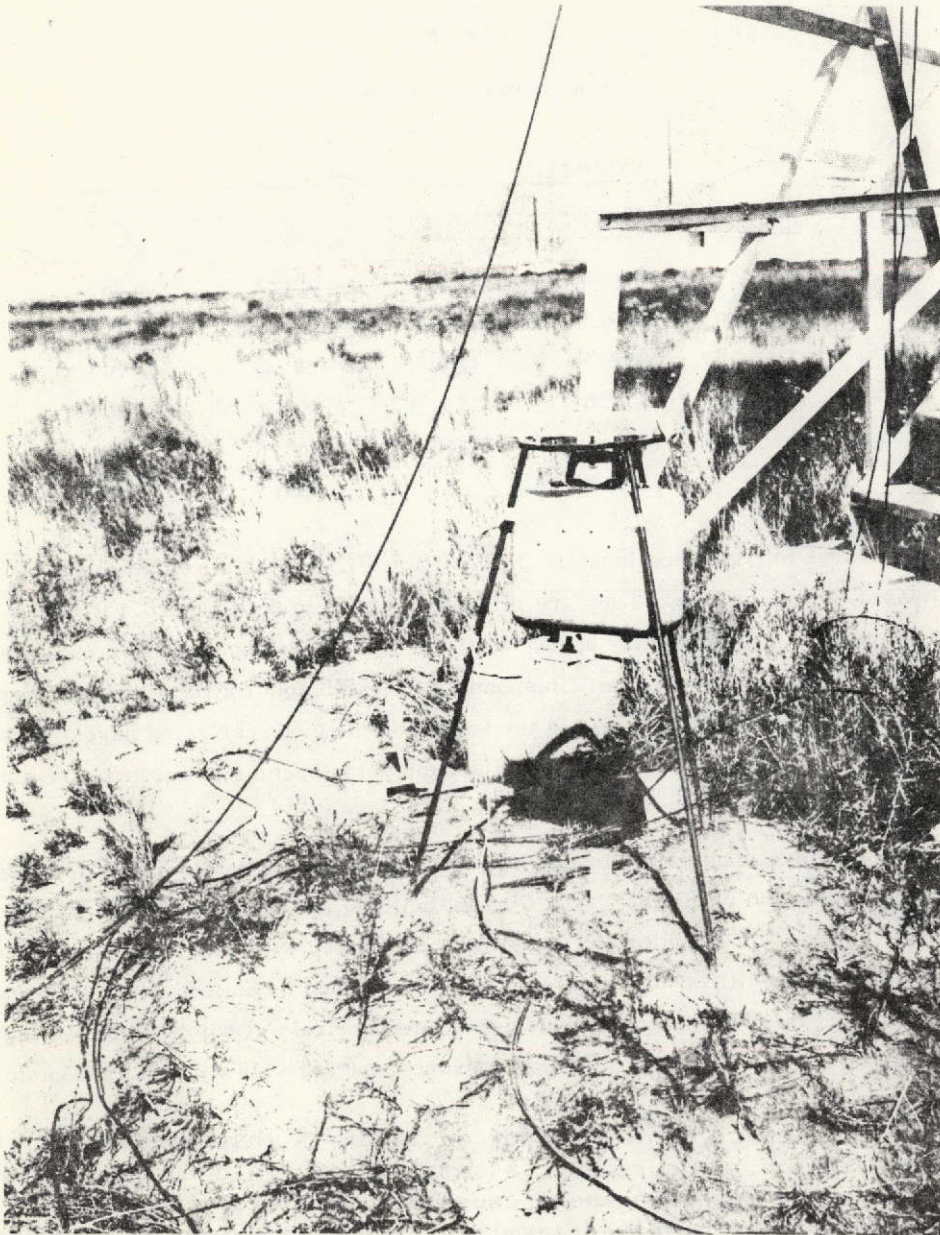


Figure 12. Canister for Mobile Pressure Transducer

Both fixed and mobile transducer systems use resistors that are switched by relay, in and out of each transducer-bridge circuit, shortly before test time. This procedure produces a known equivalent pressure step for reference to the calibration curve of each transducer.

Quick-look playbacks of four channels at one time may be made at the recording station on a Consolidated recording oscillograph. The bulk of paper recording is, however, made at the Sandia central playback Measurements Development Division I. There are available, in conjunction with the Underground Physics Division, instruction codes and digitizing equipment for automated analysis and uniform pressure wave signature graphing. These capabilities have not yet been used because experience with a variety of signal collections is needed before standardized computer analysis instructions can be determined.

Pressure transducers were calibrated against precision manometers by the Transducer Evaluation and Calibration Division.

The test field either has been or will be surveyed with four lines staked at 30.48-m (100-ft) intervals, at 305, 914, 1524, and 2134 m (1, 3, 5, and 7 kft) offset from the track (y-coordinate) and in sections where boom caustics could pass. It takes two men 1 day to move the mobile array to a new measurement location and check out equipment operation.

### Calculations

From inspection of sled trajectory data it was found that vehicle velocity could be approximated by a fourth-power polynomial in time with reasonable accuracy. Measurements of distance versus time by break switches are provided along the track, however, so these are used to compute finite-difference velocities for estimating the velocity polynomial. Thus, an rms curve fitting yields

$$\dot{x} = v = a_0 + a_1 t + a_2 t^2 + a_3 t^3 + a_4 t^4 \quad (3)$$

with calculated values of  $a_i$ . Acceleration obtains from

$$\ddot{x} = a = a_1 + 2a_2 t + 3a_3 t^2 + 4a_4 t^3 \quad (4)$$

Position estimation requires integration so that

$$x = a_k + a_0 t + \frac{1}{2} a_1 t^2 + \frac{1}{3} a_2 t^3 + \frac{1}{4} a_3 t^4 + \frac{1}{5} a_4 t^5 \quad (5)$$

and the constant  $a_k$  is obtained from the earliest (x, t) break-switch point. An appropriate root-finding subroutine in the computer library is used to determine time, t, for a given position, x, from Equation 5. This is needed to find source points for wave rays which will pass through specified gage locations (x, y).

An attempt was made to establish local sound velocity by direct observation, rather than from ambient temperature and wind observations. At various gages, blast wave arrivals from the impact explosion would give several directed velocities which could, in principle, be separated into effective sound speed (temperature) and wind speed and direction. It turned out, however, that the location and time of impact explosions were not always easily defined, and considerable errors and uncertainties resulted. Consequently, the wind and temperature observations at the control building were used to estimate sound velocities in the various required directions. One estimate for sound speed, c, in dry air is

$$c = 20.056 \left[ T \text{ K} \right]^{1/2} \text{ m/s.} \quad (6a)$$

$$= 1087.52 \left[ 1 + \frac{T^{\circ}\text{C}}{273.15} \right]^{1/2} \text{ ft/sec.} \quad (6b)$$

$$\approx 1088 + 2(T^{\circ}\text{C}) \text{ ft/sec,} \quad (6c)$$

$$\approx 331.5 + 0.607(T^{\circ}\text{C}) \text{ m/s,} \quad (6d)$$

approximations adequate for most purposes. Sound convection, if horizontal winds are assumed, is accounted for in determining sound velocity,  $V$ , from

$$V_i = c - W \cos (\theta_i - \Phi) , \quad (7)$$

where  $W$  is wind speed,  $\theta_i$  is direct bearing of interest, and  $\Phi$  is wind direction (conventionally observed as the direction from which wind blows and measured clockwise from north). Along the track, ambient sound velocity (for calculating Mach number,  $M = v/V(180^\circ)$ ) is thus

$$V(180^\circ) = c + W \cos \Phi . \quad (8)$$

At any point,  $x$ , along the track trajectory (shown in Figure 13) parameters  $(t, v, a, M)$  can be defined by manipulation of Equations 3, 4, 5, and 8. During supersonic acceleration a curved boom wave front is generated. The generated front slope expands at the Mach angle; thus,

$$\frac{dy}{dx} = f' = -(M^2 - 1)^{-1/2} \quad (9)$$

and the curvature

$$\frac{d^2y}{dx^2} = f'' = \frac{a}{V^2(M^2 - 1)^{3/2}} . \quad (10)$$

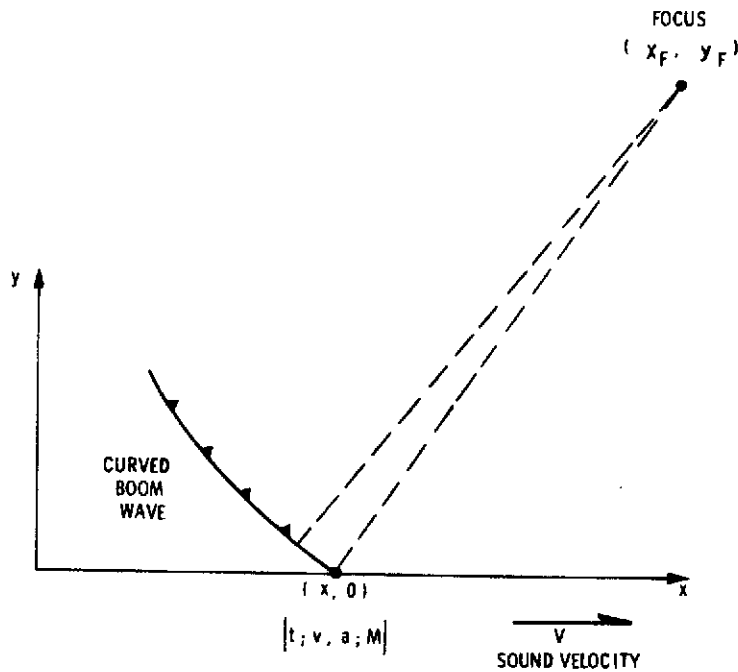


Figure 13. Sonic Boom Focusing From Accelerating Supersonic Sled

From analytic geometry the center of curvature, or focus of the emitted wave segment, falls at coordinates  $(x_F, y_F)$ , defined by

$$\begin{aligned}x_F &= x - \frac{f' [1 + (f')^2]}{f''} \\y_F &= y + \frac{1 + (f')^2}{f''}\end{aligned}\quad (11)$$

Suitable manipulation and substitution from Equations 9 and 10, with  $y = 0$  along the track coordinate system, yields

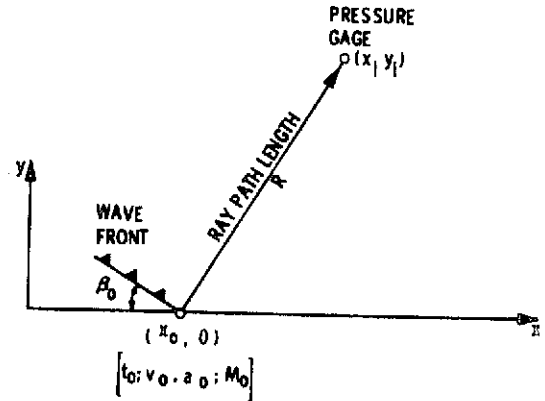
$$\begin{aligned}x_F &= x + \frac{v^2}{a} \\y_F &= \frac{v^2(v^2 - V^2)^{1/2}}{aV}\end{aligned}\quad (12)$$

Calculation of these centers for various points along the track  $(x, 0)$  yields the locus of the caustic, or focus, line for a particular accelerating supersonic sled trajectory and weather condition.

Next, a predicted arrival time and source point is calculated for each shock wave expected to pass each gage location  $(x_i, y_i)$ . From the geometry of Figure 14, a shock ray emitted from the vehicle at  $(x_o, 0)$  and perpendicular to the wave front, which extends at the Mach angle  $\beta_o$ , follows:

$$\tan \beta_o = \frac{x_i - x_o}{y_i} = V(180^\circ) / \left[ v_o^2 - V^2(180^\circ) \right]^{1/2} \quad (13)$$

Figure 14. Geometry for Wave Source Solutions



Since in Equations 3 and 5  $v_o = v(t_o)$  and  $x_o = x(t_o)$ , it is possible, by finding roots  $t(x)$ , to obtain  $v_o = v(x_o)$  for substitution in Equation 13, leaving only the variable  $x_o$  which may then be evaluated for the station location  $(x_i, y_i)$ . From transformation of  $x_o = x(t_o)$  to  $t_o = t(x_o)$  the source time may be calculated. Then the assumed acoustic travel time from  $(x_o, 0)$  to  $(x_i, y_i)$  is calculated by using the sound velocity calculated for direction  $\theta_i = \beta_o + 90^\circ$  from Equation 7.

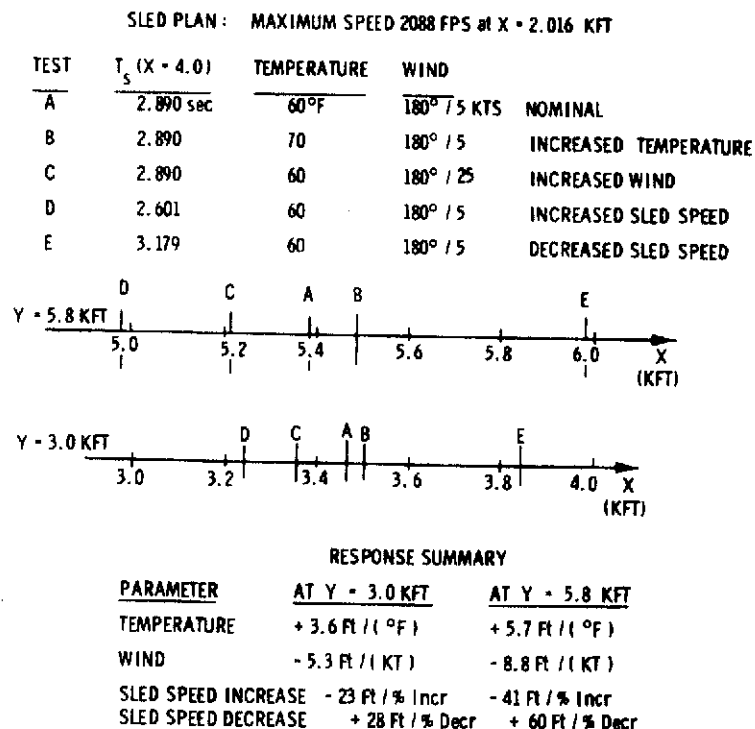
For simple trajectories, such as those which result from single-stage rocket drivers, there will usually be two solutions (sources) for wave arrivals at a gage. In more complex two-stage vehicle tests, there may be as many as four source solutions; therefore, the computer root-finder code is programmed to make the appropriate search until all solutions are found. In practice,

most predicted arrivals have fallen within a few milliseconds of observed arrivals, so this code is judged to be adequate. Meanwhile, these source parameters ( $x, t, M$ ) and the acoustic propagation distance are read out for attenuation estimation, should it be needed.

Total input to the calculation is thus a set of ( $x, t$ ) break-switch data, usually 12-15 points; position coordinates of, usually, 5 fixed (boom waves do not reach Gage B) and 12 mobile gages; temperature, in  $^{\circ}\text{F}$  as observed and reported; and wind direction in degrees and speed in knots, also as regularly reported. The output is a set of time coefficients for velocity estimation; a tabulation of trajectory values of ( $x, t, v, a, x_F, y_F$ ); and, for each gage, root, or wave source values for ( $t, x, v, a, M, R, t_a$ ), where  $R$  is acoustic travel distance and  $t_a$  is wave arrival time. If there are no roots, this is stated. Typical computer times for solution are 8 seconds for central processing and 8 seconds for peripheral processing.

A test calculation was made to show how accurately caustic locations could be predicted in spite of input errors in vehicle trajectory, air temperature, and winds. Results are summarized in Table II for parameter variations of  $10^{\circ}\text{F}$  temperature, 10 m/s (20 knots) of wind, and  $\pm 10$  percent changes in arrival times along the track. It appears that these errors can cause 60 - 90 m (200-300 ft) errors in  $x_F$  at  $y_F = 914$  m (3000 ft), 120-180 m (400-600 ft) if errors at  $y_F = 1829$  m (6000 ft). It follows that an array of 12 gages should be about 150 m (500 ft) long with 15 m (50 ft) gage spacing to intercept a caustic at  $y_F = 914$  m (3000 ft). At 1829 m (6000 ft) offset, an array should have about 30 m (100 ft) gage spacing. It is hoped that, with practice, this uncertainty may be reduced so that shorter gage spacing can be used.

TABLE II  
Caustic Location Parameter Test and Response Summary



## Results

Fifteen supersonic sled tests (summarized in Table III) have been observed to date. Seven events were recorded after the mobile array was installed. On five of these, the array was positioned to cross the caustic, and calibration shots were fired for a dynamic check on gage response to wave magnifications. Relevant data for each event, tabulated and graphed in the appendix include summaries of computer inputs and outputs, a listing of wave parameters for each recorded pulse, reproductions of all except minor pressure perturbations, and a map of calculated ray paths and caustic loci.

Although the bulk of this data collection precludes detailed evaluation at this time, it is apparent that the measurement program has been successful in obtaining satisfactory data from a previously unobserved regime in sonic boom propagation. It generally appears that boom overpressures decay in proportion to the  $-3/4$  power of offset distance from the track, where two gages were about on the same emitted wave ray. Preliminary evaluations, not detailed in the report, do not clearly show overpressure proportionality to  $(M^2 - 1)^{1/8}$ ; however, the variance is not consistent. Nevertheless, overpressures do increase rapidly with Mach number increases immediately above the transsonic regime.

The computer program for sled trajectory evaluation and boom wave arrival time prediction appears to work well, and agreement with observed arrivals is often within a few milliseconds. Comparison data are listed in even-numbered tables of the appendix. Discrepancies of 100-200 ms occur often in predicting the transsonic wave arrivals, because the waves travel longer paths and the exact source point cannot be accurately determined.

When operations allowed the positioning of the mobile gage array across the predicted caustic locus on five tests, a maximum overpressure was recorded in the array. Various methods for estimating the free-field (unfocused) overpressure have been used to estimate caustic magnification factors. Maxima from various tests range from 1.27X to 2.87X. In general, it does not appear that a sharp asymptotic approach to a very strong caustic was even observed. Rather, there was usually a "hump" in the pressure versus distance or gage number curve, about 60 m wide. This diffuse caustic may be a result of the unexpected slow compression times and thickened shock fronts, detailed in a later section. Such dampening of effects may be the result of ground reflections, sagebrush and terrain irregularities, or of attenuation by small-scale air turbulence. Data collections from gages 10-20 m above ground would probably help to resolve this question.

### Off-Site Noise Nuisance

Three noise sources have been identified from these gage records as rocket ignition and motor noise, impact explosion waves, and sonic booms from supersonic vehicles. Sonic boom waves were all emitted toward southerly bearings and do not appear to be the source for nuisance or audibility reports from either northeast or northwest directions. On February 15, 1973, however, the author observed a double bang, typical of sonic booms, at 6 km north of the track; this situation makes it appear that there can be refraction or scattering effects that do cause such wave direction change. This cannot, at this time, be explained. Therefore, only the rocket noise and impact explosions are addressed here in the context of off-site nuisance.



TABLE III  
Summary of Sled Boom Measurements

<u>Test Date</u>	<u>Sled Event</u>	<u>Stages</u>	<u>Max Mach No.</u>	<u>Gages Operated</u>		<u>Impact Wave Recorded</u>	<u>Cal Shot</u>	<u>Caustic Intercepted</u>
				<u>Fixed Array</u>	<u>Mobile Array</u>			
2/5/71	20 <sup>0</sup> Poly	2	5.058	3	-	Yes	No	-
2/23/71	2LJ-3G4	2	4.145	6	-	Yes	No	-
4/1/71	US3-7J90	2	5.074	6	-	Yes	No	-
6/22/71	Kiva	1	1.668	6	-	No	No	-
8/16/71	Unk	1	1.531	4	-	No	No	-
12/18/71	Lance	2	2.323	6	-	Yes	No	-
9/28/72	H90H.S.	1	1.710	4	-	Yes	No	-
10/12/72	Lance	2	2.202	6	-	Yes	No	-
1/5/73	Boom Spec.	1	1.897	6	12	No	Yes	Yes
1/18/73	Small Lance	1	2.715	6	12	Yes	No	No
1/24/73	Lance	2	2.383	6	12	Yes	Yes	Yes
3/2/73	25 H.W.I.	2	3.441	6	12	Yes	No	No
5/8/73	Recruit	1	3.201	6	12	Yes	Yes	Yes
5/8/73	Roadrunner	1	3.818	6	12	No	Yes	Yes
5/15/73	Kiva	1	1.552	6	12	Yes	Yes	No

### Impact Waves

Evaluating the source, or sources, for nuisance wave propagations outside Kirtland East requires an estimate of explosion energy at the source: the high-velocity impact at the end of the track. Studies of meteoritic impact explosions<sup>31</sup> have indicated that impact kinetic energy may be used to approximate an equivalent high-explosive (HE) yield for blast wave parameter estimation. Values for these sled test events are shown in Table IV, with kinetic energy (KE) calculated from

$$KE = \frac{1}{2} mv^2, \quad (14)$$

with use of a standard conversion factor: that 1 kt HE = 4.2 TJ =  $3.1 \times 10^{12}$  ft lb, so that 1 lb HE = 2.1 MJ =  $1.55 \times 10^9$  ft lb. Impact weights varied according to whether the rocket fuels were completely burned and what the empty motor cases weigh. For the purposes of this report, impact weights have been estimated from test records of payload and sled, plus an assumed 10 percent of rocket weight for the residual casing. (Full details are probably obtainable from engineering files.)

Recordings of airblast pressure from impacts were used to estimate explosion source yields, by assuming standard homogeneous atmosphere airblast propagation, from an empirical equation that<sup>11</sup>

$$\Delta p = 8.58 (W \text{ kt NE})^{0.4} (R \text{ km})^{-1.2} \text{ kPa}, \quad (15a)$$

$$\Delta p = 357 (W \text{ kt NE})^{0.4} (R \text{ kft})^{-1.2} \text{ mb} \quad (15b)$$

For a surface burst (hemispherical wave expansion) with the usually accepted 2:1 nuclear-chemical explosion equivalence, and with negative phase pressure,  $\Delta p \approx 0.35$  (as was indicated in Figure 3) peak-to-peak amplitude

$$p_K = 83.5 (W \text{ kg HE})^{0.4} (R \text{ km})^{-1.2} \text{ Pa}, \quad (16a)$$

$$p_K = 2.53 (W \text{ lb HE})^{0.4} (R \text{ kft})^{-1.2} \text{ mb}. \quad (16b)$$

A solution is required for W, obtained from

$$W = 1.57 \times 10^{-5} (R \text{ km})^3 (p_K \text{ Pa})^{2.5} \text{ kg HE}, \quad (17a)$$

$$W = 0.098 (R \text{ kft})^3 (p_K \text{ mb})^{2.5} \text{ lb HE}. \quad (17b)$$

Results from each fixed pressure gage, plus the range of values from the mobile gage array, were included in Table IV. Comparisons between calculated impacts and equivalent explosion wave energies are shown in Figure 15. Waves propagated in different directions from impact showed that apparent yields may vary by more than a factor of 400. Propagation was usually weakest up the track, and to the north, except in the March 2, 1973, test. Strongest waves were usually recorded perpendicular to the track, but there were no gages south of impact.

TABLE IV  
Summary of Sled Test Impact Explosion Data

No.	Impact Explosion Data					Fixed Gage Station and (R kft) <sup>3</sup>						Mobiles		
	Test Date	Launch Wt (lb)	Impact Wt (lb)	Velocity (fps)	Impact KE (lb HE)	B 124.85	C 14.67	D 0.45	E 19.44	F 1.04	G 7.69	Min W (lb HE)	Max W (lb HE)	Average R (kft)
1	2/5/71	3317	950	5571	9.5	-	3.3	0.26	-	14.7	-	-	-	-
2	2/23/71	3300	950	4600	6.5	-	0.96	1.28	1.77	12.8	17.0	-	-	-
3	4/1/71	6250	1130	5672	11.7	-	0.85	1.07	1.46	0.36 <sup>1</sup>	1.34	-	-	-
4	6/22/71	586	390	1917	0.46	-	No S/N	-	-	-	No S/N	-	-	-
5	8/16/71	M	M	1629	Unk.	-	No S/N	-	-	No S/N	-	-	-	-
6	12/18/71	18835	6500	2549	13.6	-	0.30	5.52	-	74.8	130	-	-	-
7	9/28/72	878	475	1938	0.58	-	-	0.64	0.30	4.45	7.67	-	-	-
8	10/12/72	20585	7200	2457	14.0	0.71	1.47	1.73	3.96	48.6	74.1	-	-	-
9	1/5/73	2612	N.I.	0	0	0	0	0	0	0	0	0	0	3.33
10	1/18/73	M	M	2984	Unk.	0.41	0.45	0.80	0.39	5.10	5.53	4.12	9.39	3.01
11	1/24/73	20472	10260	2648	23.2	0.96	0.82	1.02	2.07	71.9	200	93.7	222	3.01
12	3/2/73	3505	343	3250	1.17	5.67	3.84	1.63	5.12	1.51	0.72	1.33	3.33	3.01
13	5/8/73 <sup>1</sup>	905	395	3041	1.18	0.027	No S/N	0.033	No S/N	0.116	0.110	0.035	0.134	3.80
14	5/8/73 <sup>2</sup>	80	46	2329	0.081	No S/N	-	-	-	-	-	-	No S/N	3.80
15	5/15/73	539	380	1500	0.28	0.010	<0.05	0.0083	No S/N	0.020	0.037	-	< 0.012	3.34

Remarks:

<sup>1</sup> Arrival in tail of boom wave.

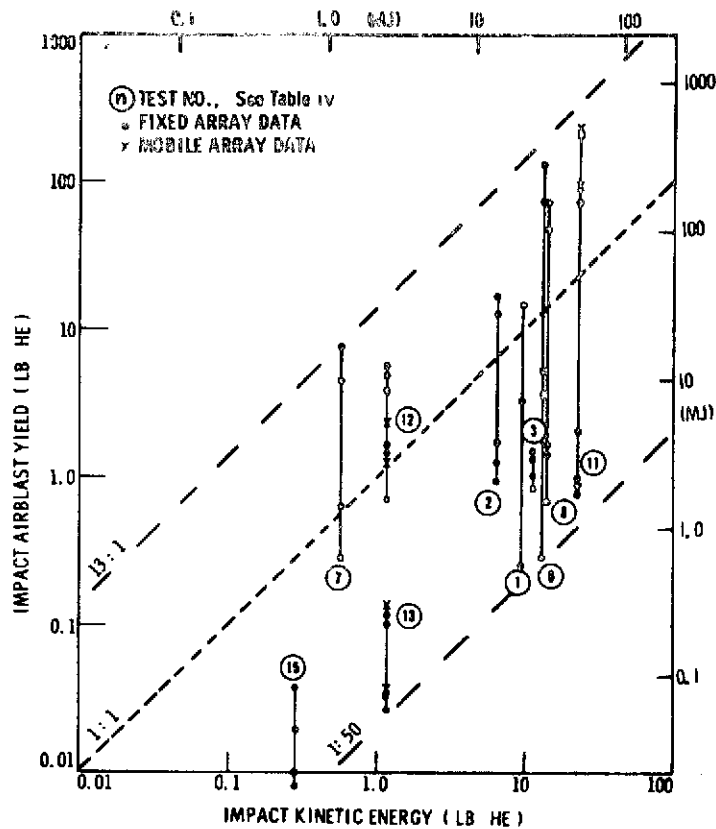


Figure 15. Energy Comparisons, Impact vs Pressure Waves

Extrapolation to longer ranges may be estimated from Figure 16, which shows standard explosion propagations for various yields. These curves, calculated from Equation 16, are for unrefracted hemispherical wave expansion. Atmospheric variations may cause amplitudes at 8-16 km ranges to scatter from 0.1 to 3 times these standard amplitudes.<sup>25</sup> It does not appear that any of these impacts would have caused more than 200-Pa (2-millibar, 0.03-psi, or 4.2-psf) amplitudes at Four Hills, even with maximum atmospheric ducting and focusing. Although about 400-Pa amplitude is an accepted rule-of-thumb for the window damage threshold, even 100-Pa amplitude can be noisy and cause buildings to rattle, and that is probably what happened in the Lance tests of 1970.

From this analysis, it would appear that a damaging 400-Pa wave at Four Hills would require, even with 5X magnification, nearly a 450-kg (1000-lb) HE equivalent impact explosion. Figure 11 indicates, however, since observed waves appear to result from as much as 13 times the impact kinetic energy because of directed blast effects, that such emissions could result from as little as a 34-kg (75-lb) HE equivalent, or 150 MJ ( $1.2 \times 10^{11}$  ft lb). This is about 3 times as energetic an impact as has been observed during this test period. It would require nearly 1500-m/s (5000-ft/sec) impact of a 4.5-Mg (5-ton) vehicle.

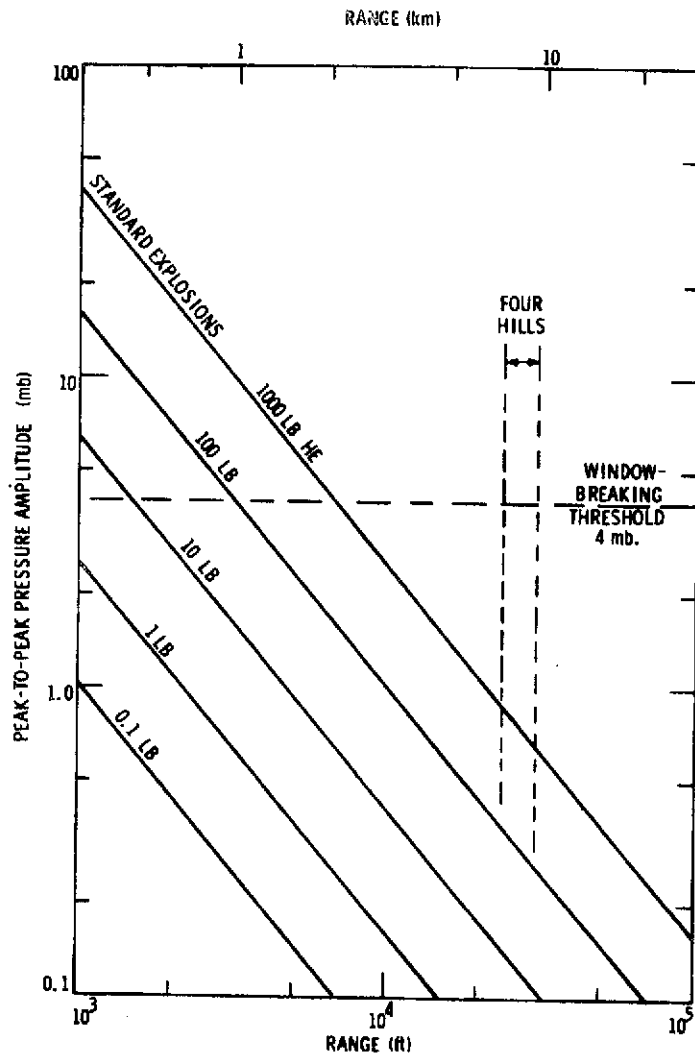


Figure 16. Comparison Curves for Impact Explosion Evaluation

#### Ignition and Rocket Engine Noise

Sounds from sled rockets are largely directed northward and could be the source of off-site annoyance, except that several reporters have heard bangs rather than roars or rumbles in both northeast and northwest directions from the test track. Distant pressure amplitudes may be estimated from the noise records obtained chiefly by Gage B. Acoustic amplitude decay, inversely proportional to distance, was assumed and no attempt was made to consider frequency-dependent sound attenuation. As shown in the data summary, Table V, noise amplitudes extrapolated to 7.62-km (25-kft) range vary from 0.5 Pa, from the small Roadrunner and Kiva tests, to well over 1.5 Pa from the December 18, 1971, Lance test. On that event, Gage B was completely saturated and driven off-scale at  $p_K \gg 400$  Pa. Only such very large rocket blasts would be more than a distant rumble at Four Hills. No nuisance damage would be expected.

TABLE V  
Rocket Engine Noise Extrapolations

Test Date	Gage	Max P <sub>K</sub> (Pa)	Range		A1 R = 25/Kft (7.62 mk) P <sub>K</sub> (Pa)
			(m)	(ft)	
4/1/71	E	85	430	1410	4.8
	G	80	1155	3790	12.1
6/22/71	C	74	181	595	2.0
8/16/71	C	83	181	995	2.0
12/18/71	B	> 3.90	302	990	> 15.4
9/28/72	E	172	371	1218	8.4
	F	226	378	1075	9.7
	G	84	607	1990	6.7
10/12/72	B	128	306	1005	5.1
	C	67	329	1080	2.9
	E	64	675	2215	5.6
1/5/73	B	243	302	990	9.6
1/18/73	B	384	302	990	15.2
1/24/73	B	298	309	1015	12.1
	E	131	724	2375	12.4
	1	65	1573	5160	13.5
	12	64	1713	5620	14.4
3/2/73	B	159.6	302	990	6.3
5/8/73 <sup>1</sup>	B	102.1	302	990	4.0
	5	19.6	1210	3970	3.1
5/8/73 <sup>2</sup>	B	12.5	302	990	0.5
5/15/73	B	12.4	302	990	0.5

## Calibration Shots

With the mobile array in operation to obtain focusing factors in caustics, the possible question of gage accuracy and reliability may be restricted by use of a dynamic pressure calibration near the time of sonic boom recording. To simulate the frequency content of sonic boom waves from sled tests, an explosion yield of 68-kg (150-lb) HE was selected by yield scaling<sup>12</sup> from a standard explosion calculation.<sup>32</sup> Figure 17 shows the explosion of one of these calibration shots. This yield should have a positive phase duration of 21 ms, a negative phase duration of 56 ms and, thus, a total wave duration of 77 ms. Measurements here have shown appreciably longer durations at overpressures below a kilopascal, a result also frequently noted at very long ranges from large explosions. It appears that finite-amplitude effects, even in such weak waves, are important in this respect and that acoustic approximations with unchanging waveform at overpressures below about 2.5 kPa (0.4 psi) are not strictly valid.

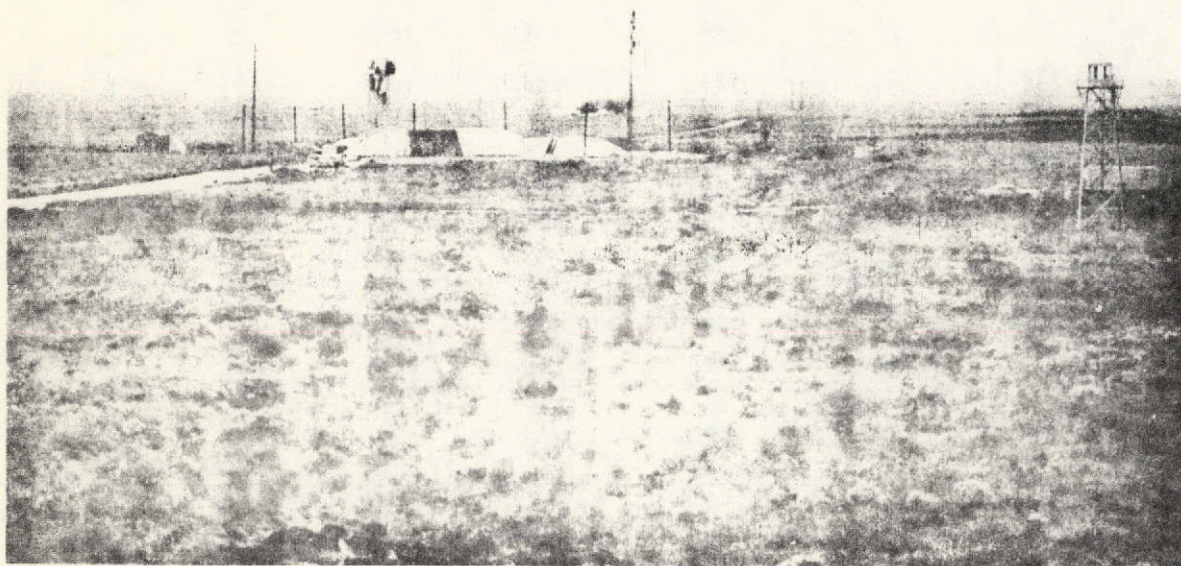


Figure 17. Calibration High-Explosives Shot, View Toward Southeast

Blast pressure amplitudes (shown in Figure 18) for five examples, to date, show reasonable agreement with the yield and ambient pressure-scaled, standard explosion, pressure/distance curve.<sup>11</sup> Pressures, generally somewhat below standard fall farther below the curve at increased range; this, no doubt, results from midday, relatively warm surface temperatures. High surface temperature causes wave rays to be refracted up, away from ground level, and this gives a reduced wave energy propagated across ray paths by scattering to ground-level gages. In these examples, at least, there was no significant ducting, such as might occur downwind in strong winds or under nighttime temperature inversions.

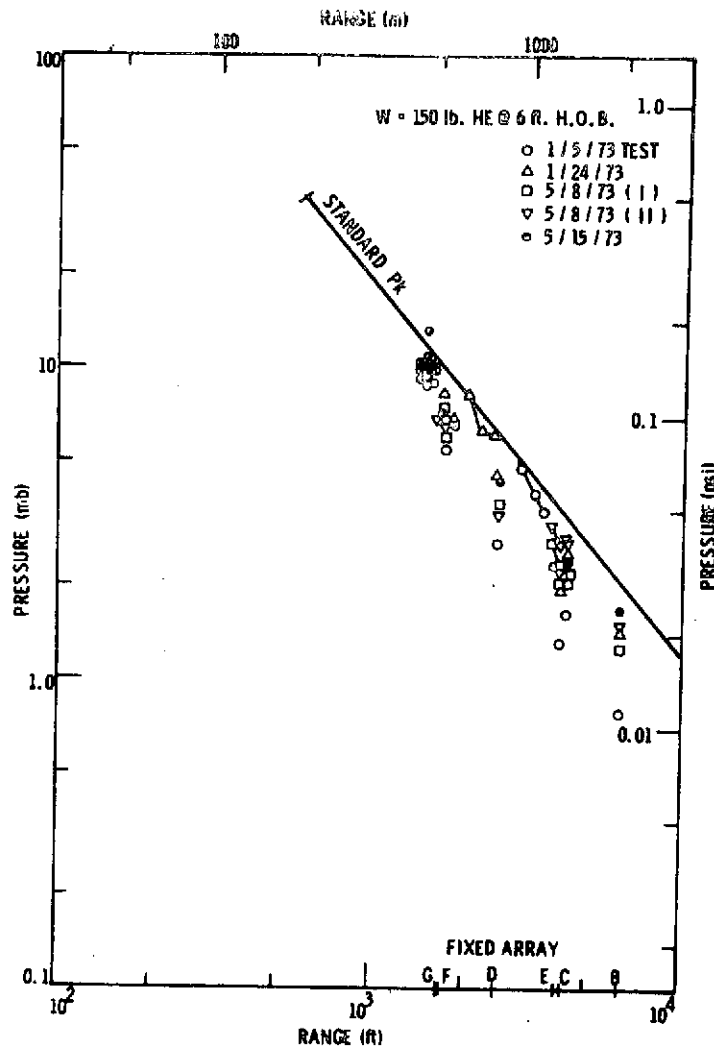


Figure 18. Calibration Shot Pressures

Pressures recorded by the mobile array (shown in Figure 19) indicate the few significant gage corrections which have been found necessary. Most of these data fall within a few percent of an rms line, which may be assumed to respond to biasing effects of specific atmospheric conditions.

Durations of the positive overpressure pulse are shown in Figure 20. The slow growth of positive phase with distance is probably caused by finite amplitude effects. Reference curves are shown for  $T_+ \sim R^{0.4}$ , which can be derived from the assumption of adiabatic, lossless propagation and  $\Delta p \sim R^{-1.2}$ . It appears that growth is less than that rate but greater than the  $T_+ \sim R^{1/4}$  which has been theorized for conical waves.<sup>10</sup>

A similar check for negative phase durations is shown in Figure 21. That these durations are considerably longer than predicted by scaling from a standard explosion<sup>32</sup> cannot be easily explained by finite amplitude effects. On the other hand, there does not appear to be any coherent change with distance, which is as expected for the rounded shape of the negative pressure signatures of explosion waves. It is very difficult to make precise determinations of negative phase duration, because it ends by almost asymptotic approach to ambient pressure. Considerable scatter in measurement results from ambient noise interference.



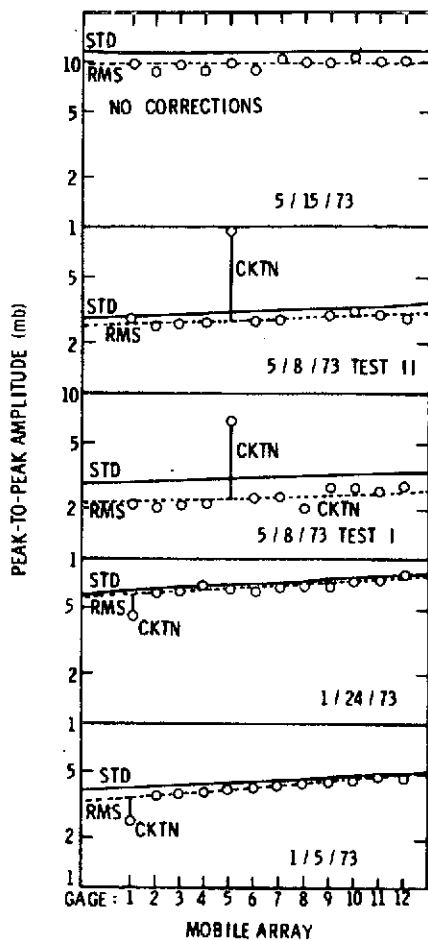


Figure 19. Calibration Shot Amplitudes and Corrections

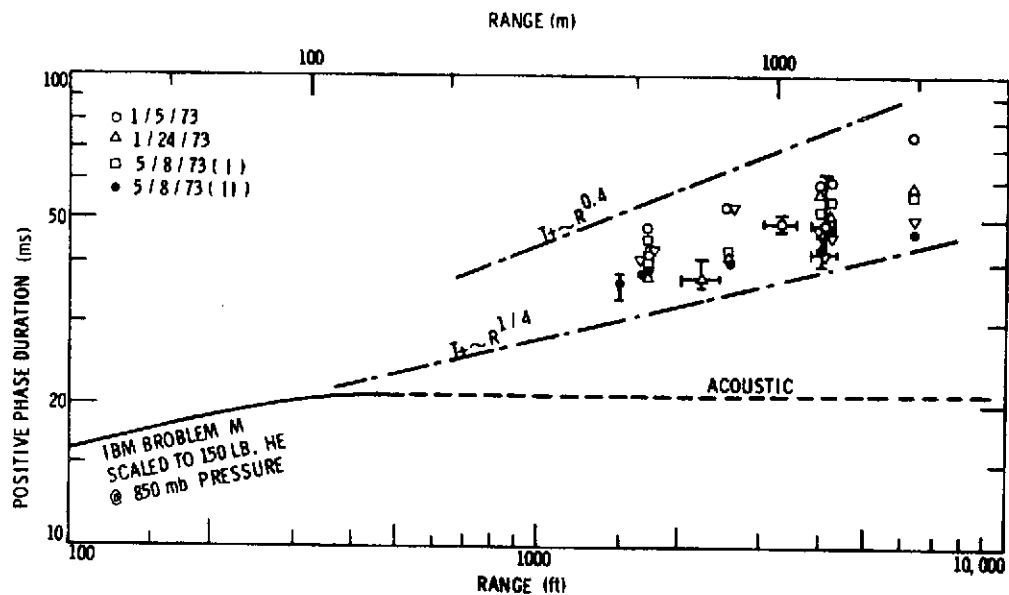
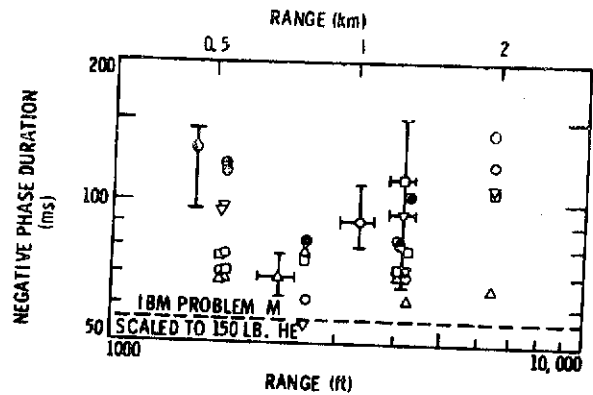


Figure 20. Calibration Shot Positive-Phase Durations

Figure 21. Calibration Shot Negative Phase Durations



### Compression Rise Times

Shock-propagation prediction theories<sup>10</sup> usually include an estimate of shock thickness, generally of the order of mean-free paths between molecules in the medium. DuMond et al<sup>12</sup> used  $\tau = (10^4 \Delta p)^{-1}$  s, for  $\Delta p$  in pascals. Experience has shown that real shocks in the free atmosphere are much thicker than theory indicates. Measurements of compression rise times from calibration shots (Figure 22) show that rise times increase roughly in inverse proportion to overpressure—a form predicted by shock theory—but they average nearly 15,000 times as long.

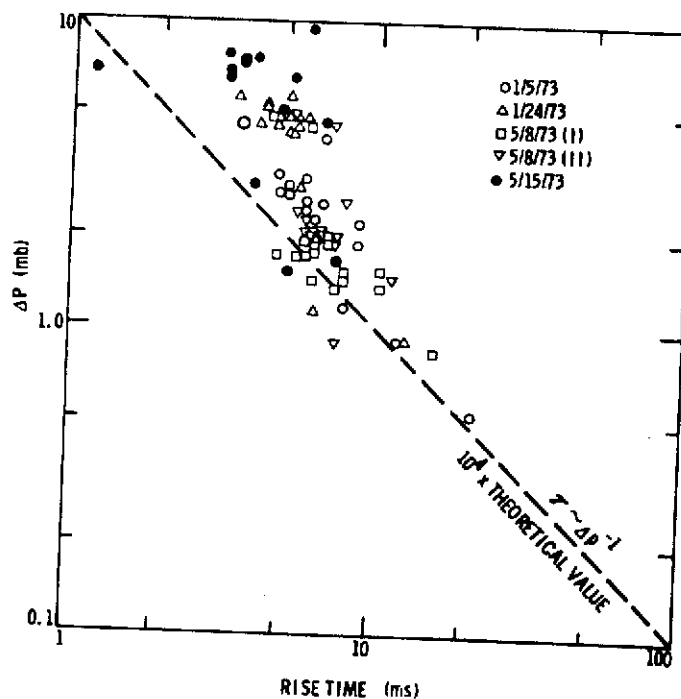


Figure 22. Compression Rise Time Observations, Calibration Shots

Rise times from sonic boom signatures (shown in Figure 23) generally follow the same pattern described by explosion waves from calibration shots. Since there are a number of cases of compression times of about 1 millisecond, it would appear that these same gages have more than adequate response characteristics for recording the vast bulk of data with 20-40 ms durations.

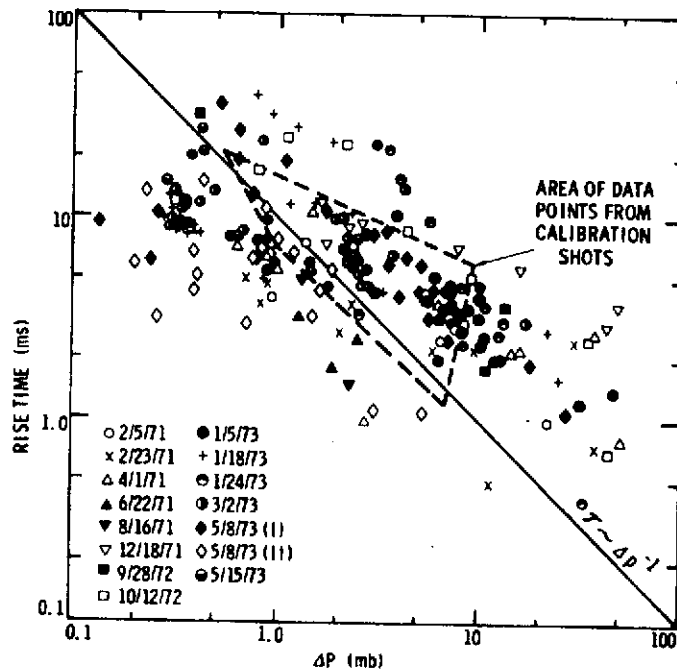


Figure 23. Rise Times From Sonic Boom Signatures

Further theoretical assessment is needed to explain these very slow observed compressions. According to the mechanisms set forth by Crow,<sup>16</sup> atmospheric microscale turbulence may cause attenuation of the high-frequency components of the sharp compression. Fwocs-Williams<sup>20</sup> has indicated that turbulence could only double shock thicknesses, not multiply them by several orders of magnitude. On the other hand, this thickening has been shown to be most pronounced in the boundary layer, a phenomenon that is contrary to any explanation based on relaxation times of the gaseous constituents. Again, it would be informative to make some measurements above ground level, possibly on the 15-m photographic towers 300 m from the track.

## Summary and Conclusions

Pressure measurements have been made at various distances, 60 m to 1 km, from 15 supersonic sled track tests. It is not clear from the results how annoying airblast noises have propagated northward into residential areas. Rocket ignition noise can cause an audible rumbling, and impact explosions may also be heard from large sled tests when there is strong atmospheric ducting and focusing (southerly upper winds). Sonic boom waves should not propagate northward from south-moving sleds, but they apparently do! Although the phenomenon is not understood at this time, it may be the mechanism for the reported disturbances.

A computer program has been prepared to take input break-switch times from the track and output sonic boom arrival times at specified gage locations. The calculations agree with observed arrival times, often within a few milliseconds, so there is good confidence in the associated analyses for such parameters as source points, Mach numbers, and wave paths. In particular, the caustic line, generated by accelerating supersonic vehicles, can be predicted within about  $\pm 30$  m at up to 1 km from the track. This range of error results from uncertainties in sled thrust and velocity, wind, and air temperature.

This small error did, however, give hope for measuring the airblast amplification or magnification which occurred in these caustics. A 12-gage mobile array was designed, built, and operated with pressure sensors at 15-m spacing on a line across predicted caustics from five tests. Results to date showing up to 2.87X magnification by the geometric wave focusing, do not reach the 9X obtained from aircraft flight experiments.

High confidence in these pressure measurements is assured by firing a 68-kg chemical high explosive, 20 seconds after sled tests, to give a relatively uniform (not focused) reference airblast on the gage array. A few instances of gage malfunction have thus been detected and corrected, so all final mobile gage data appear to be accurate within a few percent. This timely in situ dynamic calibration does not work with such confidence on the six hard-wire gages scattered over the test area because they are on different azimuths and thus their propagations may be differently affected by winds.

Measurements both of sonic booms and of explosion waves have shown that compression times are about 15,000 times as long as viscous shock theory predicts. This disparity may be a result of ground reflections, atmospheric turbulence attenuation, relaxation effects in the atmospheric constituents, or some combination of these. Further research is needed to explain the phenomenon, which may be the cause of the relatively low magnifications observed in the acceleration caustics.

Other results are that, (1) in accord with provided theory, boom overpressures appear to decrease proportionally to the  $-3/4$  power of distance perpendicular to vehicle path, and (2) overpressures do not clearly vary with the  $(M^2 - 1)^{1/8}$  that theory indicates.

Complete data tabulations have been assembled to become a basis for further analyses and theoretical evaluations as are needed to answer some serious questions about sonic booms and general airblast propagation.

## References

1. H. W. Carlson and D. J. Maglieri, "Review of Sonic-Boom Generation Theory and Prediction Methods," J. Acoust. Soc. of Amer., 51, 2 (part 3), February 1972.
2. W. D. Hayes, "Comments on the Caustic Problem," Third Conference on Sonic Boom Research, NASA SP-255, Washington, D.C., October 1970.
3. M. K. Myers and M. B. Friedman, Focusing of Supersonic Disturbances Generated by a Slender Body in a Nonhomogeneous Medium, Tech Report No. 40, Inst. Flight Structure, Columbia University, June 1966.
4. R. Seebass, "Sonic Boom Theory," J. Aircraft, 6, 3, 177-184, 1969.
5. L. W. Parker and R. G. Zalosh, Godunov Method and Computer Program to Determine the Pressure and Flow Field Associated With a Sonic Boom Focus, Mt. Auburn Research Assoc., Inc., NASA CR-2127, Washington, D.C., January 1973.
6. J. L. Wanner, J. Vallee, C. Vivier and C. Thery, "Theoretical and Experimental Studies of the Focus of Sonic Booms," J. Acoust. Soc. Amer., 52, 1 (Pt. 1), July 1972.
7. D. J. Maglieri, D. A. Hilton, V. Huckel, H. R. Henderson and N. J. McLeod, "Measurements of Sonic Boom Signatures from Flights at Cut-Off Mach Number," Third Conference on Sonic Boom Research, NASA SP-255, Washington, D.C., October 1970.
8. G. B. Whitham, "The Flow Pattern of a Supersonic Projectile," Comm. Pure and Appl. Math., 5, pp. 301-348, August 1952.
9. J. W. Reed, Microbarograph Measurements and Interpretations of B-58 Sonic Booms, SC-4634 (RR), Sandia Laboratories, December 1961.
10. J. W. M. DuMond, E. R. Cohen, W. K. H. Panofsky and E. Deeds, "A Determination of the Wave Forms and Laws of Propagation and Dissipation of Ballistic Shock Waves," J. Acoust. Soc. Amer., 18, No. 1, July 1946.
11. J. W. Reed, "Airblast Overpressure Decay at Long Ranges," J. Geophys. Res., 77, 9, March 20, 1972.
12. U. S. Department of Defense and Atomic Energy Commission, The Effects of Nuclear Weapons, Rev. Ed., S. Glasstone, editor, Washington, D.C., April 1962.
13. D. M. Maglieri, "Some Effects of Airplane Operations and the Atmosphere on Sonic Boom Signatures," J. Acoust. Soc. Amer., 39, 536-42, May 1966.
14. G. A. Herbert, W. A. Hass, and J. K. Angell, "A Preliminary Study of Atmospheric Effects on Sonic Boom," J. Appl. Meteor., 8, 618-626, 1969.
15. A. D. Pierce, "Spikes on Sonic Boom Pressure Waveform," J. Acoust. Soc. Amer., 44, 1052-1061, 1968.
16. S. C. Crow, "Distortion of Sonic Bangs by Atmospheric Turbulence," J. Fluid Mechanics, 37, 529-563, 1969.
17. B. H. K. Lee and H. S. Ribner, A Deterministic Model of Sonic Boom Propagation Through a Turbulent Atmosphere, National Aeronautical Establishment, Report LR-566 (NRC No. 12981), Ottawa, Canada, November 1972.
18. A. R. George and K. J. Plotkin, "Propagation of Weak Shock Waves Through Turbulence," Phys. Fluids, 14, 548-554, 1971.
19. K. J. Plotkin and A. R. George, "Propagation of Weak Shock Waves Through Turbulence," J. Fluid Mech., 54, 449-467, August 8, 1972.
20. J. E. F. Williams and M. S. Howe, "On the Possibility of Turbulent Thickening of Weak Shock Waves," J. Fluid Mech., 58, 461-480, 1973.
21. J. P. Hodgson, Vibrational Relaxation Effects in Weak Shock Waves in Air and the Structure of Sonic Bangs, Aero. Res. Council, Rep. No. 34, 1972.

Preceding page blank

# References (cont)

22. A. B. Bauer, "Sonic Boom and Turbulence Interactions - Laboratory Measurements Compared with Theory," Paper 71-618, AIAA 4th Fluid and Plasma Dynamics Conf., Palo Alto, California, June 1971.
23. B. Perkins, P. H. Lorrain and W. H. Townsend, Forecasting the Focus of Air Blasts Due to Meteorological Conditions in the Lower Atmosphere, Report No. 1118, Ballistic Research Laboratories, Aberdeen Proving Ground, Maryland, October 1960.
24. J. W. Reed, Explosion Wave Amplitude Statistics for a Caustic at Ranges of 30 to 45 Miles, SC-RR-67-860, Sandia Laboratories, February 1968.
25. J. W. Reed, Climatology of Airblast Propagations From Nevada Test Site Nuclear Airbursts, SC-RR-69-572, Sandia Laboratories, December 1969.
26. J. F. Goertner, Finite Amplitude Propagation of an Underwater Explosion Shock Wave Along a Strongly Refracted Ray Tube, NOLTR-71-139, U. S. Naval Ordnance Laboratory, Silver Spring, Md., December 1, 1971.
27. D. J. Maglieri and D. L. Lansing, Sonic Booms From Aircraft in Maneuvers, NASA-TN-D-2370, Washington, D.C., July 1964.
28. D. M. Maglieri and D. A. Hilton, Experiments on the Effects of Atmospheric Refraction and Airplane Acceleration on Sonic Boom Ground-Pressure Patterns, NASA-TN-D-3520, Washington, D.C., July 1966.
29. G. T. Haglund and E. J. Kane, Flight Test Measurements and Analysis of Sonic Boom Phenomena Near the Shock Wave Extremity, The Boeing Co., NASA CR 2167, Washington, D.C., February 1973.
30. J. H. Wiggins, Jr., Effects of Sonic Boom, J. H. Wiggins Co., Palos Verdes Estates, California, 1969.
31. H. C. Urey, "Cometary Collisions and Geological Periods," Nature, **242**, 32, March 2, 1973.
32. C. D. Broyles, IBM Problem M. Curves, Sandia Laboratories, SC-TM-268-56(51), December 1, 1956.

## APPENDIX

### TEST RESULTS AND DISCUSSIONS

Detailed results are included in the format and order, varied as necessary, of two tables and as many as five figures for each of the fifteen test events, as follows:

- Sonic Boom Test Calculation Summary (table)
- Sonic Boom Test Data Summary (table)
- Sonic Boom Pressures (figure)
- Impact Explosion Pressures (figure)
- Wave Propagation Paths (figure)
- Pressure Signatures, Fixed Array (figure)
- Pressure Signatures, Mobile Array (figure)

Most times were reported to the nearest millisecond, which can be easily read by comparison to the IRIG-B time code signal plotted on each record. Record playbacks were routinely produced at 25 cm/sec (10 in/sec), which allowed  $\pm 0.4$ -ms resolution from  $\pm 0.1$ -mm readings by optical comparator. The earliest tests were played back on a different oscillograph, however, and at 16 in/sec (40 cm/sec), allowing slightly more resolution. Compression rise time reports were made to 0.1 ms, but only  $\pm 0.4$ -ms resolution should be noted.

Certain abbreviations and symbols have been used as follows:

R	Rocket motor noises
B	Major sonic boom waves
T	Sonic boom waves emitted during transsonic acceleration
E	Explosion waves from vehicle impact
C	Calibration shot waves
-	Reading could not be made for any reason
$\Delta p^*$	Waves too small for separate positive and negative amplitude measurements or no negative phase occurred, so amplitude measurement was entered as an overpressure.
N.R.	No roots calculated for signal at the station; thus, in "silent" zone.
No Sig or No S/N	No signal or no signal above ambient noise level
INOP	Equipment inoperative

#### 2/5/71 Test

Computer inputs with essential and representative outputs are listed in Table A-I. All pressure measurements are recorded in Table A-II. Figures A-1 and A-2 show pressures from sonic boom and impact explosion waves. Gage D was apparently malfunctioning or had an incorrect calibration, because all pressures from that gage were low by a factor of 3 or 4. Sonic boom pressures

from Gages C and F followed the  $y^{-3/4}$  slopes. Pressure decreased with distance in the impact wave faster than  $R^{-1.2}$ , but this could be expected with surface heating in midday and light winds. Also, pressures would be expected to be lower along the up-track direction to Gage C, but not nearly so low as recorded at Gage D. Various wave ray paths are mapped in Figure A-3, and pressure wave signatures are reproduced in Figure A-4.

#### 2/23/71 Test

Pertinent data are entered in Tables A-III and A-IV. Figures A-5 and A-6 show recorded pressures from sonic boom and impact explosion waves. All primary boom waves ("B" waves) generally conformed to the  $y^{-3/4}$  slope, even though source Mach numbers ranged from 2.2 to 4.1. Transsonic waves showed an appreciable increase in strength with increase in Mach number, in order D, C, F, G, E, as shown by the ray paths in Figure A-7. Erroneous values for Gage D in the previous test appeared to be corrected in accordance with B-wave values. Wave signatures are shown in Figure A-8.

Impact wave amplitudes up-track and upwind at D, C, and E were lower than those propagated perpendicular to F and G. The latter path was about crosswind and pressures followed the  $R^{-1.2}$  slope.

#### 4/1/71 Test

Pertinent data are entered in Tables A-V and A-VI. Boom pressures in Figure A-9 show good agreement with the  $y^{-3/4}$  slope, even with Mach number sources ranging from 2.5 to 4.8. Transsonic waves again showed an increase of strength with increasing Mach number; however, the amplitude at E was nearly twice as large as could be expected from the G value on nearly the same path.

Impact waves, shown in Figure A-10, showed relatively little directional effect, in spite of the NW 8 kt (4 m/s) wind which might have given larger pressures at F and G. Asymmetry in the impact explosion appeared to be rather random and unpredictable, even for a relatively high-speed impact. Wave propagation paths are mapped in Figure A-11, and recorded pressure signatures are reproduced in Figure A-12.

#### 6/22/71 Test

Results are shown in Tables A-VII and A-VIII and Figures A-13, 14, and 15. There was no impact on a target for this test. At the south end the track was turned up to send the sled on a ballistic trajectory and to a relatively soft landing.

Pressures at D were, once more, suspiciously low by comparison with F, as the two paths and source Mach numbers were nearly the same.



#### 8/6/71 Test

Results are shown in Tables A-IX and A-X and in Figures A-16 and 17. Again, there was no detectable impact wave from this test. Boom waves at D and F were in accord with the  $y^{-3/4}$  slope. Comparison with 6/22/71 results shows, for similar vehicle and trajectory sources, low pressures at F, so it is possible that the F values from the earlier test were erroneously high, rather than the D results being suspiciously low. Small, weak wave signatures from this test have not been reproduced.

#### 12/18/71 Test

Results are recorded in Tables A-XI and A-XII and displayed in Figures A-18 through A-21. Boom pressures showed that strong waves again followed the  $y^{-3/4}$  slope for C, D, F, and G gages, with source Mach numbers ranging only from 1.59 to 2.15. Waves at E, recorded in the calculated silence zone, were apparently scattered about 500 ft from calculated ray paths, and thus showed only a small-amplitude B-wave.

Impact explosion waves increased with angle away from the track, from a minimum toward C, to medium values on the NNE line through D and E and to largest values perpendicular and east to F and G.

#### 9/28/72 Test

Results are recorded in Tables A-XIII and A-XIV and displayed in Figures A-22 through A-25. This sled was ignited at  $x = 3200$  ft (1 km) so that booms were calculated only for Gage D. Boom pressures showed that a weak wave was scattered into the silent zone at F. The wave signature at D showed the transsonic T-wave followed immediately behind the B-wave, and higher pressures were obtained from this second wave.

Impact waves propagated NNE to D and E, and appeared to obey the  $R^{-1.2}$  rule, as did waves at F and G on a bearing perpendicular to the track.

#### 10/12/72 Test

Results are shown in Tables A-XV and A-XVI and Figures A-26 through A-29. The fact that strong boom wave amplitudes at C, D, F, and G decreased in proportion to  $y^{-1}$  rather than  $y^{-3/4}$  may or may not be significant. Low pressures at E may be explained by location in the silent zone, north of calculated acoustic wave propagations. Transsonic waves at F and G were both very weak and hard to read with confidence, thus their relationship was not far out of line. Impact explosion waves gave fairly consistent values for the four NNE gage directions and the two east gage directions.

#### 1/5/73 Test

Results are shown in Tables A-XVII and A-XVIII and Figures A-30 through A-33. To save the sled hardware for repeated use this sled was designed to stop before impact. There was no impact explosion or wave.

Boom waves at C, E, and G followed the  $y^{-3/4}$  slope, and decelerating source waves propagated to F and D had successively lower relative intensities. Transsonic waves showed increased source strength, with increased source Mach number, in the correct order: D, C, F, G, E.

Extrapolation of amplitudes at C, E, and G, to  $y = 3000$  ft indicated that the free-field, unfocused amplitude at the mobile array should have been about 7.6 mb. The maximum (14.26 mb) recorded by Gage 6, thus gave a 1.88X focused magnification of amplitude. Similar extrapolation along  $y^{-3/4}$  of overpressure from 10.72 mb at E predicted 5.38 mb at the mobile array and thus a 1.99X focusing of overpressure.

#### 1/18/73 Test

Results are shown in Tables A-XIX and A-XX and Figures A-34 through A-38. Sonic boom pressures indicated a decrease in amplitude faster than  $y^{-3/4}$  between C and D, and F, G, and 12. The caustic passed south of the array, beyond mobile Gage 12, so there was no observation of caustic magnification. This special Lance instrument test had a somewhat different trajectory than previous Lance events, but this was not found out in time to move the mobile gages. Small amplitudes recorded by E were waves diffracted or scattered into the silence zone. Calculated ray paths missed that station by about 500 ft. Transsonic source waves at D, F, and G showed a small increase in source strength with Mach number increases from 1.003 to 1.216. A transsonic wave at C could not be filtered out of rocket motor noise.

Impact explosion waves showed a relatively weak wave propagated up-track to D, C, E, and B. A stronger wave emitted normal to the track to F, G, and 1-12, followed the  $R^{-1.2}$  slope quite well.

#### 1/24/73 Test

Results are shown in Tables A-XXI and A-XXII and Figures A-39 through A-43. Boom pressures generally followed  $y^{-3/4}$  through C, D, F and G. At E, low pressures were observed in the silent zone, where, it was calculated, no acoustic rays would penetrate. Free-field amplitude at the mobile array, as extrapolated from closer gage data, was about 7.3 mb, so the maximum magnification at Gage 6 was 1.96. Similar estimation from overpressures, with an extrapolated free-field value of 5.8 mb, gives 2.18X maximum magnification at Gage 6.

The only unambiguous transsonic wave recorded was at F. At C, any T-wave was lost in rocket motor noise. At both D and G, arrivals came at nearly the same time as impact wave arrivals. This mixed wave amplitude at D seemed appropriate for either source, but the amplitude at G was much too large for a T-wave, so it was not plotted as a boom wave.

Impact explosion wave pressures again showed a relatively weak wave propagated up the track to D, C, E, and B. A stronger wave propagated eastward to F, G, and 1 through 12 showed increased amplitudes with increased azimuth bearing. Stations 10, 11, and 12 showed a rapid increase in pressures; this trend may or may not have continued south of the array.

### 3/2/73 Test

Results are shown in Tables A-XXIII and A-XXIV and Figures A-44 through A-48. We were unable to move the mobile array in time for this event and the caustic passed nearly 1000 ft north of Gage 1, as shown in Figure A-46. Boom pressures, shown in Figure A-44, indicated that source strength increased with a source Mach number from C-E at near Mach 2, to D-G at Mach 3.1, and to F at near Mach 3.3. On the other hand, mobile gage data averages agreed best with F while the source was at  $2.76 \leq M \leq 3.09$  and lower than the D or G sources.

The strength of the transsonic wave at C seemed anomalously high when compared to other results. It was also noted that the strength, as related by the  $y^{-3/4}$  line, of T-waves at E, F, G, and 1-12 was remarkably constant, while source Mach numbers increased from 1.03 at F to 1.32 at Gage 1.

Impact waves, shown in Figure A-45, at C, E, and B were the strongest yet in the up-track direction. Amplitude at D appeared somewhat low without reason. Cross-track propagation to F, G, and 1 through 12 was weaker than waves from other impacts. The south wind,  $200^\circ/8$  kts, would not seem sufficient to cause such a deviation from other impact wave propagation patterns. This impact and explosion must, therefore, have been appreciably different from others.

### 5/8/73 Test (Recruit)

Results are shown in Tables A-XXV and A-XXVI and Figures A-49 through A-53. Since sonic boom amplitudes at C were high when compared to D, E, and G, an extrapolation to free-field amplitude at the mobile array was assumed to give 3.7 mb. This led to 2.21X magnification at Gage 9, and 125 ft south of the middle of the array. Transsonic wave source strengths, related to  $y^{-3/4}$ , increased monotonically with source Mach number in correct order of D, C, F, G, and E for Mach numbers increasing from 1.001 to 1.099.

Impact explosion waves from this small rocket vehicle were quite weak. They do not show very large directionality effects, with the northward propagation amplitudes at D and B about 2/3 as large as the NE and east propagations to F, G, and 1 through 12.

### 5/8/73 Test (Roadrunner)

Results are shown in Tables A-XXVII and A-XXVIII and Figures A-54 through A-57. Sonic booms at C and E were used to extrapolate a free-field amplitude of 1.00 mb at  $y = 3000$  ft. This yielded a magnification maximum at Gage 5 of 2.87X. Overpressures extrapolated to 0.70 mb, giving 2.72X maximum magnification. Despite the fact that source Mach number for the F wave was 3.28, amplitudes at D, F, and G showed decreasing values with vehicle deceleration and decreasing source Mach number along the lower end of the track. This small vehicle did not generate transsonic waves sufficiently large to be detected on fixed array records. South of the caustic, on the mobile array, four data points, from 9 through 12, showed slightly decreasing amplitudes as the source Mach number dropped from 1.76 to 1.66.

The impact explosion wave was not measurable on any gage record but a very slight ripple appeared on the records near the estimated arrival time.

#### 5/15/73 Test

Results are shown in Tables A-XXIX and A-XXX, and Figures A-58 through A-62. This vehicle was only accelerated to about  $M = 1.5$  and was beginning to decelerate about the time of wave emissions toward D, F, and 1 through 12. Although source Mach numbers for D and F were the same the relatively lower pressure at F may be an indication of a diverging wave front, convex to the south. In either case, extrapolation from D and F, to an amplitude at 3000 ft offset, showed only weak focusing in the caustic. Use of D for reference gave 1.57X magnification at Gage 7. Overpressures at D and F were in agreement with the  $y^{-3/4}$  line, and a resultant extrapolation gives 1.27X magnification at Gage 7.

A relatively low amplitude recorded at C again illustrated weakened propagation into a silence zone, although this station was probably missed by less than 100 ft by transsonic wave rays propagated toward F. It is not clear why there was no indication of a scattered wave shown on the G recording. Only D obtained a measurable transsonic wave.

Weak impact explosion waves from this small vehicle were small up-track to D and B and somewhat larger on a perpendicular toward F and G. Calibration shot waves were too strong for good recording with the sensors used. In future tests with the mobile array in the south field, the calibration shot should be moved south about 1500 ft.

TABLE A-I. SONIC BOOM TEST CALCULATION SUMMARY

SLED: 20° Poly 2 St. DATE: 2/5/71 TIME: MSG. M. T.  
 $V = -22,322 + 50,635 t - 41,885 t^2 + 15,095 t^3 - 1908.9 t^4$

PRESSURE MSG. mb  
 TEMP. 45 °F  
 WIND calm / 0 Kts

SOUND PROPAGATIONS		TRAJECTORY DATA				CAUSTIC COORDINATES		MACH NO.		
		X(ft)	t(sec)	V(fps)	A(fps <sup>2</sup> )	X <sub>F</sub> (ft)	Y <sub>F</sub> (ft)	M	V(fps)	X(ft)
C: 1102.44 fps										
Sound Velocity		825	1.936	1436	2783	1471	481		1.000	1102
Along Track:		1650	2.307	2842	4643	1847	1043	Max	5.058	4794
V(180): 1102.44 fps		3400	2.760	4966	3858	2205	1652			
		4217	2.925	5461	1967	2656	2542			
		5000	3.064	5571	-535	3854	5522			

BOOM "B" WAVES								TRANSSONIC "T" WAVES				
GAGE	X	Y	t <sub>o</sub> (sec)	X <sub>o</sub> (ft)	M	R(ft)	t <sub>a</sub> (sec)	t <sub>o</sub> (sec)	X <sub>o</sub> (ft)	M	R(ft)	t <sub>a</sub> (sec)
C	2560	200	2.568	2504	3.731	208	2.757	1.800	653	1.005	1918	3.539
D	4260	200	2.921	4219	4.946	204	3.106	1.797	650	1.002	3615	5.076
E	2504	1000	2.489	2194	3.379	1047	3.439	1.871	737	1.149	2030	3.712
F	4840	1000	2.997	4638	5.044	1020	3.922	1.812	666	1.028	4292	5.705
G	4840	1967	2.962	4444	5.010	1983	4.760	1.850	711	1.105	4563	5.989

TABLE A-II. SONIC BOOM TEST DATA SUMMARY

SLED: 20° Poly 2 St.      DATE: 2/5/71      TIME: MSG. M.S.T.

	STATION (FIXED)					
	B <sup>(1)</sup>	C	D	E <sup>(1)</sup>	F	G <sup>(1)</sup>
X(ft)	100	2560	4260	2504	4840	4840
Y(ft)	985	200	200	1000	1000	1967
BOOM WAVE						
Obs. Arrival (sec)		2.760	3.111		3.895	
Calc. Arrival (sec)		2.757	3.106		3.922	
Rise Time (ms)		1.0	3.0		2.5	
+ Phase (ms)		9.25	7.75		12.0	
Ph. Length (ms)		14.25	16.75		23.0	
$\Delta P$ (+) (mb)		21.98	7.63		6.50	
Pk (mb)		32.51	12.14		10.79	
TRANSSONIC WAVE						
Obs. Arrival (sec)		3.534	5.058		5.687	
Calc. Arrival (sec)		3.539	5.076		5.705	
Rise Time (ms)		3.0	7.5		7.5	
+ Phase (ms)		33.0	44.0		40.0	
Ph. Length (ms)		62.0	75.0		80.0	
$\Delta P$ (+) (mb)		8.36	1.40		2.45	
Pk (mb)		19.50	2.80		5.21	
IMPACT WAVE						
Arrival (sec)		5.280	3.759		3.942	
Rise Time (ms)		4.0	6.25		3.5	
+ Phase (ms)		25.0	12.5		24.25	
Ph. Length (ms)		---	25.0 *		70.0	
$\Delta P$ (+) (mb)		1.39	2.02		5.21	
Pk (mb)		1.39	2.02		7.30	

REMARKS: (1) Stations B, E, G not yet operative.

TABLE A-III. SONIC BOOM TEST CALCULATION SUMMARY

SLED: 2LJ + 3GILA-4 2 St. DATE: 2/23/71 TIME: 1145 M.S.T.  
 $V = 710.1 + 2215 t - 2053 t^2 + 3619 t^3 - 1408 t^4$

PRESSURE 837 mb  
 TEMP. 41 °F  
 WIND 330°/3 Kts

SOUND PROPAGATIONS	TRAJECTORY DATA				CAUSTIC COORDINATES		MACH NO. M		
C: 1098.00 fps	X(ft)	t(sec)	V(fps)	A(fps <sup>2</sup> )	X <sub>F</sub> (ft)	Y <sub>F</sub> (ft)			
Sound Velocity	1000	0.206	1108	1781	Not calculated		1.000	1102	975
Along Track:	2000	0.802	2450	3000			Max 4.173	4600	5000
V(180): 1102.39 fps	3000	1.137	3541	3305					
	4000	1.391	4289	2356					
	5000	1.613	4600	209					

BOOM "B" WAVES								TRANSSONIC "T" WAVES				
GAGE	X	Y	t <sub>o</sub> (sec)	X <sub>o</sub> (ft)	M	R(ft)	t <sub>a</sub> (sec)	t <sub>o</sub> (sec)	X <sub>o</sub> (ft)	M	R(ft)	t <sub>a</sub> (sec)
C	2560	200	0.979	2481	2.733	215	1.174	0.208	980	1.008	1593	1.652
D	4260	200	1.439	4208	3.986	207	1.627	0.204	976	1.002	3290	3.188
E	2504	1000	0.803	2001	2.225	1119	1.818	0.354	1161	1.247	1674	1.871
F	4840	1000	1.524	4589	4.113	1031	2.460	0.223	998	1.033	3970	3.823
G	4840	1967	1.470	4343	4.038	2005	3.290	0.280	1065	1.125	4248	4.129



TABLE A-IV. SONIC BOOM TEST DATA SUMMARY

SLED: LJ-GILA 2 St. DATE: 2/23/71 TIME: 1145 M.S.T.

	STATION (FIXED)					
	B <sup>(1)</sup>	C	D	E	F	G
X(ft)	100	2560	4260	2504	4840	4840
Y(ft)	985	200	200	1000	1000	1967
BOOM WAVE						
Obs. Arrival (sec)		1.170	1.618	1.833	2.453	3.283
Calc. Arrival (sec)		1.174	1.627	1.818	2.460	3.290
Rise Time (ms)		0.74	2.47	0.49	2.25	2.25
+ Phase (ms)		13.58	13.34	19.51	17.75	22.25
Ph. Length (ms)		16.55	21.49	22.97	43.0	50.75
$\Delta P$ (+) (mb)		38.11	29.74	11.30	9.49	5.19
Pk (mb)		48.31	43.92	12.82	14.74	8.15
TRANSSONIC WAVE						
Obs. Arrival (sec)		1.641	3.179	1.886	3.822	4.122
Calc. Arrival (sec)		1.652	3.188	1.871	3.823	4.129
Rise Time (ms)		2.72	5.0	3.75	4.75	3.75
+ Phase (ms)		24.7	30.0	33.0	28.75	30.0
Ph. Length (ms)		95.6	87.5	57.5	91.2	2.5
$\Delta P$ (+) (mb)		2.04	0.70	2.36	0.89	0.82
Pk (mb)		4.59	1.93	3.26	1.65	1.48
IMPACT WAVE						
			(2)			
Arrival (sec)		3.861	2.317	4.050	2.521	3.372
Rise Time (ms)		5.75	3.0	3.75	4.25	4.50
+ Phase (ms)		---	17.5	---	28.0	30.25
Ph. Length (ms)		---	35.0	36.0	58.0	62.0
$\Delta P$ (+) (mb)		0.85 *	2.28	0.76	4.68	2.45
Pk (mb)		0.85	3.85	0.97	6.90	3.48

REMARKS: (1) Inoperative

(2) At Station D, a nearly identical impact wave recorded at 2.364 sec.

TABLE A-V. SONIC BOOM TEST CALCULATION SUMMARY

SLED: US-3 + 7 JAV 90c 2 St. DATE: 4/1/71 TIME: 1200 M. S. T.  
 $V = -2285 + 8976 t - 9323 t^2 + 4660 t^3 - 733.4 t^4$

PRESSURE 851 mb  
 TEMP. 52 °F  
 WIND. 304°/8 Kts

SOUND PROPAGATIONS		TRAJECTORY DATA				CAUSTIC COORDINATES		MACH NO. M V(fps) X(ft)		
C: 1110.22 fps		X(ft)	t(sec)	V(fps)	A(fps <sup>2</sup> )	X <sub>F</sub> (ft)	Y <sub>F</sub> (ft)			
Sound Velocity		1000	1.201	1594	1663	1961	750	1.000	1118	559
Along Track:		2000	1.668	2695	3152	2442	1419	Max 5.074	5672	5018
V(180): 1117.78 fps		3000	1.981	3840	4090	2840	2075			
		4000	2.233	4918	4378	4174	4808			
		4900	2.408	5672	4171	4722	6174			

BOOM "B" WAVES								TRANSSONIC "T" WAVES				
GAGE	X	Y	t <sub>o</sub> (sec)	X <sub>o</sub> (ft)	M	R(ft)	t <sub>a</sub> (sec)	t <sub>o</sub> (sec)	X <sub>o</sub> (ft)	M	R(ft)	t <sub>a</sub> (sec)
C	2650	200	1.840	2488	2.942	213	2.030	0.876	560	1.005	2010	2.672
D	4260	200	2.258	4214	4.497	205	2.441	0.873	557	1.001	3708	4.188
E	2504	1000	1.703	2070	2.512	1090	2.673	0.988	695	2.512	1090	2.673
F	4840	1000	2.337	4627	4.806	1022	3.248	0.893	581	1.027	4375	4.799
G	4840	1967	2.297	4412	4.648	1990	4.069	0.955	654	1.102	4615	5.069

TABLE A-VI. SONIC BOOM TEST DATA SUMMARY

SLED: US-JAV 2 St. DATE: 4/1/71 TIME: 1200 M. S. T.

	STATION (FIXED)					
	B <sup>(1)</sup>	C	D	E	F	G
X(ft)	100	2560	4260	2504	4840	4840
Y(ft)	985	200	200	1000	1000	1967
BOOM WAVE						
Obs. Arrival (sec)		2.016	2.441	2.668	3.250	4.064
Calc. Arrival (sec)		2.030	2.441	2.673	3.248	4.069
Rise Time (ms)		0.8	2.7	2.2	2.2	3.7
+ Phase (ms)		29.8	23.3	40.0	38.0	36.7
Ph. Length (ms)		---	84.6	---	---	---
$\Delta P$ (+) (mb)		50.47	36.63	16.06	14.92	6.52
Pk (mb)		56.24	43.64	18.28	16.88	8.58
TRANSSONIC WAVE						
Obs. Arrival (sec)		2.564	4.062	2.788	4.665	5.024
Calc. Arrival (sec)		2.672	4.138	2.830	4.799	5.069
Rise Time (ms)		1.0	5.7	10.7	7.4	7.2
+ Phase (ms)		21.1	17.1	32.6	19.6	32.0
Ph. Length (ms)		---	---	66.5	---	65.0
$\Delta P$ (+) (mb)		2.82	1.00	1.51	0.93	0.63
Pk (mb)		2.82	1.00	2.88	0.93	1.03
IMPACT WAVE						
Arrival (sec)		4.676	3.129	4.852	3.389	4.221
Rise Time (ms)		12	7.9	7.4	2.5	5.0
+ Phase (ms)		25	17.1	32.8	---	---
Ph. Length (ms)			54.3	---	---	---
$\Delta P$ (+) (mb)			1.86	0.47	1.65	1.26
Pk (mb)		0.81	3.58	0.90	1.65	1.26

MOTOR NOISE

Time (sec)	3.385	4.918
$\Delta P$ (+) (mb)	0.47	0.80*
Pk (mb)	0.85	0.80
Freq. (Hz)	36	53

OTHER WAVES

Time (sec)	No Sig.	3.006	4.755	3.296	4.125
Rise Time (ms)		5.7	---	14.4	9.5
+ Phase (ms)		14.1	---	46.4	67.8
Ph. Length (ms)		25.4	---	110.2	163.8
$\Delta P$ (+) (mb)		0.57*	0.24*	4.94	2.98
Pk (mb)		0.57	0.24	9.21	5.49
SOURCE	EXPLOSIVE TARGET @ X = 4900 ft.				

REMARKS: (1) Erratic Signal Channel, Station F.



TABLE A-VIII. SONIC BOOM TEST DATA SUMMARY

SLED: KIVA TUBE    DATE: 6/22/71    TIME: 1122 M.D.T.

	STATION (FIXED)					
	B <sup>(1)</sup>	C	D	E	F	G <sup>(2)</sup>
X(ft)	100	2560	4260	2504	4840	4840
Y(ft)	985	200	200	1000	1000	1967
BOOM WAVE						
Obs. Arrival (sec)		No Sig.	5.553	No Sig.	6.406	
Calc. Arrival (sec)		None	5.551	None	6.404	None
Rise Time (ms)			1.8		2.5	
+ Phase (ms)			7.0		9.5	
Ph. Length (ms)			9.5		---	
$\Delta P$ (+) (mb)			1.89		2.54	
Pk (mb)			3.16		2.54	
TRANSSONIC WAVE						
Obs. Arrival (sec)			No Sig.		6.479	
Calc. Arrival (sec)			5.834		6.490	
Rise Time (ms)					3.2	
+ Phase (ms)					12.2	
Ph. Length (ms)					24.1	
$\Delta P$ (+) (mb)					1.27	
Pk (mb)					2.11	
IMPACT WAVE (NO TARGET IMPACT)						
MOTOR NOISE						
Time (sec)		4.363				
$\Delta P$ (+) (mb)		0.46				
Pk (mb)		0.74				
Freq. (Hz)		< 18				

REMARKS: (1) Erratic Signal Channel, Station B.  
 (2) Station G Inoperative.





TABLE A-X. SONIC BOOM TEST DATA SUMMARY

SLED: MSG.      DATE: 8/16/71      TIME: 1500 M.D.T.

	STATION (FIXED)					
	B	C	D	E	F	G
X(ft)	100	2560	4260	2504	4840	4840
Y(ft)	985	200	200	1000	1000	1967
BOOM WAVE	INOP.					INOP.
Obs. Arrival (sec)	No Sig.		5.455	No Sig.		6.313
Calc. Arrival (sec)			5.470			6.322
Rise Time (ms)			1.5			5.0
+ Phase (ms)			9.2			29.9
Ph. Length (ms)			---			---
$\Delta P$ (+) (mb)			2.268			1.303 *
Pk (mb)			3.528			1.303
TRANSSONIC WAVE						
Obs. Arrival (sec)			No S/N			6.406
Calc. Arrival (sec)			5.704			6.373
Rise Time (ms)						---
+ Phase (ms)						---
Ph. Length (ms)						22.4
$\Delta P$ (+) (mb)						0.890 *
Pk (mb)						0.890
IMPACT WAVE						
Arrival (sec)	(7.9)		(6.4)			(6.6)
Rise Time (ms)	No S/N		No S/N			No S/N
+ Phase (ms)						
Ph. Length						
$\Delta P$ (+) (mb)						
Pk (mb)						
MOTOR NOISE						
Time (sec)	4.284					
$\Delta P$ (+) (mb)	---					
Pk (mb)	0.834					
Freq. (Hz)	57					

TABLE A-XI. SONIC BOOM TEST CALCULATION SUMMARY

SLED: LANCE-585    DATE: 12/18/71    TIME: 1450 M. S. T.  
 $V = 1494 - 2344 t + 1651 t^2 + 374.0 t^3 + 30.25 t^4$

PRESSURE 845 mb  
 TEMP. 33 °F  
 WIND 350°/2 Kts

SOUND PROPAGATIONS	TRAJECTORY DATA				CAUSTIC COORDINATES		MACH NO. M	V(fps)	x(ft)
	X(ft)	t(sec)	V(fps)	A(fps <sup>2</sup> )	X <sub>F</sub> (ft)	Y <sub>F</sub> (ft)			
C: 1089.11 fps							1.000	1096	1194
Sound Velocity	1000	2.076	959	758	2914	468	Max 2.323	2546	4982
Along Track:	2000	2.850	1562	754	3567	1264			
V(180): 1095.76 fps	3000	3.417	1964	666	5236	3287			
	4000	3.888	2269	645	6167	4553			
	5000	4.302	2549	730	6991	5752			

BOOM "B" WAVES								TRANSSONIC "T" WAVES				
GAGE	X	Y	t <sub>o</sub> (sec)	x <sub>o</sub> (ft)	M	R(ft)	t <sub>a</sub> (sec)	t <sub>o</sub> (sec)	x <sub>o</sub> (ft)	M	R(ft)	t <sub>a</sub> (sec)
C	2560	200	3.091	2398	1.587	258	3.327	2.269	1222	1.011	1353	3.503
D	4260	200	3.955	4152	2.110	227	4.163	2.256	1208	1.002	3058	5.047
E	2504	1000	No Roots									
F	4840	1000	4.025	4315	2.152	1129	5.058	2.307	1265	1.038	3712	5.694
G	4840	1967	3.761	3715	1.996	2245	5.814	2.466	1456	1.153	3902	6.028

TABLE A-XII. SONIC BOOM TEST DATA SUMMARY

SLED: LANCE-585 2 St.      DATE: 12/18/71      TIME: 1450 M.S.T.

	STATION (FIXED)					
	B	C	D	E	F	G
X(ft)	100	2560	4260	2504	4840	4840
Y(ft)	985	200	200	1000	1000	1967
BOOM WAVE						
Obs. Arrival (sec)		3.318	4.147	3.666	5.042	5.797
Calc. Arrival (sec)		3.327	4.163	N/R	5.058	5.814
Rise Time (ms)		2.9	3.8	9.4	5.7	7.2
+ Phase (ms)		15.4	14.1	---	22.1	27.3
Ph. Length (ms)		23.8	22.1	58.1	32.2	38.5
$\Delta P$ (+) (mb)		43.39	49.14	2.61	15.71	8.83
Pk (mb)		61.22	64.75	3.26	17.42	8.83
TRANSSONIC WAVE						
		(1)			(2)	(3)
Obs. Arrival (sec)		3.479	5.016	3.931	5.660	Unk.
Calc. Arrival (sec)		3.503	5.047	N/R	5.694	6.028
Rise Time (ms)		---	9	7.4	12	
+ Phase (ms)		---	---	12	32	
Ph. Length (ms)		15	---	25	50	
$\Delta P$ (+) (mb)		9.32*	2.30	1.74*	1.60	
Pk (mb)		9.32	2.30	1.74	2.14	
IMPACT WAVE						
						(3)
Arrival (sec)		6.609	5.064	6.796	5.240	6.073
Rise Time (ms)		12	5	10.2	7.4	23.8
+ Phase (ms)		---	17	25	26.8	59.6
Ph. Length (ms)		---	46	54	60.1	86.4
$\Delta P$ (+) (mb)		0.532*	4.35	0.869	7.59	5.49
Pk (mb)		0.532	6.91	1.303	14.00	7.86
MOTOR NOISE						
Time (sec)		3.679				
$\Delta P$ (+) (mb)		Limited				
Pk (mb)		> 3.9				
Freq. (Hz)		---				

REMARKS: (1) Signal embedded in engine noise.  
 (2) Two similar cycles in sequence.  
 (3) Interfering arrivals of "T" & impact waves plus engine noise.



TABLE A-XIV. SONIC BOOM TEST DATA SUMMARY

SLED: HYB 90° HALF SCALE      DATE: 9/28/72      TIME: 1103 M.D.T.

	STATION (FIXED)					
	B	C	D	E	F	G
X(ft)	100	2560	4260	2504	4840	4840
Y(ft)	985	200	200	1000	1000	1967
BOOM WAVE	INOP.	INOP.		NO SIG.		NO SIG.
Obs. Arrival (sec)			1.463		2.30	
Calc. Arrival (sec)			1.469	N.R.	N.R.	N.R.
Rise Time (ms)			1.8		32	
+ Phase (ms)			6.2		---	
Ph. Length (ms)			---		---	
$\Delta P$ (+) (mb)			10.86		.412	
Pk (mb)			14.04		.412	
TRANSSONIC WAVE						
Obs. Arrival (sec)			1.473			
Calc. Arrival (sec)			1.473	N.R.	N.R.	N.R.
Rise Time (ms)			3.7			
+ Phase (ms)			9.2			
Ph. Length (ms)			11.7			
$\Delta P$ (+) (mb)			13.51			
Pk (mb)			15.90			
IMPACT WAVE						
Arrival (sec)			2.481	4.130	2.666	3.471
Rise Time (ms)			---	8.0	2.5	4.7
+ Phase (ms)			11	16.2	10.5	12.2
Ph. Length (ms)			---	25	20.9	23.5
$\Delta P$ (+) (mb)			2.12	.479*	2.47	1.47
Pk (mb)			2.92	.479	4.53	2.53
MOTOR NOISE						
Time (sec)				1.110	2.413	3.240
$\Delta P$ (+) (mb)				1.72	2.26*	.842*
Pk (mb)				1.72	2.26	.842
Freq. (Hz)				29	131	103

TABLE A-XV. SONIC BOOM TEST CALCULATION SUMMARY

SLED: LANCE LZ4/STU-12 DATE: 10/12/72 TIME: 1642 M.D.T.

$$V = -2086 + 4656 t - 2898 t^2 + 864.8 t^3 - 89.98 t^4$$

 PRESSURE 852 mb  
 TEMP. 78 °F  
 WIND 180°/6 Kts

SOUND PROPAGATIONS	TRAJECTORY DATA				CAUSTIC COORDINATES		MACH NO.	V(fps)	X(ft)
	X(ft)	t(sec)	V(fps)	A(fps <sup>2</sup> )	X <sub>F</sub> (ft)	Y <sub>F</sub> (ft)	M		
C: 1139.11 fps							1.000	1129	990
Sound Velocity	1000	2.050	1143	577	3276	102	Max	2.202	4647
Along Track:	2000	2.764	1655	857	3349	436			
V(180): 1128.98 fps	3000	3.295	2125	851	3741	1217			
	4000	3.734	2427	450	4140	1833			
	5000	4.133	2457	-391	5194	3352			

BOOM "B" WAVES								TRANSSONIC "T" WAVES				
GAGE	X	Y	t <sub>o</sub> (sec)	x <sub>o</sub> (ft)	M	R(ft)	t <sub>a</sub> (sec)	t <sub>o</sub> (sec)	x <sub>o</sub> (ft)	M	R(ft)	t <sub>a</sub> (sec)
C	2560	200	2.994	2404	1.628	253	3.218	2.065	1031	1.009	1542	3.431
D	4260	200	3.794	4155	2.148	226	3.993	2.052	1017	1.002	3250	4.931
E	2504	1000	N.R.									
F	4840	1000	3.861	4319	2.165	1127	4.854	2.116	1091	1.035	3880	5.553
G	4840	1967	3.637	3777	2.083	2215	5.590	2.311	1332	1.143	4010	5.859

TABLE A-XVI. SONIC BOOM TEST DATA SUMMARY

SLED: LANCE LZ4/STU-12      DATE: 10/12/72      TIME: 1642 M.D.T.

	STATION (FIXED)					
	B	C	D	E	F	G
X(ft)	100	2560	4260	2504	4840	4840
Y(ft)	985	200	200	1000	1000	1967
BOOM WAVE						
Obs. Arrival (sec)		3.207	3.979	3.683	4.841	5.581
Calc. Arrival (sec)		3.218	3.993	N.R.	4.854	5.590
Rise Time (ms)		2.5	0.7	23.4	5.0	8.5
+ Phase (ms)		15.4	14.9	182	89.6	120
Ph. Length (ms)		20.9	17.7	320	---	---
$\Delta P$ (+) (mb)		35.13	44.17	2.15	9.01	4.42
Pk (mb)		49.05	50.69	3.63	10.49	5.04
TRANSSONIC WAVE						
		NO S/N				
Obs. Arrival (sec)		~ 3.4	4.967	---	5.536	5.786
Calc. Arrival (sec)		3.431	4.931	N.R.	5.553	5.859
Rise Time (ms)		---	25		17	12
+ Phase (ms)		---	---		54	---
Ph. Length (ms)		---	---		98	---
$\Delta P$ (+) (mb)		---	1.09		.79*	.31
Pk (mb)		$\leq 13.5$	1.45		.79	.31
IMPACT WAVE						
Arrival (sec)	8.503	6.280	4.819	6.469	5.102	5.831
Rise Time (ms)	17.4	10.4	18.2	14.4	5.0	10.0
+ Phase (ms)	33.8	25.1	35	32.8	32.8	43.3
Ph. Length (ms)	50.5	46.0 *	50	48.3	76.6	93
$\Delta P$ (+) (mb)	.217	1.01	3.44	0.92	6.53	3.39
Pk (mb)	.320	1.01	4.34	1.34	11.78	6.27
MOTOR NOISE						
Time (sec)	0.913	2.595		2.745		
$\Delta P$ (+) (mb)	0.56	.67		0.35*		
Pk (mb)	0.56	.67		0.35		
Freq. (Hz)	2.4	6.2		8.0		
Time (sec)	2.215			3.449		
Pk (mb)	1.28			.635		
Freq. (Hz)	5.2			12		



TABLE A-XVII. SONIC BOOM TEST CALCULATION SUMMARY

SLED: BOOM TEST SPECIAL DATE: 1/5/73 TIME: 1141 M.S.T.  
 $V = 174.7 + 53.48 t + 3205 t^2 - 2132 t^3 + 361.5 t^4$

PRESSURE 843 mb  
 TEMP. 40 °F  
 WIND 300°/15 Kts

SOUND PROPAGATIONS			TRAJECTORY DATA				CAUSTIC COORDINATES		MACH NO. M			V(fps)	X(ft)	
C: 1096.89 fps			X(ft)	t(sec)	V(fps)	A(fps <sup>2</sup> )	X <sub>F</sub> (ft)	Y <sub>F</sub> (ft)						
Sound Velocity			244	1.400	2070	460	1306	392			Max	1.000	1110	423
Along Track:			1570	1.610	2100	-170	1891	1048				1.897	2105	1949
V(180): 1109.56 fps			2050	2.330	1387	-1440	2685	2038						
			3350	2.530	1112	-1248	3553	3228						
			3600	0.500	759	1840	4782	5029						

BOOM "B" WAVES								TRANSSONIC "T" WAVES				
GAGE	X	Y	t <sub>o</sub> (sec)	X <sub>o</sub> (ft)	M	R(ft)	t <sub>a</sub> (sec)	t <sub>o</sub> (sec)	X <sub>o</sub> (ft)	M	R(ft)	t <sub>a</sub> (sec)
C	2560	200	1.788	2429	1.825	239	2.001	0.688	422	1.004	2147	2.619
D	4260	200	2.495	3582	1.043	707	3.129	0.686	420	1.001	3845	4.148
E	2504	1000	1.526	1883	1.896	1177	2.575	0.754	500	1.118	2239	2.757
F	4840	1000	2.354	3405	1.219	1749	3.916	0.700	436	1.025	4516	4.754
G	4840	1967	2.140	3084	1.491	2619	4.476	0.741	484	1.095	4770	5.009
1	3245	3000	N.R.									
2	3300	3000	N.R.									
3	3355	3000	1.233	1282	1.759	3647	4.482	1.128	1083	1.656	3763	4.482
4	3410	3000	1.307	1430	1.816	3594	4.510	Single Root in Caustic				
5	3465	3000	1.356	1530	1.845	3570	4.538	1.035	919	1.545	3935	4.543
6	3520	3000	1.397	1613	1.864	3555	4.565	1.011	877	1.513	3998	4.575
7	3575	3000						*				
8	3630	3000	1.465	1755	1.887	3538	4.617	0.973	815	1.462	4114	4.641
9	3685	3000						*				
10	3740	3000	1.523	1878	1.896	3531	4.670	0.946	771	1.422	4221	4.710
11	3795	3000						*				
12	3850	3000	1.576	1988	1.896	3531	4.722	0.923	736	1.389	4324	4.780

\* Details calculated but not transcribed to this summary.

TABLE A-XVIII. SONIC BOOM TEST DATA SUMMARY

SLED: BOOM TEST SPECIAL DATE: 1/5/73 TIME 1411 M.S.T.

	STATION (FIXED)							(MOBILE)											
	B	C	D	E	F	G	I	J	K	L	M	N	O	P	Q	R	S	T	U
X(ft)	100	2560	4260	7504	4840	4840	3245	3300	3355	3410	3465	3520	3575	3630	3685	3740	3795	3850	
Y(ft)	985	200	200	1000	1000	1767	3000												3000
BOOM WAVE																			
Obs. Arrival (sec)		2.012	3.179	2.612	3.761	4.404	4.469	4.498	4.529	4.559	4.587	4.615	4.642	4.669	4.696	4.721	4.747	4.772	
Calc. Arrival (sec)		2.001	3.120	2.575	3.916	4.476	N.R.	N.R.	4.482	4.510	4.538	4.565	4.591	4.617	4.644	4.670	4.696	4.722	
Rise Time (ms)		1.2	2.4	2.0	3.2	4.0	8.7	10.3	5.2	3.6	3.2	2.6	4.0	3.0	3.2	4.4	4.4	3.6	
+ Phase (ms)		12.7	23.4	20	25.0	34.6	30.9	27.3	23.8	20.6	21.0	21.8	23.0	25.0	29.7	30.5	23.0	26.9	
Ph. Length (ms)		24.6	51.5	31	57.3	59	46.4	47.5	46.4	44.8	46.8	46.0	44.8	42.4	44.0	43.6	44.4	42.8	
AP (+) (mb)		31.74	10.05	12.27	6.32	5.61	2.81	3.91	6.10	8.51	11.52	13.01	14.26	12.78	11.33	10.47	8.48	8.09	8.28
Pk (mb)		52.65	18.42	16.60	11.65	10.08	3.79	5.31	8.51	11.52	13.01	14.26	12.78	11.33	10.47	8.48	8.09	8.28	
TRANS-SONIC WAVE																			
							(NONE) →												
Obs. Arrival (sec)		2.619	4.132	2.765	4.766	5.005													
Calc. Arrival (sec)		2.619	4.148	2.757	4.754	5.009													
Rise Time (ms)		-	26	36	10	24													
+ Phase (ms)		-	38	59	26	-													
Ph. Length (ms)		41.2	61	82	50	68													
AP (+) (mb)		2.05	1.46*	1.61	1.74*	1.73*													
Pk (mb)		3.51	1.46	3.22	1.74	1.73													
CAL SHOT WAVE																			
Arrival (sec)	26.166	24.067	22.642	23.916	21.854	21.840	23.529	23.483	23.438	23.92	23.349	23.302	23.257	23.213	23.168	23.123	23.079	23.034	
Rise Time (ms)	21	8	8.7	12	6.7	3.6	8.7	6.3	6.3	5.9	6.7	5.9	5.2	4.8	5.9	5.2	4.8	4.8	
+ Phase (ms)	75	60	53	59	42	48	48.3	50.7	48.3	49.1	49.5	49.5	50.3	49.9	49.5	47.5	47.5	47.5	
Ph. Length (ms)	196	130	115	143	119	119	123	131	147	143	121	145	143	121	152	157	151	139	
AP (+) (mb)	0.53	1.17	1.88	0.91	4.09	4.59	2.18	2.27	2.27	2.46	2.55	2.58	2.74	2.76	3.06	2.88	3.17	3.18	
Pk (mb)	0.78	1.61	2.72	1.31	5.45	6.69	3.43	3.54	3.64	3.77	3.95	3.94	4.16	4.21	4.45	4.51	4.78	4.72	
MOTOR NOISE																			
Time (sec)	0.872																		
AP (+) (mb)	1.37																		
Pk (mb)	2.43																		
Freq. (Hz)	-																		

TABLE A-XIX. SONIC BOOM TEST CALCULATION SUMMARY

SLED: SMALL LANCE ; DATE: 1/18/73 TIME: Unk M. T.  
 $V = 67.34 + 190.6 t + 1657 t^2 - 1083 t^3 + 212.3 t^4$ .

PRESSURE	U	mb
TEMP.	<u>42</u>	°F
WIND	calm/0	Kts

SOUND PROPAGATIONS	TRAJECTORY DATA				CAUSTIC COORDINATES		MACH NO.		
	X(ft)	t(sec)	V(fps)	A(fps <sup>2</sup> )	X <sub>F</sub> (ft)	Y <sub>F</sub> (ft)	M	V(fps)	X(ft)
C: 1099.11 fps									
Sound Velocity	1216	0.200	163	730	3383	726			
Along Track:	1715	1.031	1078	1085	4014	1357	Max	1.000	1736
V(180): 1099.11 fps	2337	1.521	1517	705	4763	2142		2.715	5009
	4200	2.531	2323	1540	5623	3105			
	5009	2.840	2984	2857	7618	5617			

[illegible]

TABLE A-XX. SONIC BOOM TEST DATA SUMMARY

SLED: SMALL LANCE DATE: 1/18/73 TIME: UNX M.S.T.

STATION (FIXED)																		
	B	C	D	E	F	G	1	2	3	4	5	6	7	8	9	10	11	12
X(ft)	100	2560	4260	5904	4840	4840	4550	4600	4650	4700	4750	4800	4850	4900	4950	5000	5050	5100
Y(ft)	985	200	200	1000	1000	1067	3000											3000
BOOM WAVE																		
	(1)																	
Obs. Arrival (sec)		1.793	2.719	2.366	4.507	4.344	4.684	4.916	4.941	4.771	5.004	5.035	5.063	5.092	5.124	5.156	5.187	5.218
Calc. Arrival (sec)		1.779	2.702	N.R.	3.593	4.330	N.R.											
Rise Time (ms)		1.6	2.8	5	4.0	4.3	11	13	9.5	9.1	8.3	8.3	8.3	9.9	8.7	9.9	8.7	N.R.
+ Phase (ms)		11.5	7.5	0	1.5	2	20	24	17	19	20	20	20	20	24	24	24	24
Ph. Length (ms)		15.8	9.1	-	-	4	-	-	-	-	-	-	-	-	-	-	-	-
ΔP (+) (mb)		25.25	22.01	0.859	1.30	1.31	1.30	1.293	1.317	1.357	1.383	1.420	1.358	1.329	1.335	1.282	1.330	1.338
Pk (mb)		34.32	29.06	0.859	6.08	2.23	-	-	-	-	-	-	-	-	-	-	-	-
TRANS-SONIC WAVE																		
	(2)																	
Obs. Arrival (sec)	No S/N	3.354	1.603	4.017	4.418		5.018	5.035	5.060	5.084	5.105	5.134	5.163	5.188	5.216	5.239	5.263	5.286
Calc. Arrival (sec)	1.822	3.354	N.R.	4.018	4.339		N.R.											N.R.
Rise Time (ms)		10.6	13	12	11.8													
+ Phase (ms)		34.8	30	47	41		-120	-120	-120	120	95	87	79	71	40	32	28	24
Ph. Length		71	38	71	95						158	158	148	134	121	111	97	55
ΔP (+) (mb)		2.31	0.327	1.51	1.16		1.163	1.232	1.229	1.306	1.340	1.390	1.426	1.511	1.788	1.930	1.234	1.865
Pk (mb)		4.29	0.327	2.55	2.01		-	-	-	-	1.532	1.660	1.783	1.005	1.340	1.544	2.086	2.942
IMPACT WAVE																		
Arrival (sec)	7.339	5.074	3.545	5.260	3.763	4.604	5.589	5.583	5.576	5.569	5.565	5.561	5.559	5.555	5.554	5.553	5.552	5.551
Rise Time (ms)	8.7	6	4.0	6.3	3.6	5.1	6.3	7.1	7.5	7.5	6.3	7.5	6.7	6.7	7	7	8	8
+ Phase (ms)	18.2	-	11.1	-	13.4	18.2	18.6	19.4	19	22	21	21	22	21	23	21	20	22
Ph. Length (ms)	42	32	30	29	34	36	67	63	63	55	40	40	51	53	42	51	51	51
ΔP (+) (mb)	0.126	0.627*	1.98	0.532*	3.07	1.21	1.753	1.788	1.739	1.789	1.744	1.826	1.800	1.774	1.847	1.880	1.852	1.981
Pk (mb)	0.257	0.627	3.19	0.532	4.78	2.22	1.261	1.220	1.285	1.289	1.191	1.381	1.379	1.350	1.418	1.428	1.495	1.656
MOTOR NOISE																		
Time (sec)	1.342																	
ΔP (+) (mb)	2.90																	
Pk (mb)	3.84																	
Freq. (Hz)	12																	

REMARKS: (1) 41 ms gradual compression prior to strong shock arrival.

(2) Indefinite arrival time; time of peak pressure recorded for Gages 1-12.

TABLE A-XXI. SONIC BOOM CALCULATION SUMMARY

SLED: LANCE DATE: 1/24/73 TIME: 1541 M.S.T.  
 $V = -0.6968 + 197.9 t + 393.8 t^2 - 119.3 t^3 + 12.37 t^4$

PRESSURE 845 mb  
 TEMP. 46 °F  
 WIND 320°/6 Kts

SOUND PROPAGATIONS	TRAJECTORY DATA				CAUSTIC COORDINATES		MACH NO.		
	X(ft)	t(sec)	V(fps)	A(fps <sup>2</sup> )	X <sub>F</sub> (ft)	Y <sub>F</sub> (ft)	M	V(fps)	X(ft)
C: 1103.56 fps							1.000	1111	887
Sound Velocity	1000	1.960	1184	739	2897	698	Max 2.383	2648	4950
Along Track:	2000	2.674	1696	691	3713	1635			
V(180): 1111.32 fps	3000	3.210	2059	675	5297	3571			
	4000	3.657	2367	711	7072	6091			
	4950	4.032	2648	798	4845	3000			

BOOM "B" WAVES								TRANSSONIC "T" WAVES				
GAGE	X	Y	t <sub>0</sub> (sec)	X <sub>0</sub> (ft)	M	R(ft)	t <sub>a</sub> (sec)	t <sub>0</sub> (sec)	X <sub>0</sub> (ft)	M	R(ft)	t <sub>a</sub> (sec)
C	2560	200	2.888	2409	1.657	251	3.113	1.873	899	1.007	1673	3.37'
D	4260	200	3.712	4156	2.165	225	3.914	1.864	890	1.002	3376	4.901
E	2504	1000	N.R.					N.R.				
F	4840	1000	3.785	4333	2.213	1121	4.792	1.910	942	1.032	4024	5.52'
G	4840	1967	3.543	3759	2.057	2223	5.540	2.054	1115	1.128	4202	5.828
1	4550	3000	N.R.					N.R.				
2	4600	3000	N.R.					N.R.				
3	4650	3000	2.823	2291	1.618	3816	6.251	2.618	1936	1.491	4046	6.251
4	4700	3000	2.926	2479	1.680	3733	6.278	2.537	1805	1.440	4169	6.281
5	4750	3000	2.997	2613	1.724	3683	6.305	2.487	1726	1.409	4260	6.312
6	4800	3000	3.056	2728	1.760	3646	6.331	2.450	1667	1.385	4338	6.344
7	4850	3000	3.109	2832	1.792	3615	6.356	2.418	1620	1.365	4409	6.377
8	4900	3000	3.157	2930	1.821	3590	6.381	2.392	1579	1.348	4475	6.410
9	4950	3000	3.202	3020	1.848	3567	6.406	2.368	1545	1.333	4538	6.443
10	5000	3000	3.244	3106	1.873	3548	6.430	2.347	1514	1.319	4599	6.477
11	5050	3000	3.283	3190	1.898	3530	6.454	2.329	1486	1.307	4658	6.511
12	5100	3000	3.322	3271	1.921	3514	6.478	2.311	1461	1.296	4716	6.540

TABLE A-XXII. SONIC BOOM TEST DATA SUMMARY

SLED: LANCE DATE: 1/24/73 TIME: 1941 M.S.T.

	STATION (FIXED)																	
	B	C	D	E	F	G	1	2	3	4	5	6	7	8	9	10	11	12
X(ft)	100	2560	4260	2504	4840	4840	4550	4690	4650	4700	4750	4800	4850	4900	4950	5000	5050	5100
Y (ft)	985	200	200	1000	1000	1967	3000											3000
BOOM WAVE																		
Obs. Arrival (sec)		3.123	3.908	3.602	4.780	5.527	6.172	6.206	6.240	6.272	6.302	6.331		6.357	6.382	6.405	6.430	6.453
Calc. Arrival (sec)		3.113	3.914	N.R.	4.792	5.540	N.	N.R.	6.251	6.278	6.305	6.331		6.356	6.381	6.406	6.430	6.454
Rise Time (ms)		0.4	1.4	22	3.1	3.5	3.4	16.0	9.8	4.6	4.7	2.7		3.7	2.4	4.7	3.7	3.9
+ Phase (ms)		15	14.1	180	80		55	50	46	41	34	47		45	61	110	114	104
Ph. Length (ms)		22	18.8	400		112	55	50	46	41	34	47		45	61	110	114	104
ΔP (+) (mb)		33.34	46.80	1.65	13.46	7.93	1.09	4.05	5.68	8.01	9.98	12.63		10.88	8.38	7.21	6.71	7.18
Pk (mb)		50.55	29.05	2.45	15.76	9.32	4.60	5.74	7.47	9.88	11.74	14.31		12.67	9.90	8.84	8.22	8.48
TRANS-SONIC WAVE																		
			(2)			(2)	(4)											
Obs. Arrival (sec)		No S/N	4.785		5.498													
Calc. Arrival (sec)		3.377	4.901	N.R.	5.527	5.828	N.R.	N.R.	6.251	6.281	6.312	6.344		6.377	6.410	6.443	6.477	6.511
Rise Time (ms)			3.3		10.2													
+ Phase (ms)			16.3		34.5													
Ph. Length (ms)			50		65													
ΔP (+) (mb)			2.61		.871													
Pk (mb)			3.51		1.940													
IMPACT WAVE																		
			(2)			(2)												
Arrival (sec)	8.576	6.308	-	6.493	4.961	5.793	6.777	6.770	6.763	6.757	6.752	6.746		6.743	6.737	6.735	6.733	6.732
Rise Time (ms)	10.2	10.4		7.8	3.1	5.1	7.0	6.2	5.9	4.7	6.6	6.6		8.6	6.3	5.5	5.9	3.1
+ Phase (ms)	40	30.2		33	30	34	37.5	35.2	37.9	36.8	43.0	40		44	45	45	47	53
Ph. Length (ms)	128	62		56	63	109	115	113	111	109	110	149		147	129	126	135	130
ΔP (+) (mb)	.271	0.50		.724	9.82	6.24	2.60	2.67	2.75	3.16	2.94	3.01		2.52	2.51	3.22	3.27	3.59
Pk (mb)	.361	0.80		1.034	13.78	9.32	4.11	4.33	4.64	4.96	4.89	4.82		4.54	4.53	4.80	4.65	4.82
CAL SHOT WAVE																		
Arrival (sec)	5.841	3.817	2.407	3.676	1.631	1.618	2.280	2.244	2.209	2.173	2.138	2.104		2.071	2.037	2.004	1.971	1.940
Rise Time (ms)	12.5	6.3	5.5	6.3	5.9	5.1	5.3	5.5	4.1	5.1	5.5	5.1		4.7	4.7	4.7	4.3	4.3
+ Phase (ms)	58	51	41	51	43	38	36	36	37	36	38	40		36	37	41	38	38
Ph. Length (ms)	123	113	119	127	112	106	108	107	106	113	104	104		107	104	104	104	112
ΔP (+) (mb)	.922	1.940	2.86	1.138	4.79	5.71	4.23	4.47	4.64	4.80	4.76	4.30		4.54	4.81	4.53	5.26	5.15
Pk (mb)	1.398	2.538	4.41	1.965	6.65	8.17	6.03	6.27	6.52	6.76	6.72	6.21		6.73	6.93	6.70	7.42	7.33
MOTOR NOISE																		
			(3)				(3)											(3)
Time (sec)	0.817			2.661			4.972											5.513
ΔP (+) (mb)	1.00			.379			.245*											.336*
Pk (mb)	2.44			.793			.245											.336
Freq. (Hz)	140			15														
Time (sec)	2.481			3.382			5.857											6.266
Pk (mb)	2.98			1.31*			.654											.639
Freq. (Hz)	50			15			13											
REMARKS: (1) Overpressure possibly limited by gage response limits.																		
(2) Waves "r" & "i" inseparable in arrival time and phase duration.																		
(3) First & Second stage ignition blasts recorded. All mobile array records similar to two recorded.																		
(4) Two booms not separable in mobile array records.																		

TABLE A-XXIII. SONIC BOOM TEST CALCULATION SUMMARY

SLED: 25 HVAR W.I. + JAV 2 St. DATE: 3/2/73 TIME: 1420 M. S. T.

$$V = 51.58 + 1403 t - 910.8 t^2 + 535.7 t^3 - 82.72 t^4$$

 PRESSURE 840 mb  
 TEMP. 59 °F  
 WIND 200°/8 Kts

SOUND PROPAGATIONS	TRAJECTORY DATA				CAUSTIC COORDINATES		MACH NO.		
	X(ft)	t(sec)	V(fps)	A(fps <sup>2</sup> )	X <sub>F</sub> (ft)	Y <sub>F</sub> (ft)	M	V(fps)	X(ft)
C: 1118.00 fps							1.000	1105	617
Sound Velocity	1000	1.430	1416	1117	2142	521	Max 3.441	3803	5000
Along Track:	2000	1.994	2167	1537	2796	1437			
V(180): 1105.30 fps	3000	2.392	2820	1713	3344	2222			
	4000	2.711	3366	1683	4408	3954			
	5000	2.984	3803	1486	5703	6456			

BOOM "B" WAVES								TRANSSONIC "T" WAVES				
GAGE	X	Y	t <sub>o</sub> (sec)	X <sub>o</sub> (ft)	M	R(ft)	t <sub>a</sub> (sec)	t <sub>o</sub> (sec)	X <sub>o</sub> (ft)	M	R(ft)	t <sub>a</sub> (sec)
C	2560	200	2.192	2461	2.247	223	2.392	1.129	622	1.005	1948	2.891
D	4260	200	2.774	4193	3.141	211	2.963	1.125	617	1.002	3648	4.424
E	2504	1000	1.936	1876	1.880	1181	2.994	1.313	843	1.167	1939	3.061
F	4840	1000	2.866	4520	3.276	1050	3.805	1.156	653	1.028	4305	5.046
G	4840	1967	2.772	4187	3.138	2050	4.605	1.248	761	1.108	4518	5.324
1	4550	3000	2.526	3384	2.760	3219	5.406	1.466	1052	1.317	4608	5.612
2	4600	3000	2.548	3450	2.793	3213	5.422	1.456	1038	1.307	4657	5.647
3	4650	3000	2.569	3515	2.826	3208	5.438	1.447	1025	1.298	4705	5.682
4	4700	3000	2.589	3580	2.858	3202	5.454	1.438	1013	1.289	4754	5.717
5	4750	3000	2.609	3643	2.889	3198	5.470	1.430	1001	1.281	4802	5.752
6	4800	3000	2.629	3706	2.920	3193	5.485	1.422	990	1.273	4850	5.788
7	4850	3000	2.648	3769	2.949	3189	5.500	1.414	979	1.265	4898	5.823
8	4900	3000	2.667	3831	2.978	3185	5.516	1.407	969	1.258	4945	5.859
9	4950	3000	2.686	3892	3.007	3181	5.531	1.401	959	1.251	4993	5.895
10	5000	3000	2.704	3953	3.035	3177	5.546	1.394	950	1.244	5040	5.932
11	5050	3000	2.722	4013	3.062	3174	5.560	1.387	941	1.238	5087	5.968
12	5100	3000	2.739	4074	3.089	3171	5.575	1.381	933	1.232	5135	6.005

TABLE A-XXIV. SONIC BOOM TEST DATA SUMMARY

SLED: 25 HVAR W. I. DATE: 4/2/73 TIME: 14.00 M. S. T.

STATION (FIXED)																		
	B	C	D	E	F	G	I	J	K	L	M	N	O	P	Q	R	S	T
X(ft)	100	2560	4260	2504	4840	4840	4550	4600	4650	4700	4750	4800	4850	4900	4950	5000	5050	5100
Y(ft)	985	200	200	1000	1000	1967	3000		4650	4700	4750	4800	4850	4900	4950	5000	5050	5100
BOOM WAVE																		
Obs. Arrival (sec)		2.389	2.949	3.011	3.787	4.582	5.194	5.409	5.424	5.429	5.455	5.470	5.484	5.598	5.514	5.529	5.544	5.557
Calc. Arrival (sec)		2.392	2.963	2.994	3.809	4.605	5.406	5.422	5.438	5.454	5.470	5.485	5.500	5.516	5.531	5.546	5.560	5.575
Rise Time (ms)		2.0	3.1	6.7	4.0	5.6	5.7	4.7	6.0	6.1	6.0	5.5	7.1	10.3	8.1	6.4	5.8	6.7
+ Phase (ms)		23	18	43	17	26	28	31	28	29	33	27	31	28	31	32	29	30
Ph. Length (ms)		65	52	55	66	65	72	76	91	98	56	58	64	77	69	90	98	103
ΔP (+) (mb)		12.75	16.94	3.77	5.56	5.86	2.77	2.61	2.43	2.53	2.36	2.57	2.14	2.10	2.26	2.26	2.34	2.41
Pk (mb)		15.42	20.19	4.23	6.94	3.58	3.72	3.30	3.08	3.09	2.80	3.23	2.83	2.80	3.05	2.88	2.89	3.06
TRANS-SONIC WAVE																		
Obs. Arrival (sec)		2.876	4.403	3.075	5.008	5.274	5.586	5.623	5.657	5.688	5.726	5.751	5.795	5.833	5.868	5.906	5.934	5.978
Calc. Arrival (sec)		2.891	4.424	3.061	5.046	5.324	5.612	5.647	5.682	5.717	5.752	5.788	5.823	5.859	5.895	5.932	5.968	6.005
Rise Time (ms)		14	10	5.5	24	14	12.0	9.4	9.7	12.1	9.2	8.6	13.6	8.1	11.8	10.0	9.9	11.2
+ Phase (ms)		40	37	16	52	30	24	21	20	26	24	26	38	40	24	22	20	22
Ph. Length (ms)		75	82	-	86	-	-	-	-	-	-	-	96	82	-	-	-	-
ΔP (+) (mb)		4.25	1.966	.881	.839	.492	.415	.347	.327	.338	.339	.667	.322	.579	.332	.298	.319	.338
Pk (mb)		11.66	4.991	1.727	2.020	.849	-	-	-	-	-	-	.746	.860	.780	.789	.756	.756
IMPACT WAVE																		
Arrival (sec)	7.640	5.432	3.938	5.606	4.007	4.814	5.793	5.784	5.774	5.765	5.757	-	5.748	5.743	5.739	5.736	5.731	5.729
Rise Time (ms)	8.3	5.2	3.4	6.7	5.2	5.9	7.6	6.2	7.9	8.6	9.1	-	6.9	8.3	8.3	8.0	7.9	8.0
+ Phase (ms)	20	18	15	16	19	24	24	21	24	26	19	-	22	24	22	22	22	22
Ph. Length (ms)	46	38	37	36	35	48	45	41	47	52	-	-	-	44	44	43	41	41
ΔP (+) (mb)	.530	1.038	3.18	1.026	2.32	.849	.773	.743	.638	.757	.446	-	.644	.827	.647	.736	.689	.740
Pk (mb)	.735	1.482	4.24	1.485	2.94	.984	1.094	1.007	.758	.821	1.071	-	-	-	.846	.912	.790	.852
MOTOR NOISE																		
Time (sec)	0.927																	
ΔP (+) (mb)	1.024																	
Pk (mb)	1.596																	
Freq. (Hz)	91																	
Time (sec)	1.908																	
Pk (mb)	1.366																	
Freq. (Hz)	100																	

(1)

REMARKS: (1) Waves "T" and "I" near same arrival time, inseparable results.



TABLE A-XXV. SONIC BOOM TEST CALCULATION SUMMARY

SLED: RECRUIT MONORAIL DATE: 5/8/73 TIME: 1045 M. D. T.  
 $V = 376.2 + 351.3 t + 3819 t^2 - 2162 t^3 + 265.2 t^4$

PRESSURE 847 mb  
 TEMP. 67 °F  
 WIND 270°/3 Kts

SOUND PROPAGATIONS	TRAJECTORY DATA				CAUSTIC COORDINATES		MACH NO. M	V(fps)	X(ft)
	X(ft)	t(sec)	V(fps)	A(fps <sup>2</sup> )	X <sub>F</sub> (ft)	Y <sub>F</sub> (ft)			
C: 1126.89 fps							1.000	1127	263
Sound Velocity	1000	0.875	2315	2780	799	136	Max 3.201	3608	3511
Along Track:	2000	1.241	3191	1869	1905	1656			
V(180): 1126.89 fps	3000	1.532	3565	645	2958	3543			
	4000	1.805	3555	-754	3865	5446			
	5100	2.121	3041	-2503	4803	7610			

BOOM "B" WAVES								TRANSSONIC "T" WAVES				
GAGE	X	Y	t <sub>o</sub> (sec)	X <sub>o</sub> (ft)	M	R(ft)	t <sub>a</sub> (sec)	t <sub>o</sub> (sec)	X <sub>o</sub> (ft)	M	R(ft)	t <sub>a</sub> (sec)
C	2560	200	1.387	2490	3.038	212	1.574	0.454	265	1.004	2304	2.498
D	4260	200	1.866	4192	3.105	211	2.052	0.463	263	1.001	4002	4.003
E	2504	1000	1.281	2136	2.896	1066	2.223	0.495	313	1.099	2408	2.628
F	4840	1000	1.951	4487	3.004	1060	2.888	0.462	275	1.024	4674	4.606
G	4840	1967	1.862	4180	3.108	2052	3.676	0.490	307	1.088	4932	4.858
1	2400	3000	N. R.					N. R.				
2	2450	3000	N. R.					N. R.				
3	2500	3000	N. R.					N. R.				
4	2550	3000	N. R.					N. R.				
5	2600	3000	N. R.					N. R.				
6	2650	3000	N. R.					N. R.				
7	2700	3000	0.992	1276	2.333	3321	3.927	N. R.				
8	2750	3000	1.037	1399	2.435	3290	3.945	0.785	792	1.829	3583	3.953
9	2800	3000	1.073	1498	2.512	3270	3.963	0.761	743	1.768	3637	3.977
10	2850	3000	1.104	1586	2.576	3255	3.980	0.742	706	1.720	3688	4.003
11	2900	3000	1.131	1668	2.632	3243	3.998	0.726	675	1.670	3735	4.020
12	2950	3000	1.157	1744	2.682	3233	4.014	0.712	640	1.643	3781	4.056

TABLE A-KXVI. SONIC BOOM TEST DATA SUMMARY

SLED: RECRUIT MONORAIL DATE: 2/8/73 TIME: 1045 M.D.T.

STATION (FIXED)																		
	B	C	D	E	F	G	1	2	3	4	5	6	7	8	9	10	11	12
X(ft)	100	2560	4260	5904	7440	8840	2400	2450	2500	2550	2600	2650	2700	2750	2800	2850	2900	2950
Y(ft)	282	700	700	1000	1000	1907	3000	3000	3000	3000	3000	3000	3000	3000	3000	3000	3000	3000
BOOM WAVE																		
Obs. Arrival (sec)		1.580	1.048	1.298	1.893	1.670	3.767	3.806	3.834	3.858	3.879	3.898	3.921	3.943	3.962	3.980	3.996	4.013
Calc. Arrival (sec)		1.574	1.052	1.293	1.888	1.676	N.R.	N.R.	N.R.	N.R.	N.R.	N.R.	3.927	3.945	3.963	3.980	3.998	4.014
Rise Time (ms)		1.1	1.9	1.5	4.1	4.5	37	19	19	11	8.3	8.7	5.9	3.2	4.3	4.3	6.3	5.9
+ Phase (ms)		11.6	9.7	20	15	17	61	40	33	28	28	26	21	20	22	25	29	33
Ph. Length (ms)		66	32	77	47	44	127	112	92	72	79	82	80	73	78	76	87	96
AP(+) (mb)		26.88	17.67	5.91	4.06	2.95	0.501	0.645	1.109	1.711	2.87	3.54	5.09	5.68	5.80	5.02	4.39	3.62
Pk (mb)		32.02	26.18	7.55	6.24	4.38	1.139	1.336	2.065	3.185	4.80	5.49	7.58	7.35	8.16	7.13	5.88	4.94
TRANS-SONIC WAVE																		
Obs. Arrival (sec)		2.459	4.030	2.632	4.811	4.826								(3)				(3)
Calc. Arrival (sec)		2.408	4.003	2.628	4.606	4.858	N.R.	N.R.	N.R.	N.R.	N.R.	N.R.	N.R.	3.853	3.977	4.003	4.029	4.056
Rise Time (ms)		27	6.3	13.4	9.6	10.5												
+ Phase (ms)		39	-	24	22	20												
Ph. Length (ms)		139	39	81	103	86												
AP(+) (mb)		0.634	0.238*	0.741	0.132	0.265												
Pk (mb)		1.198	0.238	1.432	0.580	0.663												
IMPACT WAVE																		
Arrival (sec)	6.61	No S/N	1.886	No S/N	3.067	3.888	5.727	5.686	5.667	5.648	5.599	5.571	5.548	5.525	5.492	5.460	5.439	5.407
Rise Time (ms)	19		6.3		3.4	6.6												
+ Phase (ms)	-		12.6		8.2	9.7												
Ph. Length (ms)	48		28		17	22	28											
AP(+) (mb)	0.052		0.654		0.685	0.464*												28
Pk (mb)	0.087		0.892		1.053	0.464	0.177	0.203	0.134	0.167	0.165	0.216	0.153	0.174	0.162	0.229	0.199	0.229
CAL SHOT WAVE																		
Arrival (sec)	5.670	3.684	2.293	3.541	1.533	1.525	3.874	3.829	3.787	3.746	3.705	3.664	3.622	3.581	3.540	3.498	3.457	3.417
Rise Time (ms)	15.3	10.3	7.7	10.4	6.0	4.6	6.3	7.5	7.9	7.9	5.9	4.8	5.5	6.3	7.1	7.1	6.3	5.9
+ Phase (ms)	56	55	43	52	45	40	52	52	52	62	47	47	49	44	44	48	43	46
Ph. Length (ms)	161	136	118	124	117	117	182	136	137	152	154	153	159	149	186	159	194	162
AP(+) (mb)	1.848	1.515	2.56	1.360	4.53	4.84	1.424	1.355	1.443	1.518	1.729	1.714	1.715	1.761	1.884	1.954	1.816	1.906
Pk (mb)	1.264	2.043	3.63	1.970	6.00	7.30	2.170	2.027	2.151	2.193	2.387	2.345	2.424	2.459	2.703	2.732	2.583	2.744
MOTOR NOISE																		
Time (sec)	0.874																	
AP(+) (mb)	0.806						3.374	3.407	3.443	3.471	3.495	3.531	3.555	3.592	3.611	3.649	3.682	3.710
Pk (mb)	1.021																	
Freq. (Hz)	21						137	175	115	167	196	108	172	106	162	109	104	106
Time (sec)	1.538																	
Pk (mb)	0.358																	
Freq. (Hz)	125																	
OTHER WAVES																		
Time (sec)					3.034													
Rise Time (ms)					5.0													
+ Phase (ms)					11													
Ph. Length (ms)					19.7													
AP(+) (mb)					0.369													
Pk (mb)					00.500													
SOURCE					2d Imp.													

REMARKS: (1) Arrival times based on wave arrival at Gage #1.  
 (2) Weak impact wave time parameters not detailed.  
 (3) Trans-sonic waves not separable from main beam waves.

TABLE A-XXVII. SONIC BOOM TEST CALCULATION SUMMARY

SLED: ROADRUNNER MONORAILDATE: 5/8/73TIME: 1405 M.D.T.

$$V = 785.1 - 2583 t + 7515 t^2 - 2542 t^3 - 180.9 t^4$$

 PRESSURE 843 mb  
 TEMP. 73 °F  
 WIND 270°/4 Kts

SOUND PROPAGATIONS	TRAJECTORY DATA				CAUSTIC COORDINATES		MACH NO. M		
C: 1133.56 fps	X(ft)	t(sec)	V(fps)	A(fps <sup>2</sup> )	X <sub>F</sub> (ft)	Y <sub>F</sub> (ft)		V(fps)	X(ft)
Sound Velocity	1000	0.881	2495	4244	843	158	Max	1134	375
Along Track:	2000	1.203	3748	3200	1387	900		4328	3375
V(180): 1133.56 fps	3000	1.456	4295	898	1861	1682			
	4000	1.693	4129	-2510	2467	2876			
	5120	2.013	2329	-9137	2543	3039			

BOOM "B" WAVES								TRANSSONIC "T" WAVES				
GAGE	X	Y	t <sub>o</sub> (sec)	X <sub>o</sub> (ft)	M	R(ft)	t <sub>a</sub> (sec)	t <sub>o</sub> (sec)	X <sub>o</sub> (ft)	M	R(ft)	t <sub>a</sub> (sec)
C	2560	200	1.327	2502	3.608	208	1.510	0.531	376	1.004	2193	2.465
D	4260	200	1.728	4201	3.555	208	1.911	0.530	375	1.001	3890	3.961
E	2504	1000	1.252	2200	3.437	1045	2.168	0.568	420	1.109	2312	2.602
F	4840	1000	1.810	4519	3.275	1050	2.731	0.539	384	1.025	4566	4.562
G	4840	1967	1.743	4263	3.511	2027	3.521	0.562	413	1.092	4835	4.817
1	2400	3000	N.R.					N.R.				
2	2450	3000	N.R.					N.R.				
3	2500	3000	N.R.					N.R.				
4	2550	3000	0.996	1315	2.627	3244	3.842	N.R.				
5	2600	3000	1.037	1440	2.773	3216	3.859	N.R.				
6	2650	3000	1.068	1540	2.881	3199	3.874	0.807	828	1.926	3510	3.888
7	2700	3000	1.094	1628	2.971	3186	3.889	0.790	791	1.863	3556	3.911
8	2750	3000	1.118	1708	3.048	3176	3.904	0.776	761	1.810	3600	3.936
9	2800	3000	1.140	1784	3.118	3167	3.918	0.763	735	1.764	3642	3.960
10	2850	3000	1.160	1856	3.181	3160	3.932	0.752	714	1.724	3683	3.986
11	2900	3000	1.179	1926	3.238	3154	3.946	0.742	695	1.688	3723	4.011
12	2950	3000	1.197	1993	3.291	3149	3.960	0.733	678	1.656	3764	4.038

TABLE A-XXVIII. SONIC BOOM TEST DATA SUMMARY

SLED: ROADRUNNER MONORAIL DATE: 5/8/73 TIME: 1405 M.D.T.

	STATION (FIXED)																		
	B	C	D	E	F	G	1	2	3	4	5	6	7	8	9	10	11	12	
X(ft)	100	2560	4260	2504	4840	4840	2400	2450	2500	2550	2600	2650	2700	2750	2800	2850	2900	2950	
Y(ft)	985	200	200	1000	1000	1967	3000											3000	
BOOM WAVE																			
Obs. Arrival (sec)		1.508	1.903	2.175	2.719	3.498	3.764	3.781	3.808	3.833	3.850	3.864	3.877		3.904	3.916	3.929	3.941	
Calc. Arrival (sec)		1.510	1.911	2.168	2.731	3.521	N.R.	N.R.	N.R.	3.842	3.859	3.874	3.889	3.904	3.918	3.932	3.946	3.960	
Rise Time (ms)		1.1	1.1	3.3	3.0	5.1	13.8	15.0	11.1	4.4	5.5	6.7	7.9		6.3	7.1	6.3	6.7	
+ Phase (ms)		6.8	4.8	8.4	7.4	8.9	21.4	23.7	17.6	11.9	12.3	16.2	14.7		13.9	13.1	13.1	13.9	
Ph. Length (ms)		14.1	9.2	19.6	14.3	17.4	39	36	41	28	31	42	57		33	26	26	27	
AP(+) (mb)		5.28	3.02	1.489	0.695	0.402	.223	.436	.877	1.637	1.901	1.229	1.011		.777	.839	.782	.908	
Pk (mb)		7.79	6.51	2.247	1.497	0.704	.419	.787	1.325	2.666	2.866	1.945	1.526		1.084	1.249	1.154	1.279	
TRANS-SONIC WAVE																			
Obs. Arrival (sec)		No S/N	No S/N	No S/N	No S/N	No S/N	N.R.	N.R.	N.R.	N.R.	N.R.	3.888	3.911	3.936	3.947	3.971	3.995	4.021	
Calc. Arrival (sec)		2.465	3.961	2.602	4.562	4.817									3.960	3.986	4.011	4.038	
Rise Time (ms)															4.4	3.2	5.9	6.7	
+ Phase (ms)															9.9	10.7	11.5	13.5	
Ph. Length (ms)															29	28	32	33	
AP(+) (mb)															.309	.261	.201	.391	
Pk (mb)															.726	.634	.544	.694	
IMPACT WAVE																			
Arrival (sec)		No S/N	2.8	No S/N	2.9	3.7	No Signal/Noise												No S/N
Rise Time (ms)			(1)		(1)	(1)													
+ Phase (ms)																			
Ph. Length (ms)																			
AP(+) (mb)																			
Pk (mb)																			
CAL SHOT WAVE																			
Arrival (sec)	5.611	3.664	2.293	3.514	1.529	1.509	3.834	3.790	3.774	3.708	3.667	3.624	3.584		3.504	3.462	3.421	3.379	
Rise Time (ms)	7.6	7.4	7.8	11.4	7.1	5.2	6.7	6.3	5.9	6.7	6.3	6.3	6.3		5.9	5.5	5.9	7.5	
+ Phase (ms)	50	46	53	48	43	41	44	44	40	42	43	42	40		41	40	42	46	
Ph. Length (ms)	156	119	108	120	141	137	110	118	125	147	168	155	128		154	136	129	135	
AP(+) (mb)	.907	1.876	2.54	1.489	4.49	4.82	2.09	1.96	2.04	2.03	2.07	2.10	2.10		2.23	2.39	2.22	2.00	
Pk (mb)	1.494	2.690	3.37	2.301	6.36	6.70	2.80	2.54	2.62	2.69	2.74	2.68	2.74		2.93	3.12	2.98	2.81	
MOTOR NOISE																			
Time (sec)	0.840																		
AP(+) (mb)	.0834																		
Pk (mb)	.1251																		
Freq. (Hz)	60																		

REMARKS: (1) Very weak ripple, possible signal, on recording.

TABLE A-XXIX. SONIC BOOM TEST CALCULATION SUMMARY

SLED: KIVA-I MONORAIL DATE: 5/15/73 TIME: 1022 M.D.T.  
 $V = -2633 + 4319 t - 2135 t^2 + 460.4 t^3 - 34.35 t^4$

PRESSURE 855 mb  
 TEMP. 55 °F  
 WIND 110°/1 Kts

SOUND PROPAGATIONS	TRAJECTORY DATA				CAUSTIC COORDINATES		MACH NO.		
	X(ft)	t(sec)	V(fps)	A(fps <sup>2</sup> )	X <sub>F</sub> (ft)	Y <sub>F</sub> (ft)	M	V(fps)	X(ft)
C: 1113.56 fps							1.000	1113	1944
Sound Velocity	1000	2.887	734	198	4407	530	Max 1.552	1727	3971
Along Track:	2000	3.969	1140	540	4781	1141			
V(180): 1112.98 fps	3000	4.742	1565	479	5417	1919			
	4000	5.371	1727	-59	6252	2870			
	4150	5.457	1716	-179	7398	4175			

BOOM "B" WAVES								TRANSSONIC "T" WAVES				
GAGE	X	Y	t <sub>o</sub> (sec)	X <sub>o</sub> (ft)	M	R(ft)	t <sub>a</sub> (sec)	t <sub>o</sub> (sec)	X <sub>o</sub> (ft)	M	R(ft)	t <sub>a</sub> (sec)
C	2560	200	N.R.					N.R.				
D	4260	200	5.355	4091	1.552	262	5.601	3.927	1953	1.004	2316	6.008
E	2504	1000	N.R.									
F	4840	1000	5.311	3998	1.552	1307	6.487	4.051	2095	1.064	2921	6.677
G	4840	1967	N.R.									
1	6200	3000	5.064	3574	1.518	3987	8.649	4.588	2812	1.336	4525	8.657
2	6250	3000	5.113	3658	1.530	3965	8.679	4.552	2760	1.319	4602	8.690
3	6300	3000	5.157	3732	1.538	3949	8.708	4.523	2717	1.304	4673	8.725
4	6350	3000	5.196	3799	1.544	3938	8.737	4.497	2681	1.292	4740	8.759
5	6400	3000	5.232	3860	1.548	3931	8.766	4.475	2648	1.280	4804	8.794
6	6450	3000	5.265	3918	1.550	3926	8.795	4.455	2620	1.270	4865	8.830
7	6500	3000	5.297	3972	1.552	3923	8.824	4.436	2593	1.261	4926	8.865
8	6550	3000	5.326	4024	1.552	3922	8.853	4.419	2570	1.252	4984	8.901
9	6600	3000	5.354	4072	1.552	3923	8.882	4.403	2548	1.244	5042	8.937
10	6650	3000	5.381	4119	1.551	3925	8.911	4.389	2528	1.237	5098	8.973
11	6700	3000	5.407	4163	1.549	3929	8.940	4.375	2509	1.230	5154	9.009
12	6750	3000	5.431	4205	1.546	3934	8.969	4.362	2491	1.223	5209	9.046

TABLE A-XXX. SONIC BOOM TEST DATA SUMMARY

SLED: KIVA-I MONORAIL DATE: 7/12/73 TIME: 10:20 M.D.T.

STATION (FIXED)																		
	B	C	D	E	F	G	I	J	K	L	M	N	O	P	Q	R	S	T
X(ft)	100	2560	4260	5504	6840	8040	9200	10500	11800	13000	14200	15400	16500	17600	18700	19800	20900	22000
Y(ft)	985	200	200	1000	1000	1967	2000	2000	2000	2000	2000	2000	2000	2000	2000	2000	2000	2000
BOOM WAVE																		
Obs. Arrival (sec)		4.497	5.655	No Sig.	6.541	No Sig.	8.669	8.704	8.722	8.760	8.809	8.840	8.870	8.900	8.928	8.955	8.981	
Calc. Arrival (sec)		N.R.	5.601	N.R.	6.487	N.R.	8.649	8.679	8.708	8.737	8.766	8.795	8.824	8.853	8.882	8.911	8.940	
Rise Time (ms)		7.9	2.0		4.4		20.6	15.5	27.8	21.4	8.3	7.1	5.9	5.2	6.3	5.9	7.5	8.969
+ Phase (ms)		21	5.2		10.3		44	39	50	46	30	30	30	29	26	28	32	28
Ph. Length (ms)		-	-		-		71	83	92	87	118	86	88	74	78	83	90	57
AP(+) (mb)		2.50	6.26		1.760		.374	.292	.430	.431	.649	.959	1.443	1.429	.891	.984	.861	.808
Pk (mb)		3.92	9.75		2.117		.708	.546	.736	.843	1.136	1.512	2.141	2.115	1.520	1.578	1.429	1.198
TRANS-SONIC WAVE																		
Obs. Arrival (sec)		(1)	5.992	No Sig.	6.666	No Sig.												(1)
Calc. Arrival (sec)		N.R.	6.487	N.R.	6.677	N.R.	8.657	8.690	8.725	8.754	8.794	8.830	8.865	8.901	8.937	8.973	9.009	9.046
Rise Time (ms)		-	-		4.0													
+ Phase (ms)		-	16		11.1													
Ph. Length (ms)		-	32		23													
AP(+) (mb)		-	.616*		.951*													
Pk (mb)		-	.616		.951													
IMPACT WAVE																		
No Signal/Noise $\pm$ 0.1 mb.																		
Arrival (sec)	10.438	-8.2	6.677	No S/N	6.871	7.706												
Rise Time (ms)	4.8	-	-		3.6	-												
+ Phase (ms)	12.7	-	-		7.5	-												
Ph. Length (ms)	40	-	29		20	-												
AP(+) (mb)	.059*	<.26*	.513*		.523*	.300*												
Pk (mb)	.059	<.26	.513		.523	.300												
CAL SHOT WAVE																		
Arrival (sec)	5.709	3.715	2.312	3.576	1.548	1.543	1.364	1.354	1.345	1.337	1.335	1.331	1.329	1.329	1.332	1.335	1.340	1.347
Rise Time (ms)	8.3	7.5	4.0	5.2	6.7	4.8	5.9	5.2	3.2	1.2	4.0	3.2	3.6	3.2	3.6	3.6	3.6	3.6
+ Phase (ms)	47	47	41	43	39	38	37	38	35	38	34	38	38	34	38	38	37	36
Ph. Length (ms)	188	151	123	127	155	155	179	174	175	166	146	134	173	147	181	174	179	168
AP(+) (mb)	1.225	1.655	2.92	1.508	4.61	5.02	6.87	6.48	6.78	6.80	7.54	6.53	7.36	7.65	7.14	7.48	7.07	7.35
Pk (mb)	1.666	2.391	4.41	2.298	6.28	7.21	9.68	8.80	9.55	8.94	9.97	9.11	10.18	9.86	(9.78)	10.73	9.87	(10.06)
MOTOR NOISE																		
Time (sec)	0.882																	
AP(+) (mb)	.096																	
Ph (ms)	.124																	
Freq. (Hz)	53																	

REMARKS: (1) Near caustic, two waves not separable.

(2) Negative phase off plot scale on playback; pressures estimated (...).

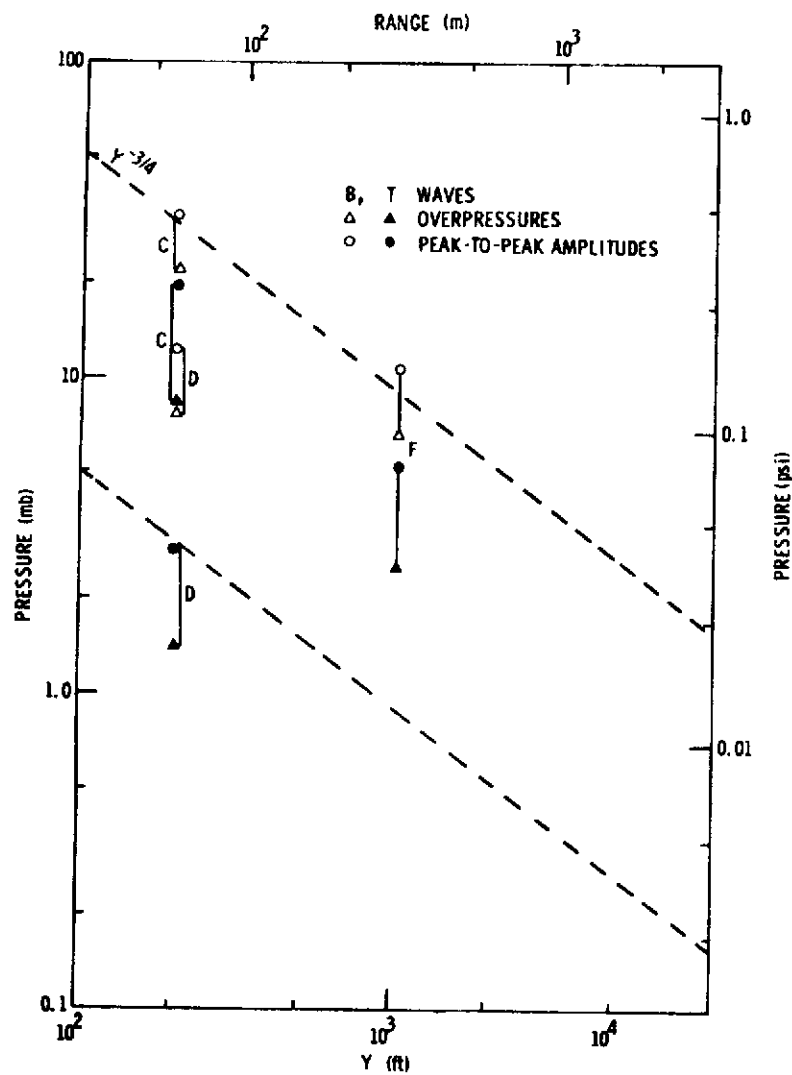


Figure A-1. Sonic Boom Pressures, 2/5/71 Sled Test

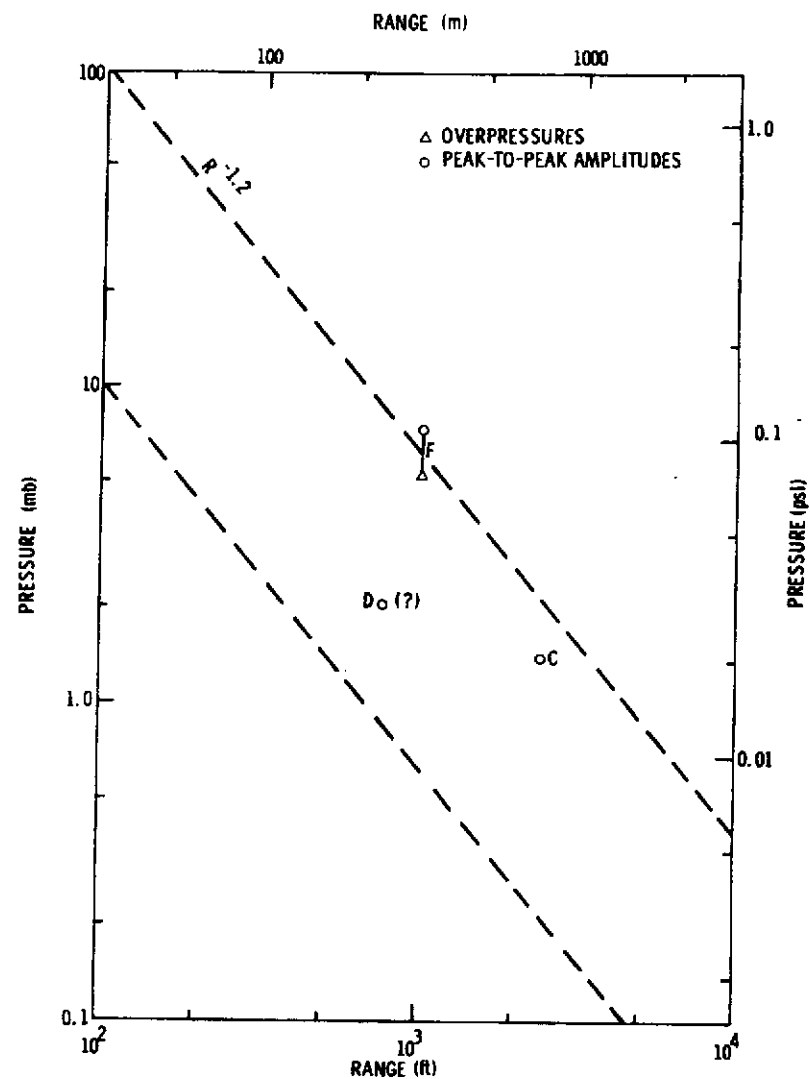


Figure A-2. Impact Explosion Pressures, 2/5/71 Sled Test

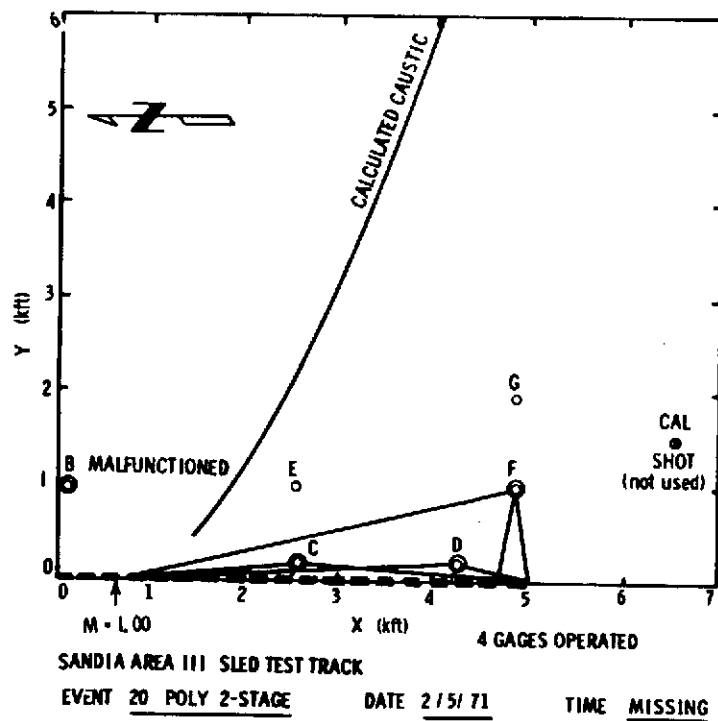


Figure A-3. Wave Propagation Paths

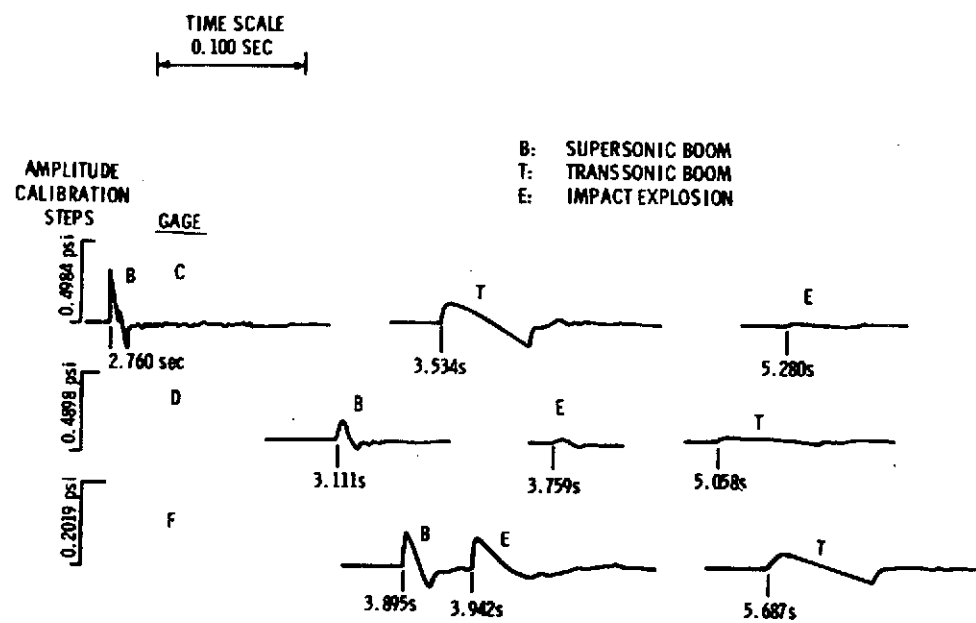


Figure A-4. Pressure Signatures Fixed Gages  
2/5/71 Test



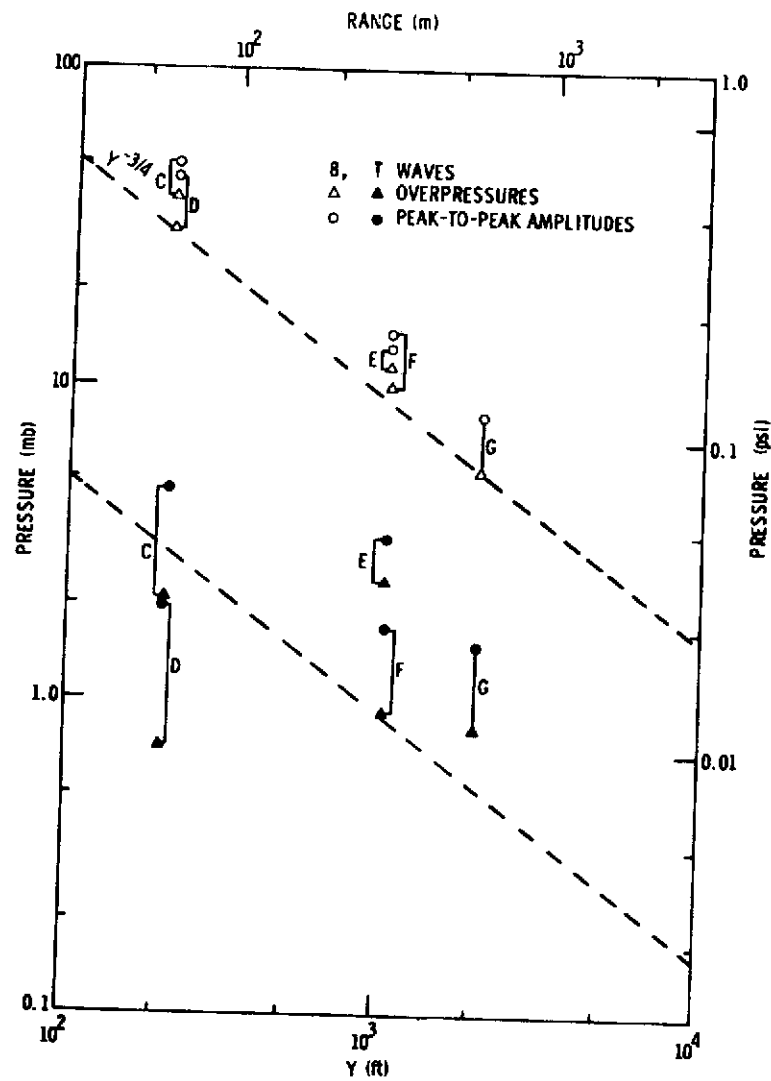


Figure A-5. Sonic Boom Pressures, 2/23/71 Sled Test

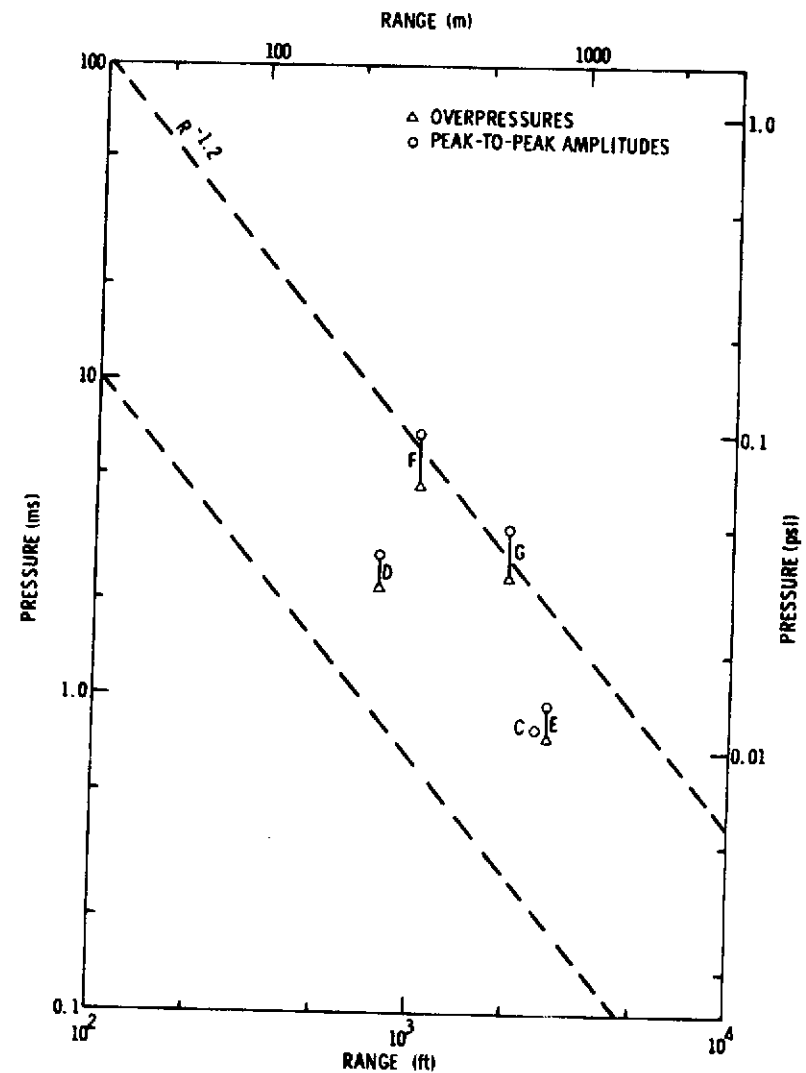


Figure A-6. Impact Explosion Pressures, 2/23/71 Sled Test

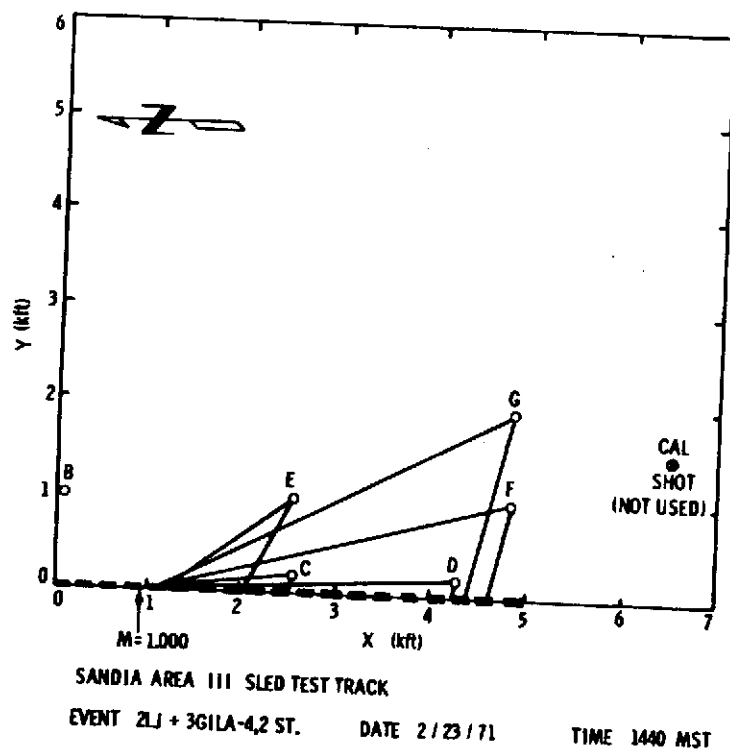


Figure A-7. Wave Propagation Paths

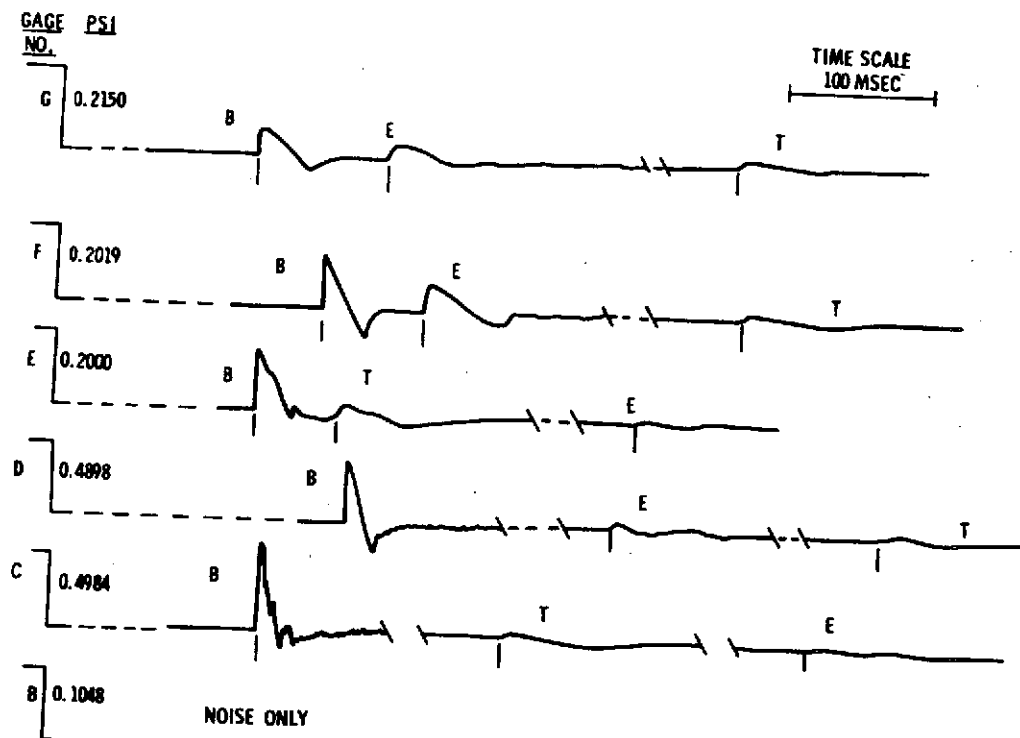


Figure A-8. Pressure Signatures, Fixed Gages, 2/23/71

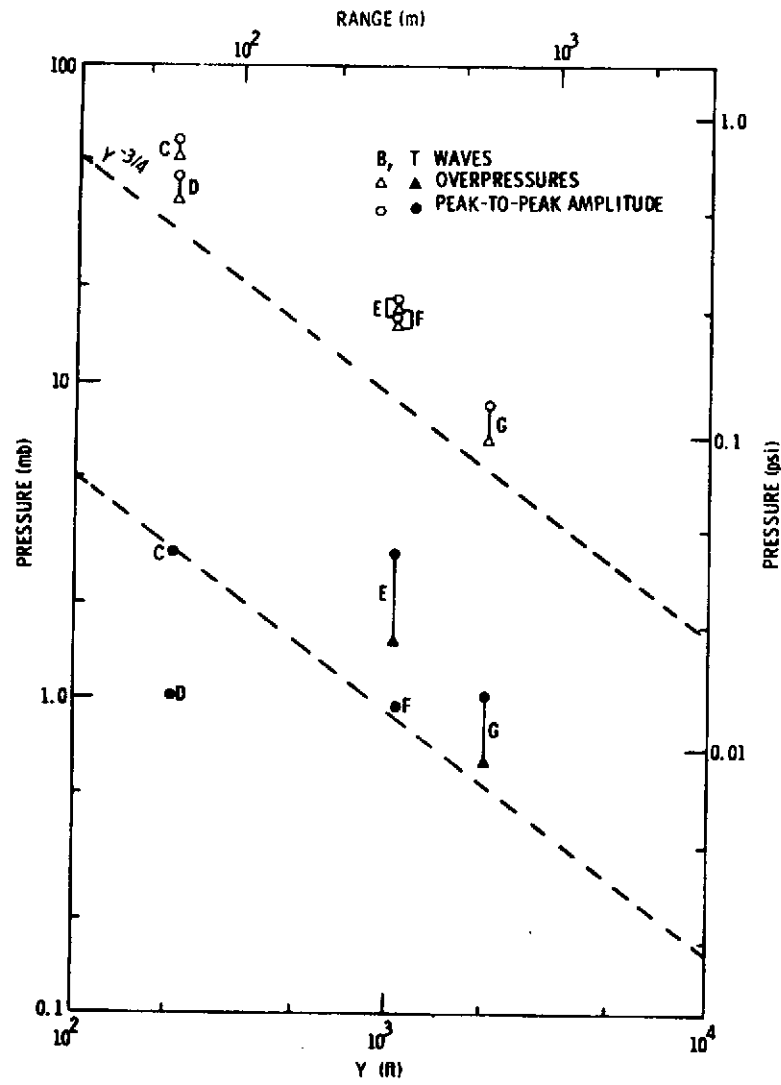


Figure A-9. Sonic Boom Pressures, 4/1/71 Sled Test

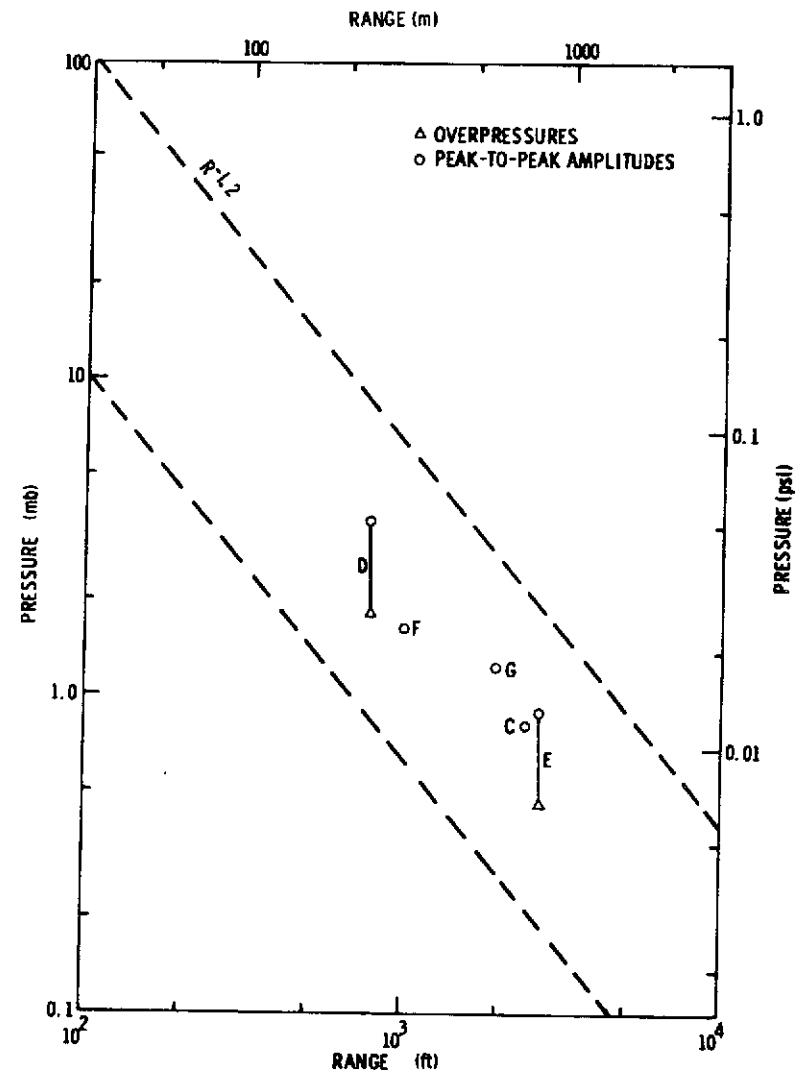


Figure A-10. Impact Explosion Pressures, 4/1/71 Sled Test

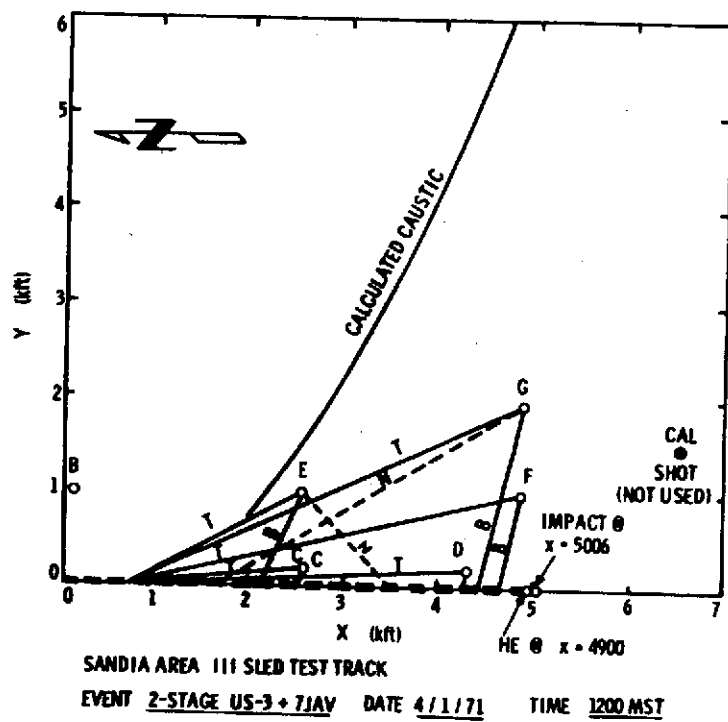


Figure A-11. Wave Propagation Paths

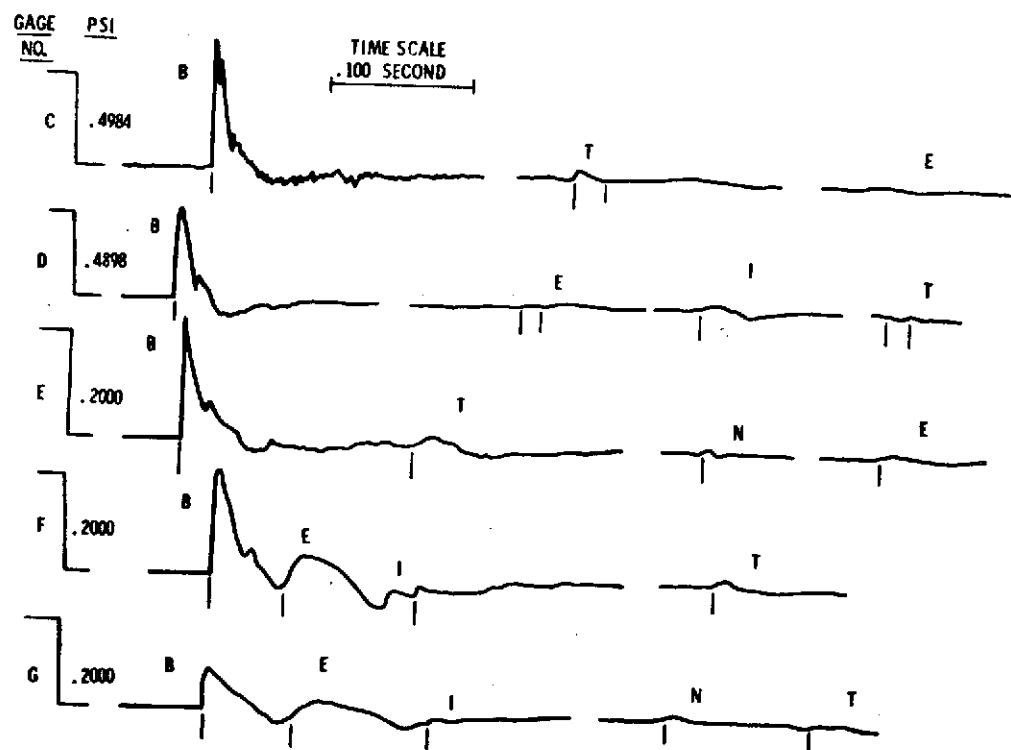


Figure A-12. Pressure Signatures Fixed Gages,  
4/1/71

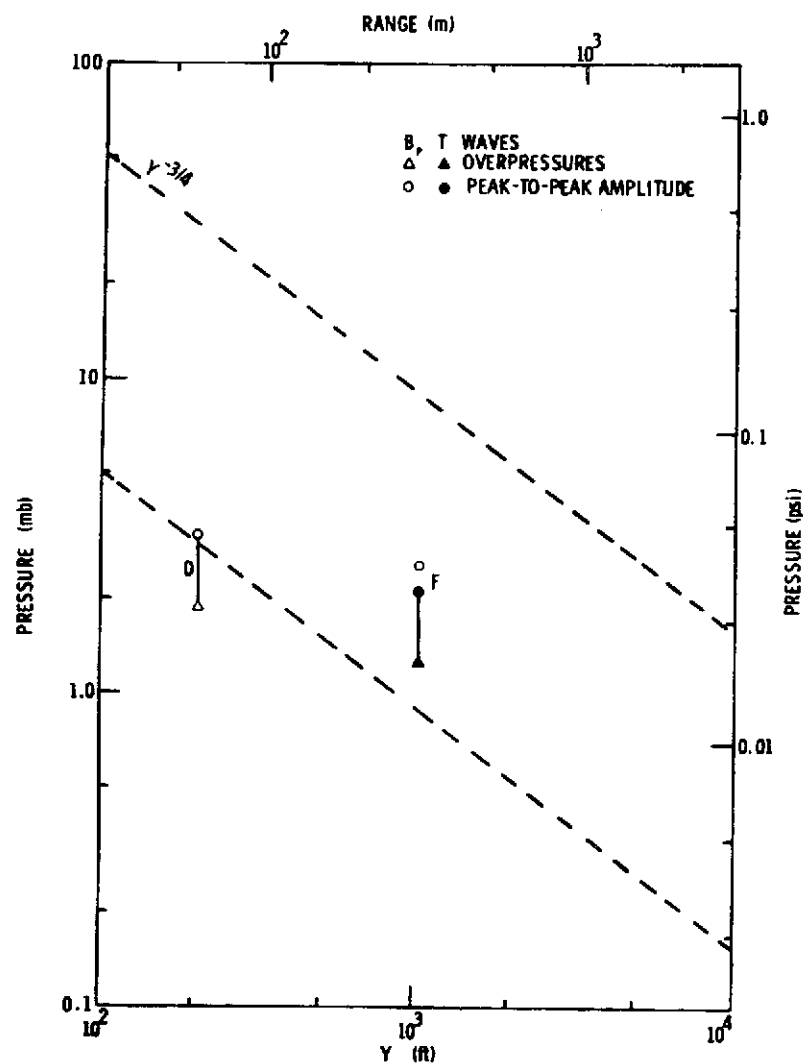


Figure A-13. Sonic Boom Pressures,  
6/22/71 Sled Test

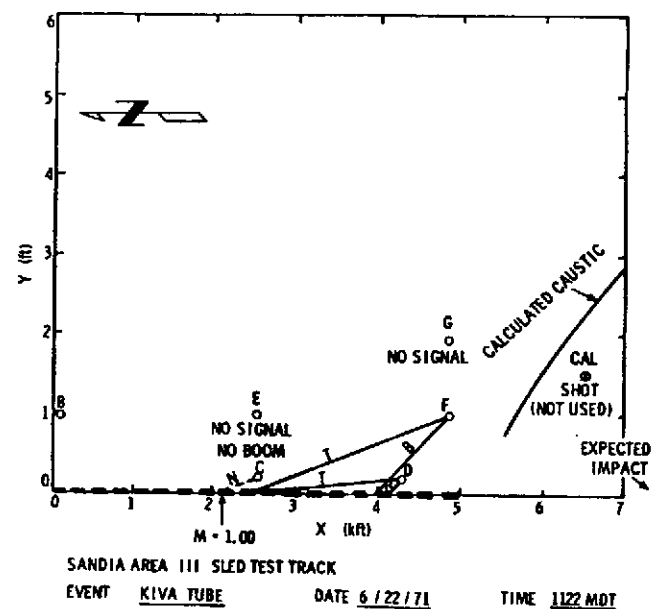


Figure A-14. Wave Propagation Paths

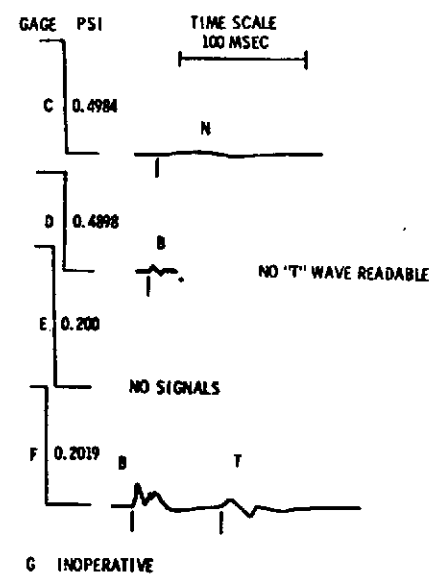


Figure A-15. Pressure Signatures  
Fixed Gages, 6/22/71

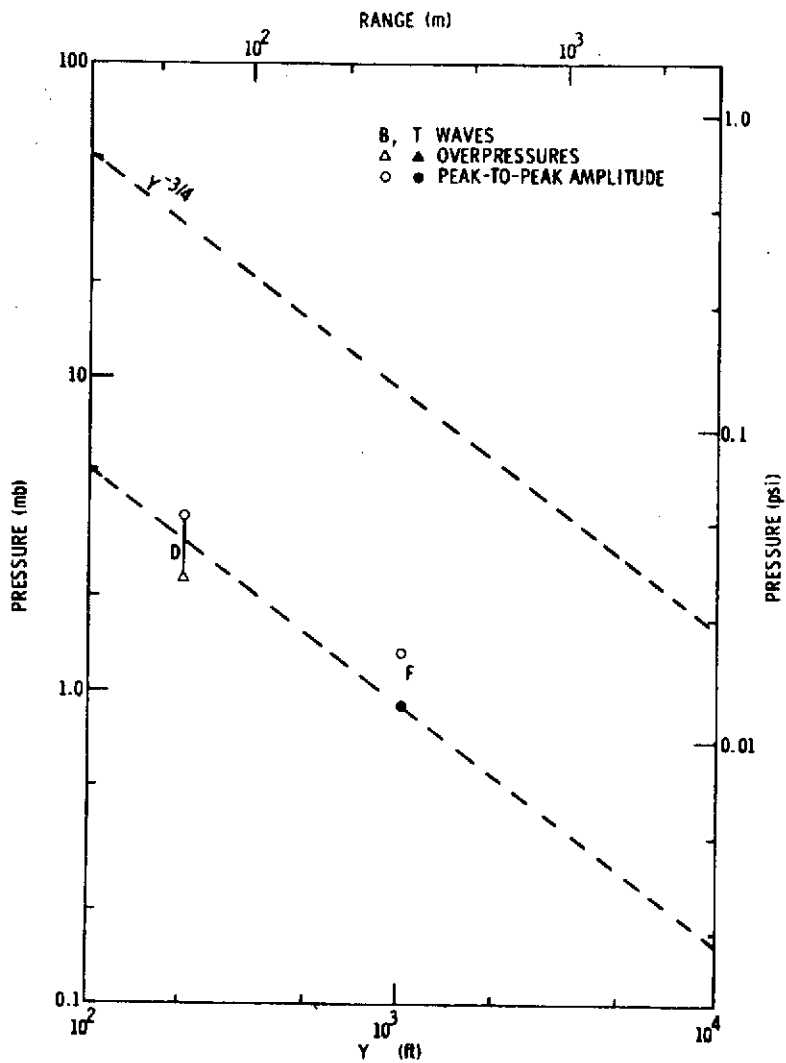


Figure A-16. Sonic Boom Pressures,  
8/16/71 Sled Test

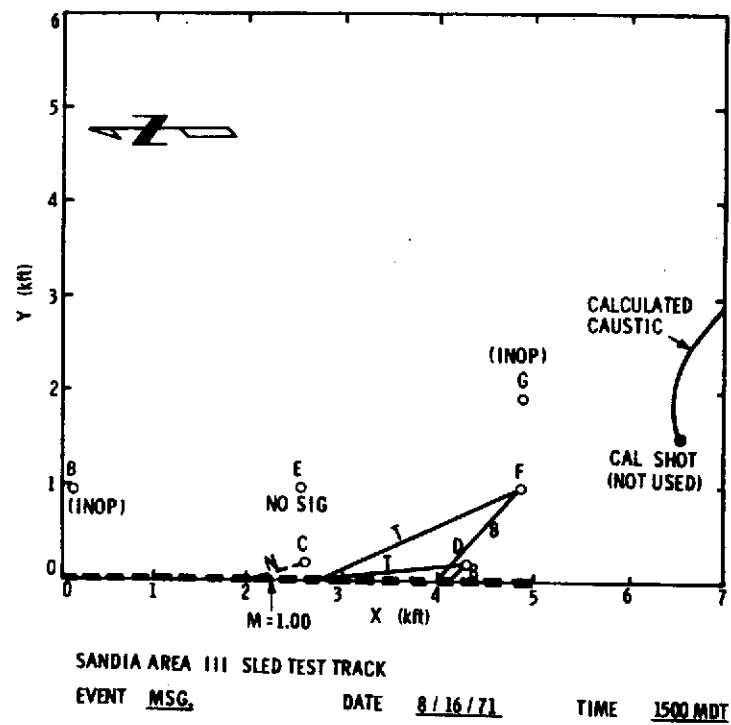


Figure A-17. Wave Propagation Paths

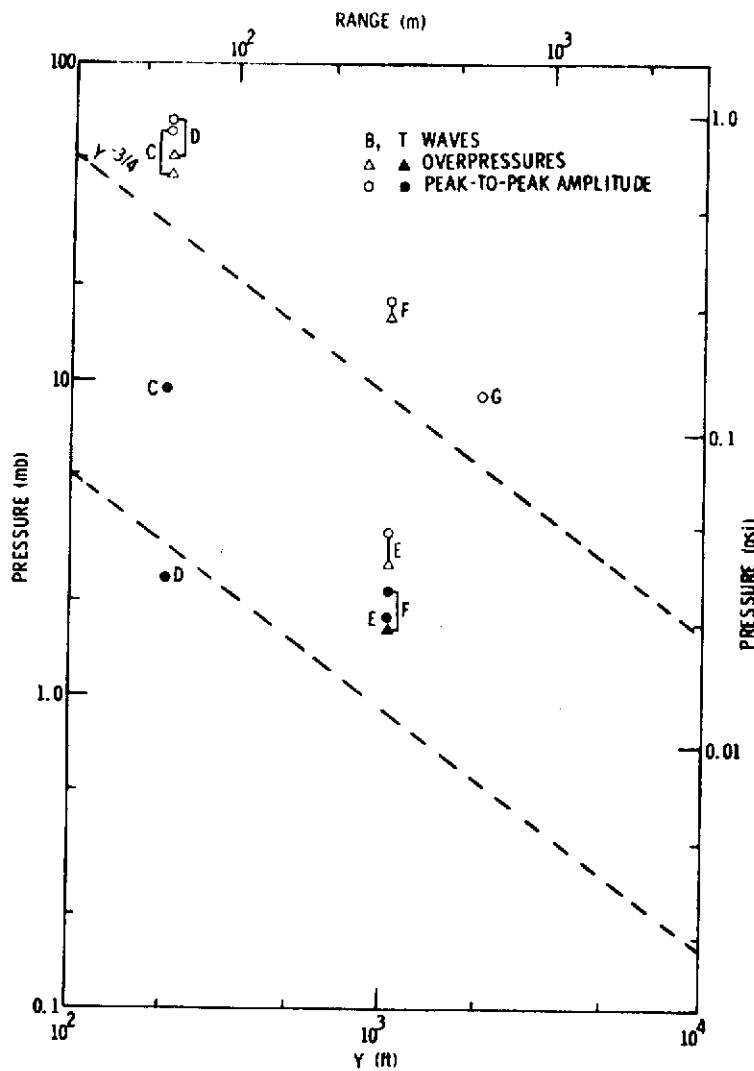


Figure A-18. Sonic Boom Pressures, 12/18/71 Sled Test

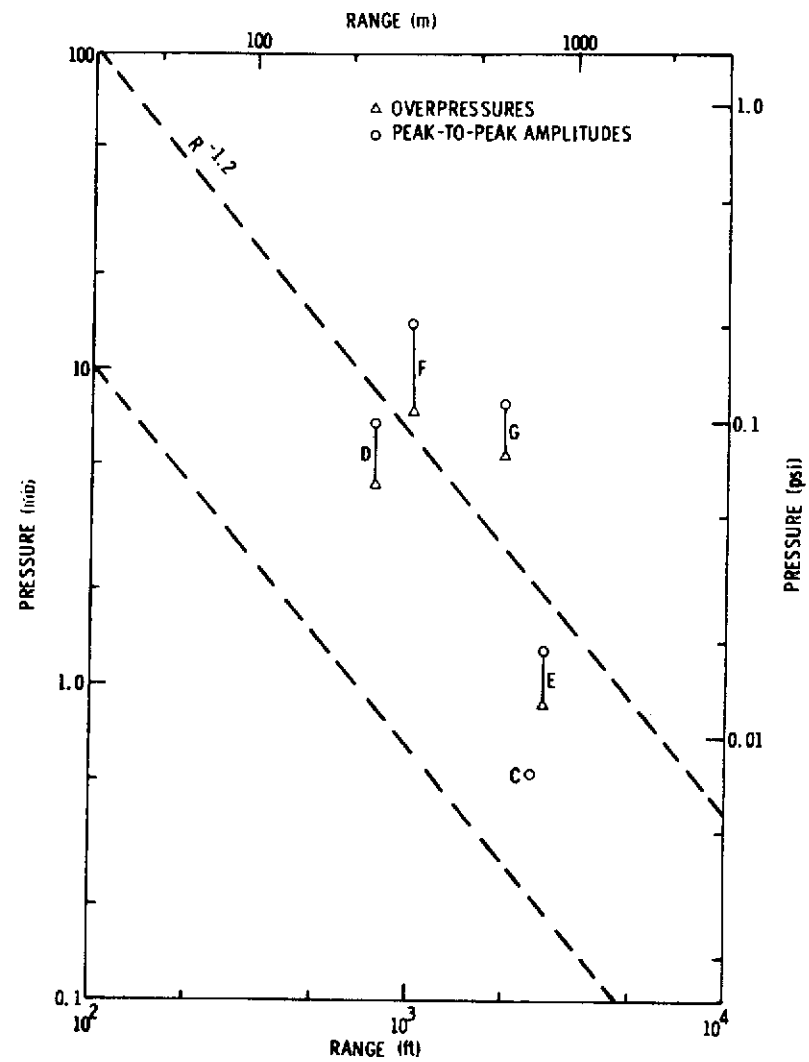


Figure A-19. Impact Explosion Pressures, 12/18/71 Sled Test

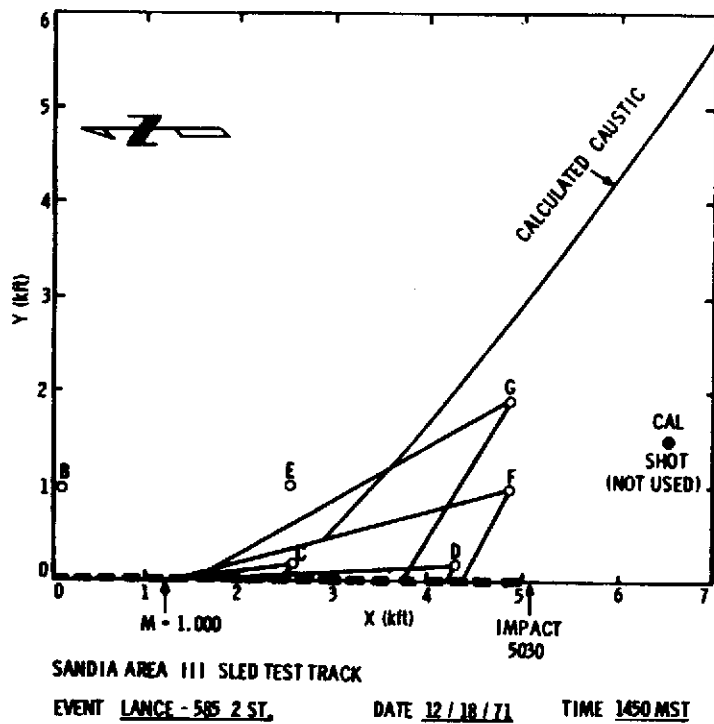


Figure A-20. Wave Propagation Paths

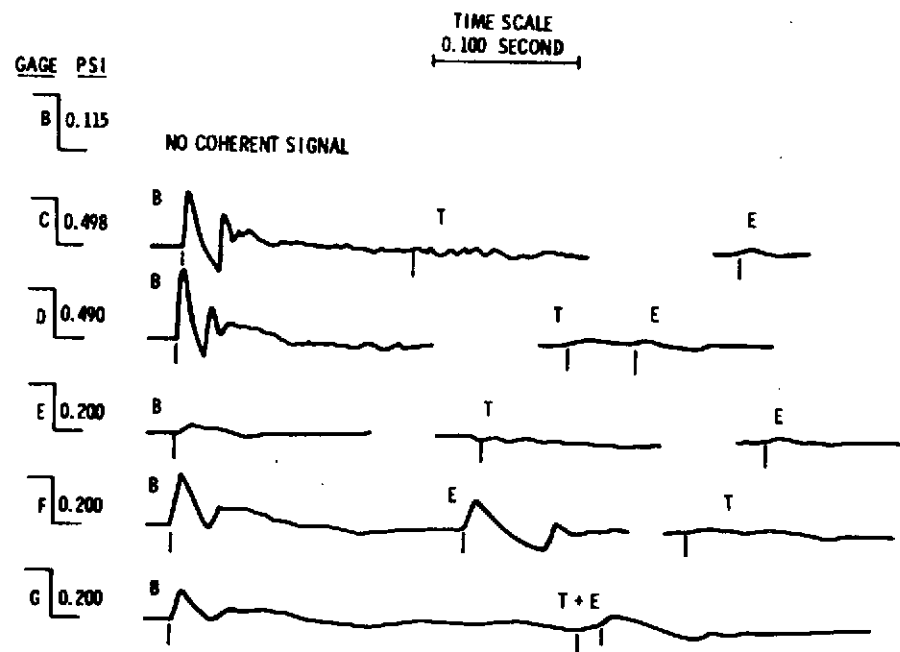


Figure A-21. Pressure Signatures, Fixed Array 12/18/71



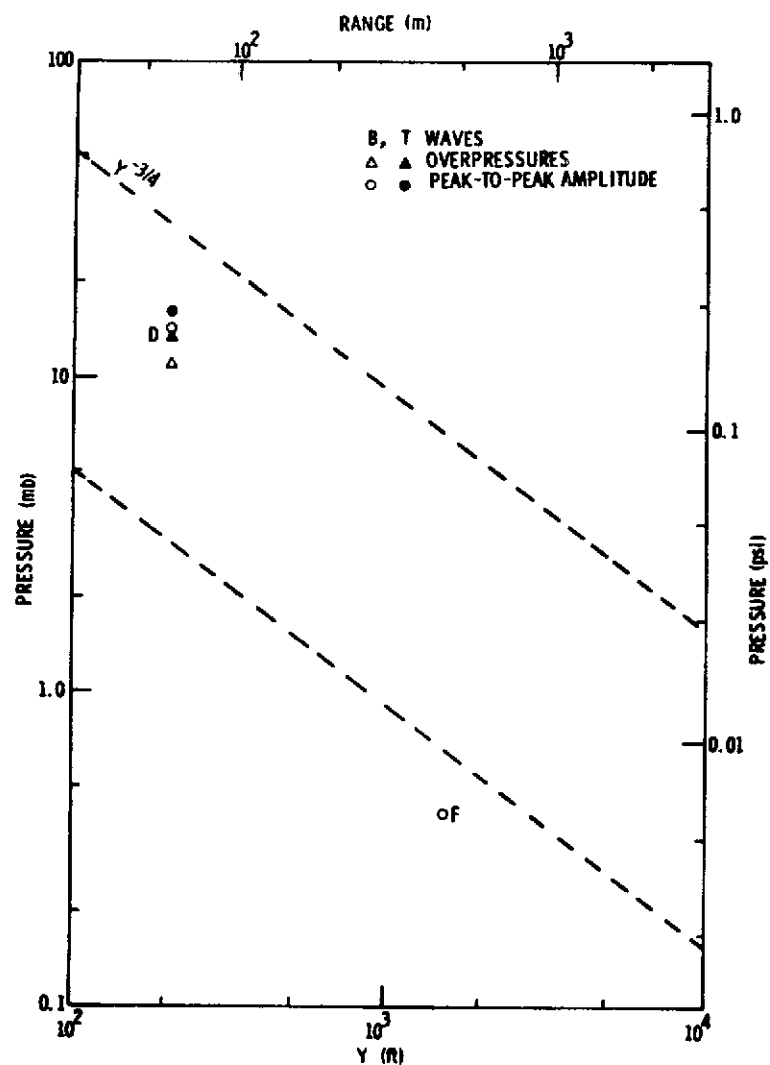


Figure A-22. Sonic Boom Pressures,  
9/28/73 Sled Test

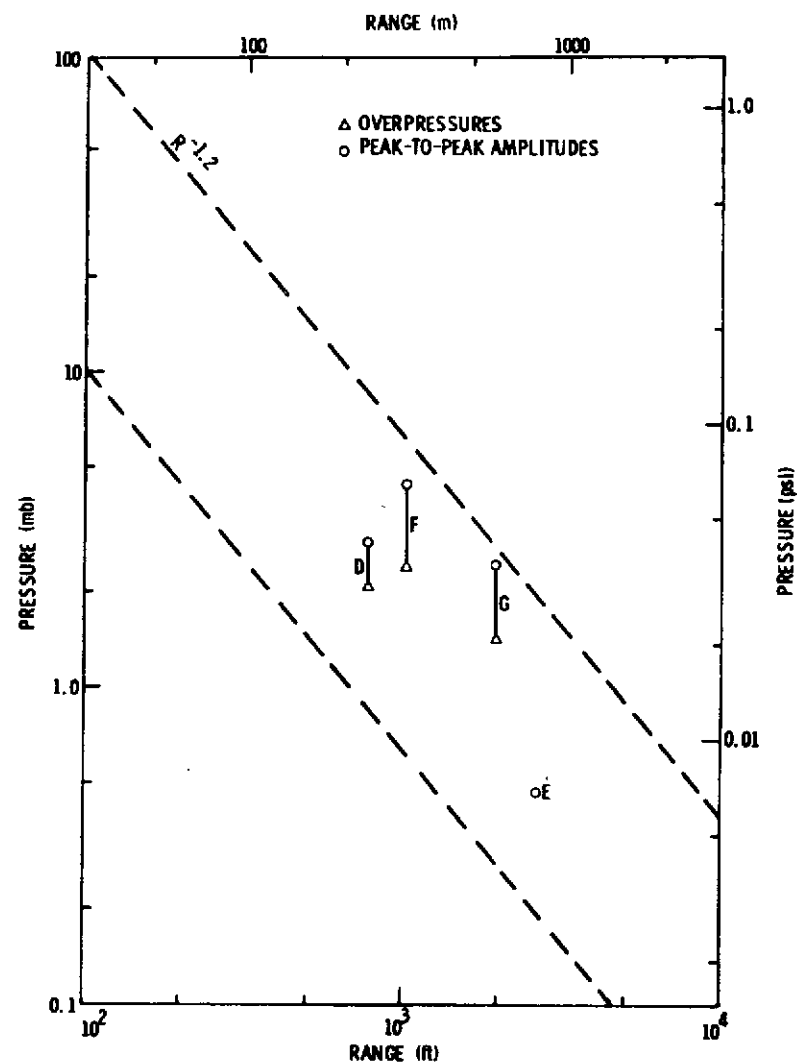


Figure A-23. Impact Explosion Pressures, 9/28/72 Sled Test

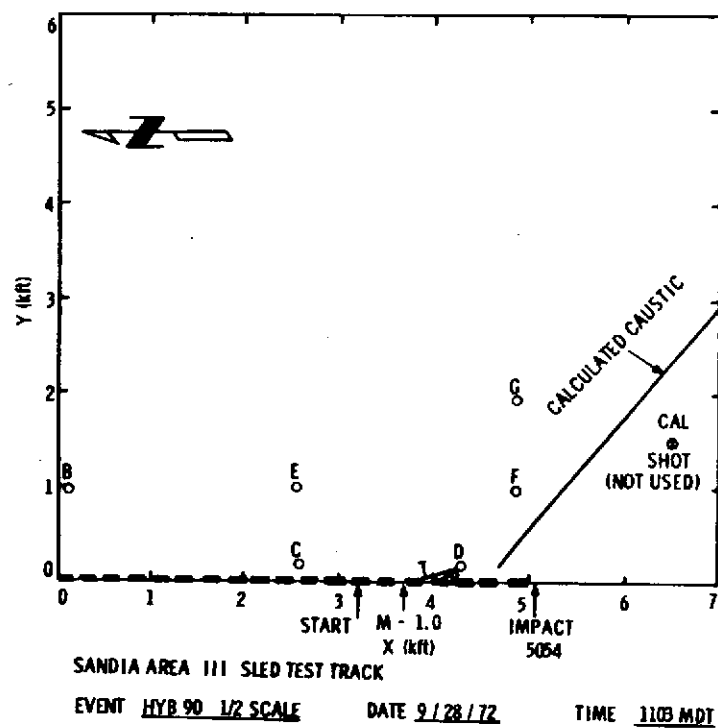


Figure A-24. Wave Propagation Paths

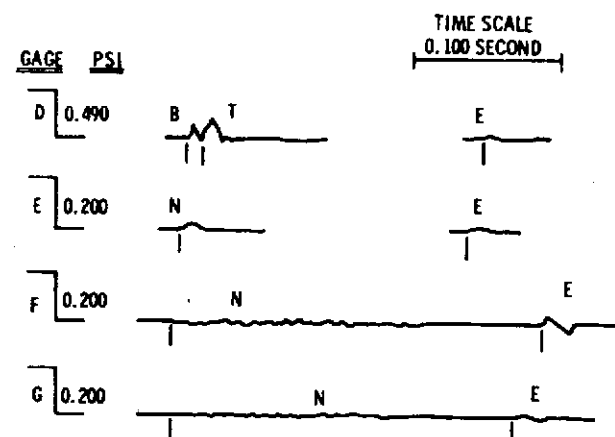


Figure A-25 Pressure Signatures, Fixed Array  
9/28/72 Test

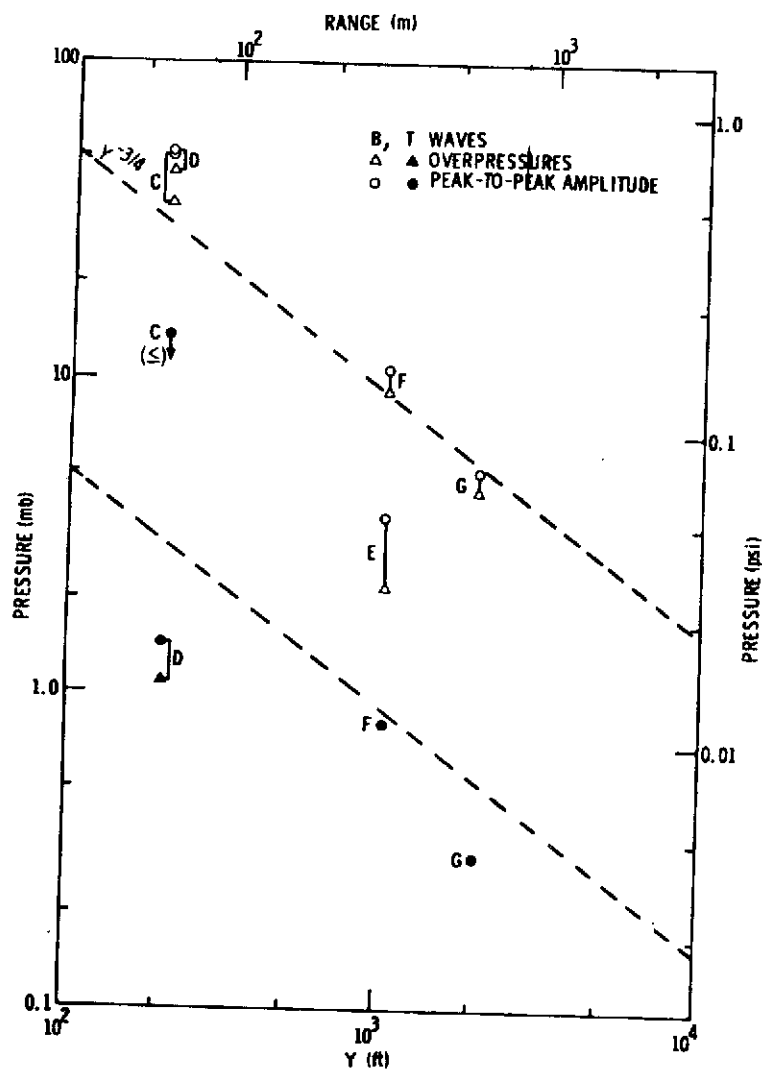


Figure A-26. Sonic Boom Pressures,  
10/12/73 Sled Test

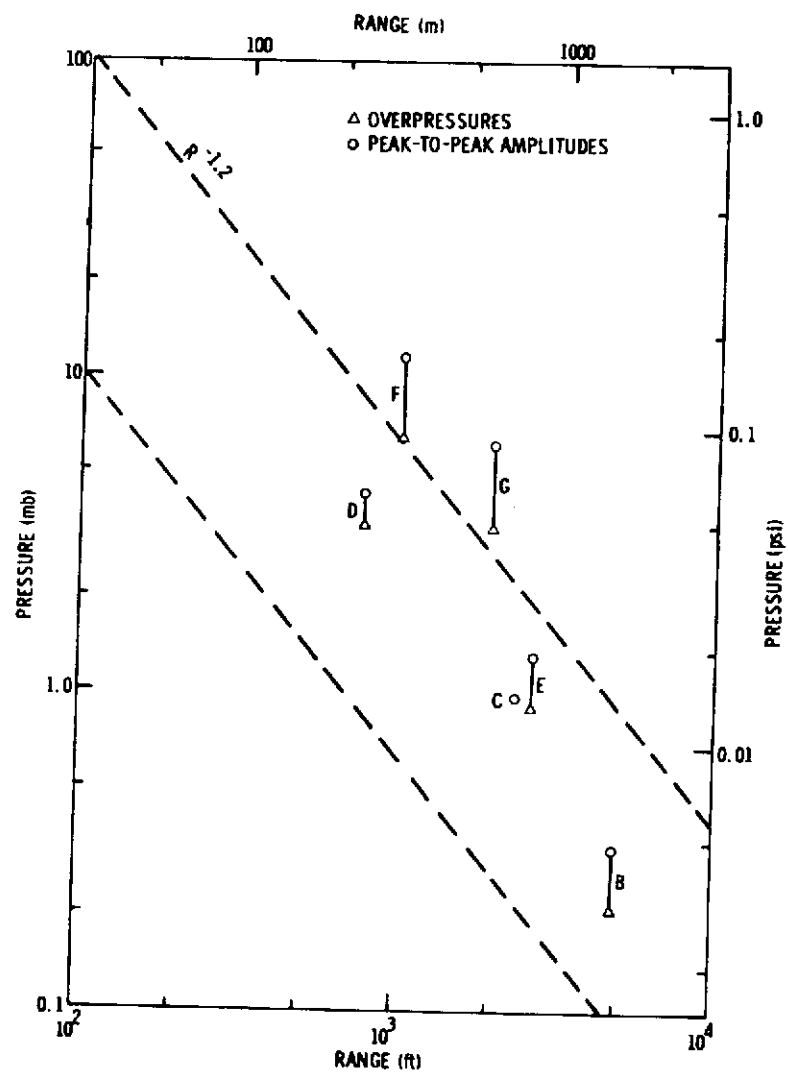


Figure A-27. Impact Explosion Pressures  
10/12/73 Sled Test

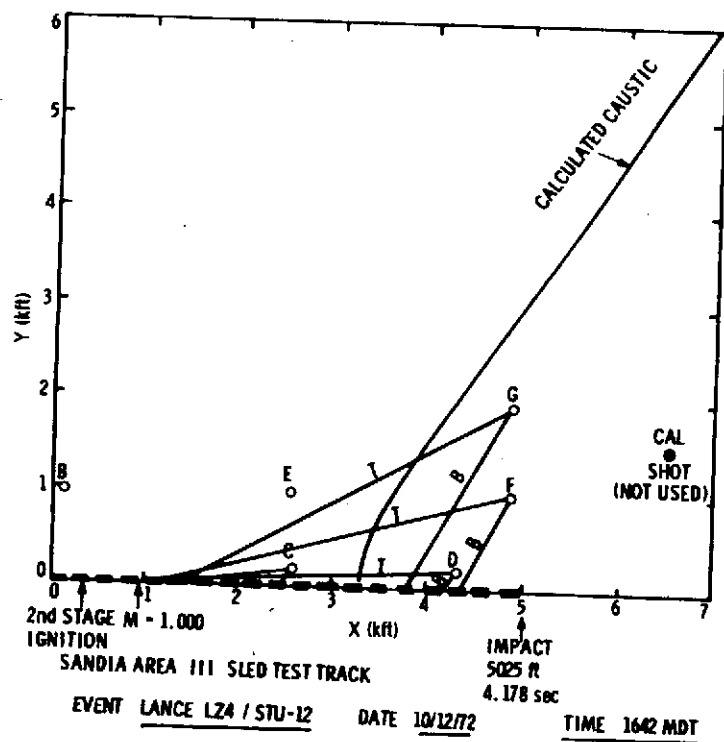


Figure A-28. Wave Propagation Paths

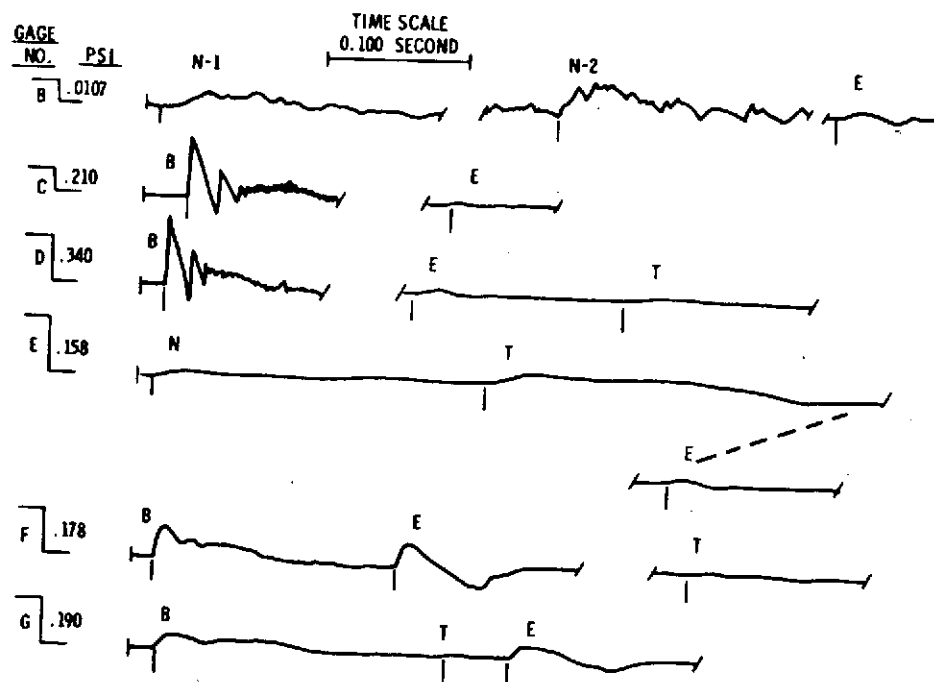


Figure A-29. Pressure Signatures, Fixed Array 10/12/72 Test

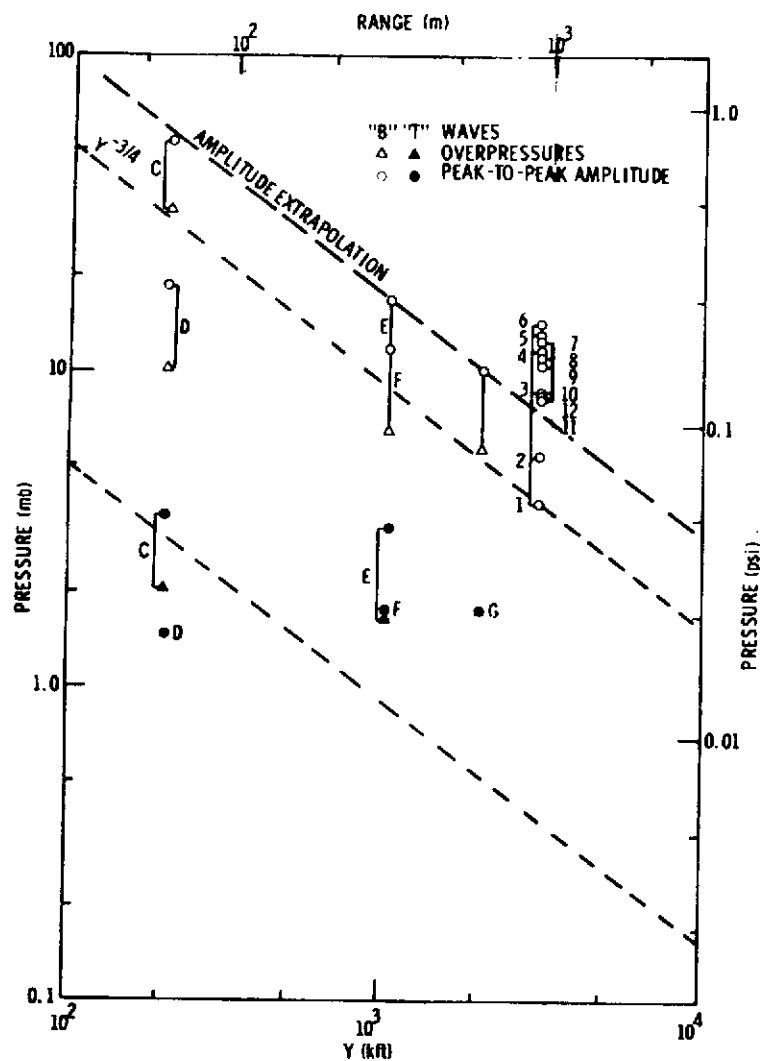


Figure A-30. Sonic Boom Pressures,  
1/5/73 Sled Test

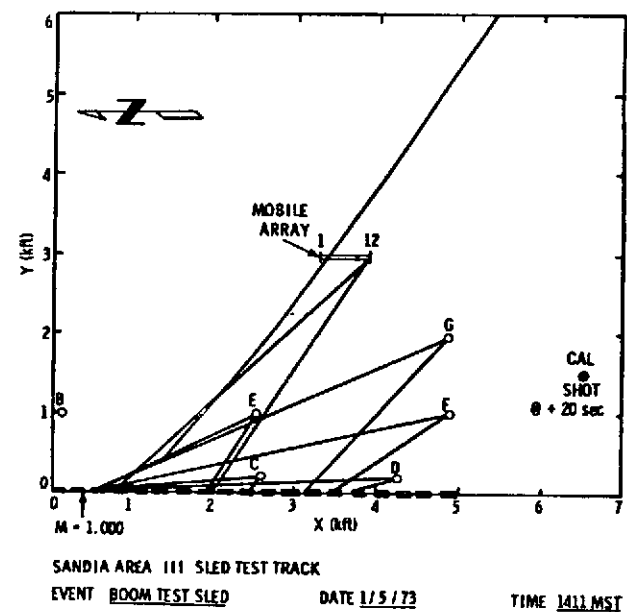


Figure A-31. Wave Propagation Paths

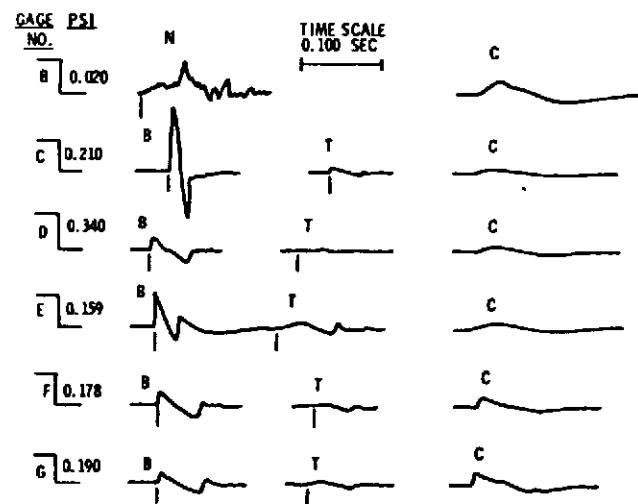


Figure A-32. Pressure Signatures, Fixed Array  
1/5/73 Test

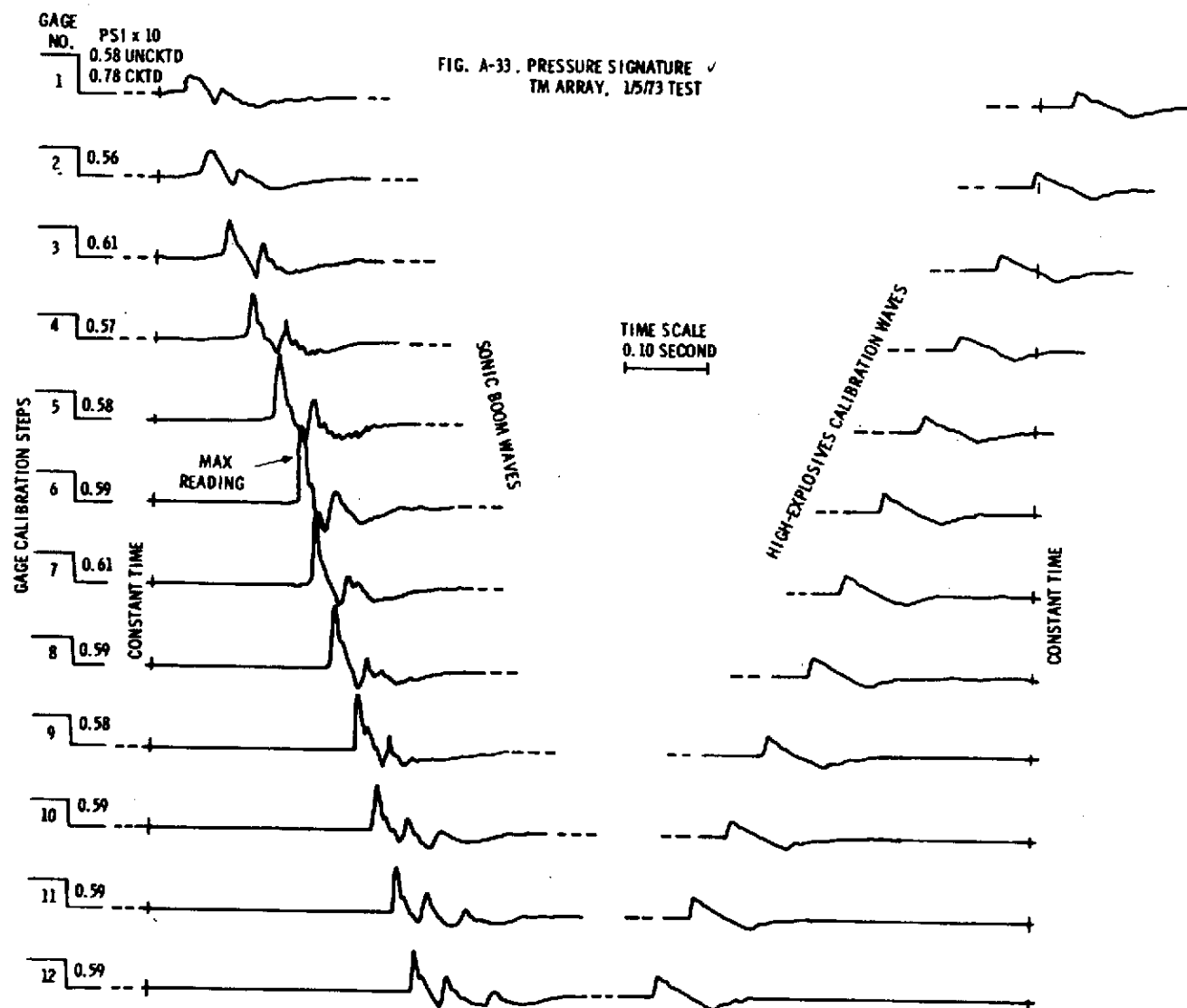


Figure A-33. Pressure Signature TM Array,  
1/5/73 Test

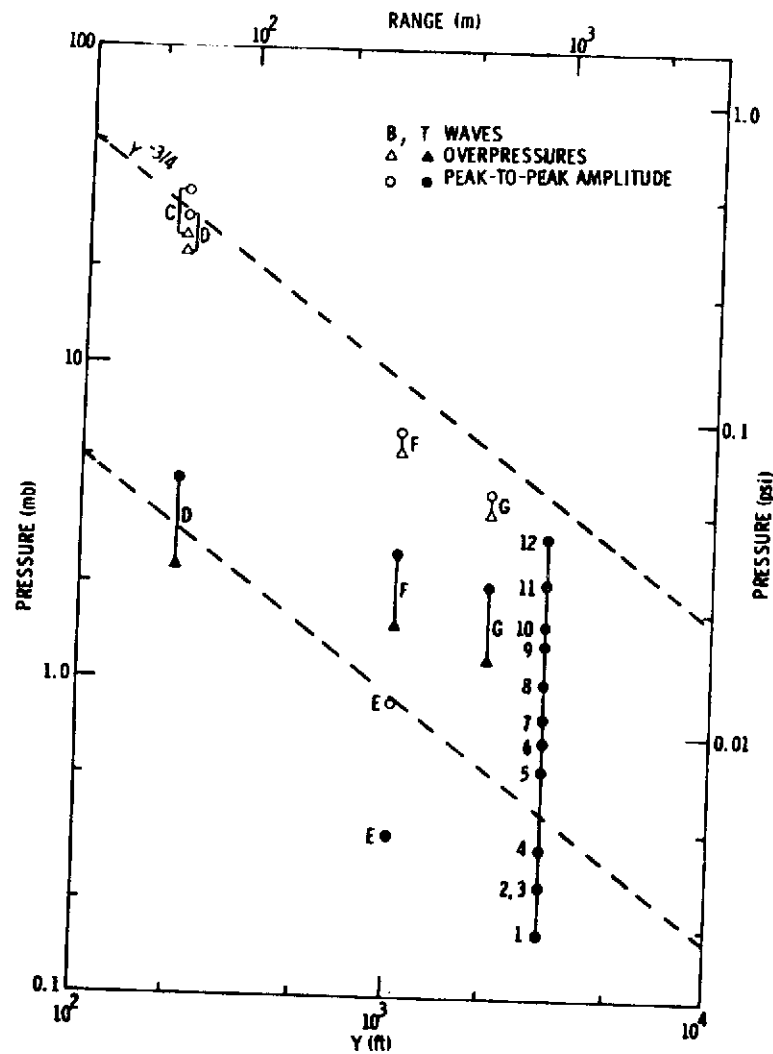


Figure A-34. Sonic Boom Pressures,  
1/18/73 Sled Test

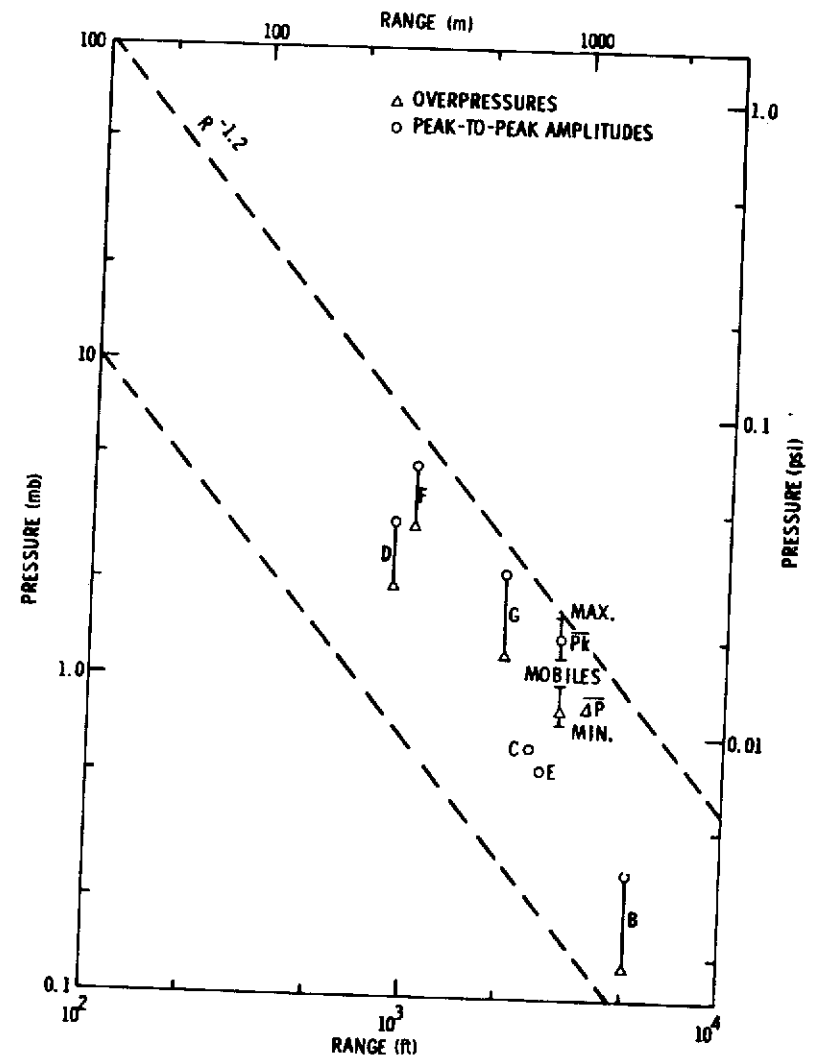


Figure A-35. Impact Explosion Pressures,  
1/18/73 Sled Test

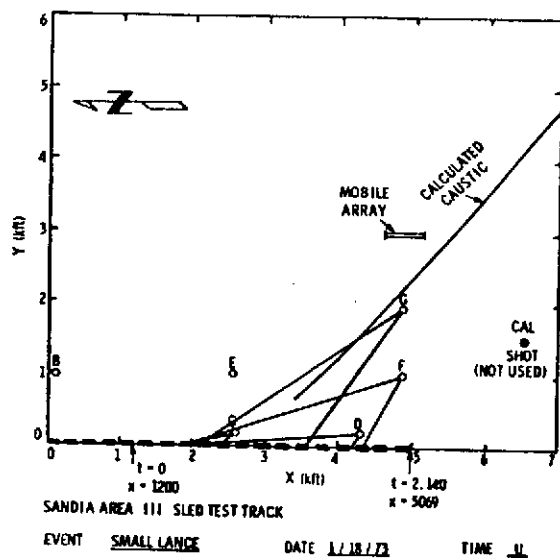


Figure A-36. Wave Propagation Paths

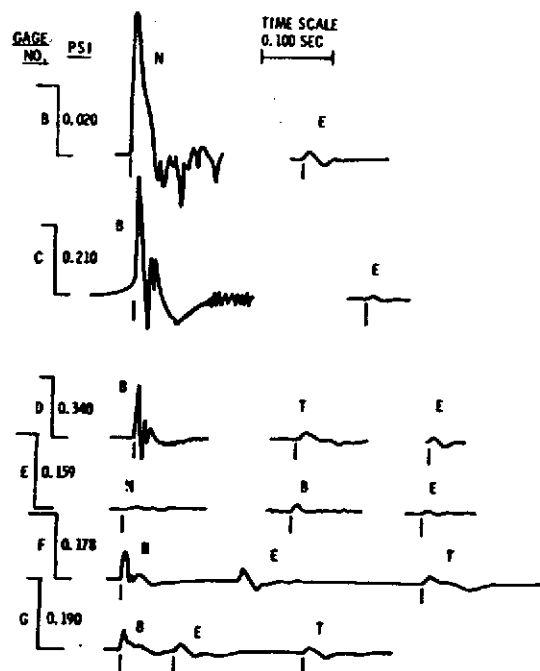


Figure A-37. Pressure Signatures. Fixed Array, 1/18/73 Test

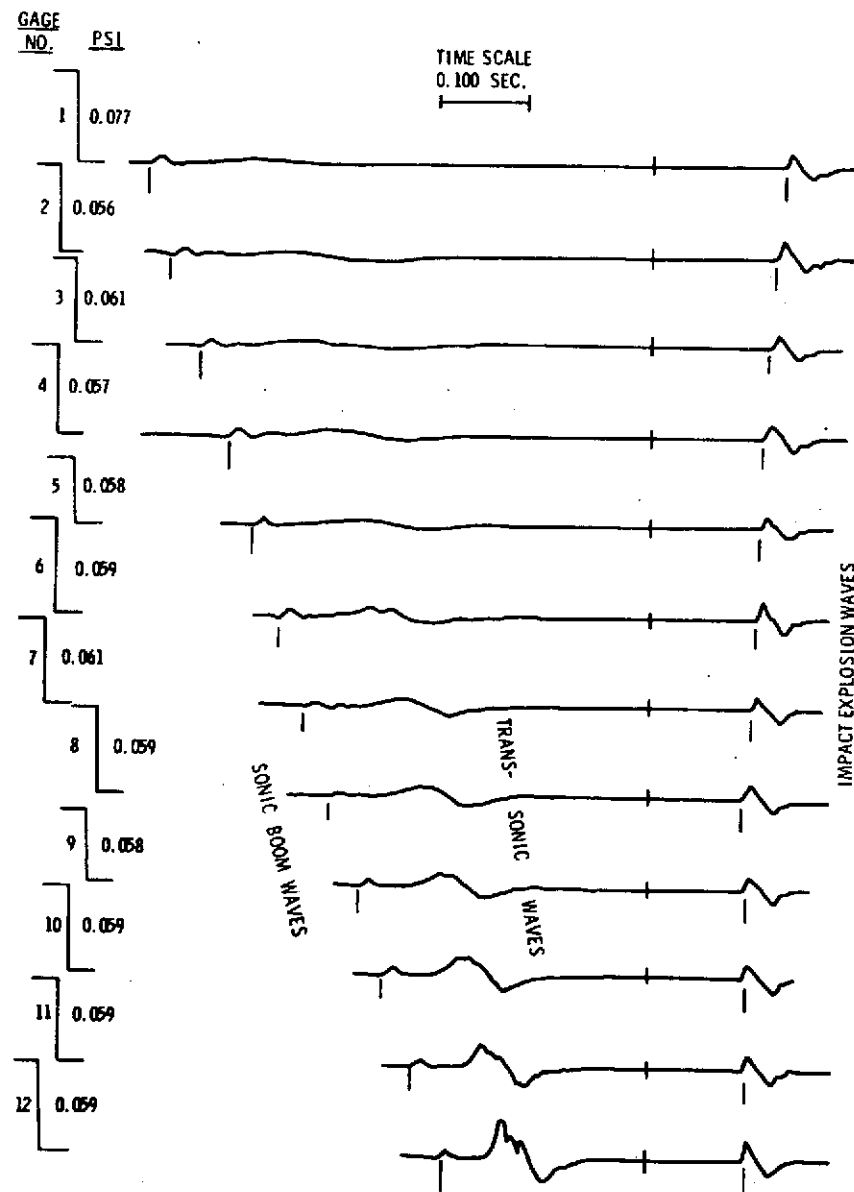


Figure A-38. Pressure Signatures, Mobile Array, 1/18/73 Test



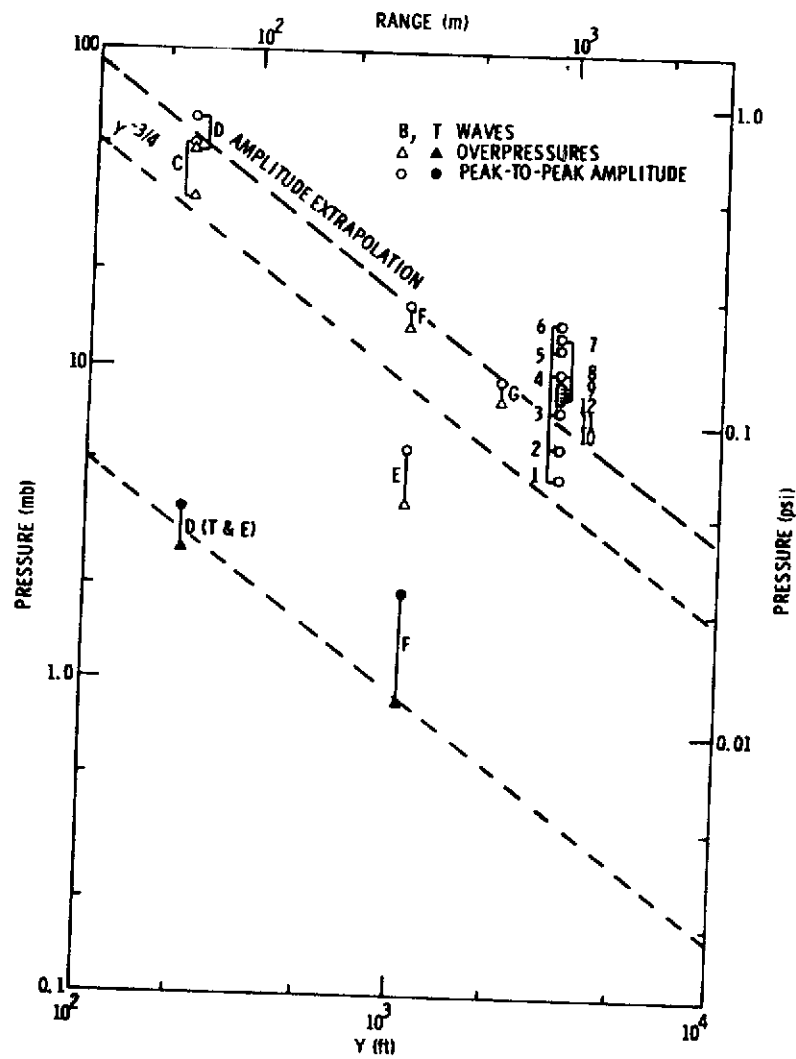


Figure A-39. Sonic Boom Pressures,  
1/24/73 Sled Test

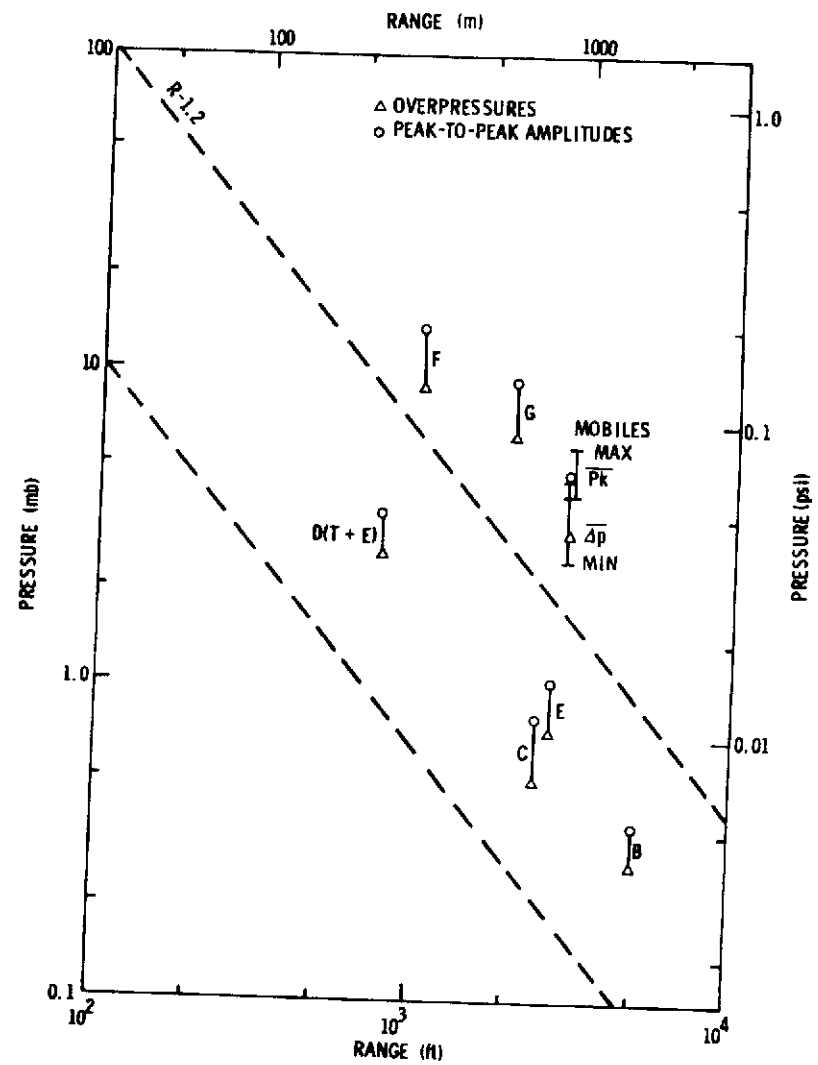


Figure A-40. Impact Explosion Pressures,  
1/24/73 Sled Test

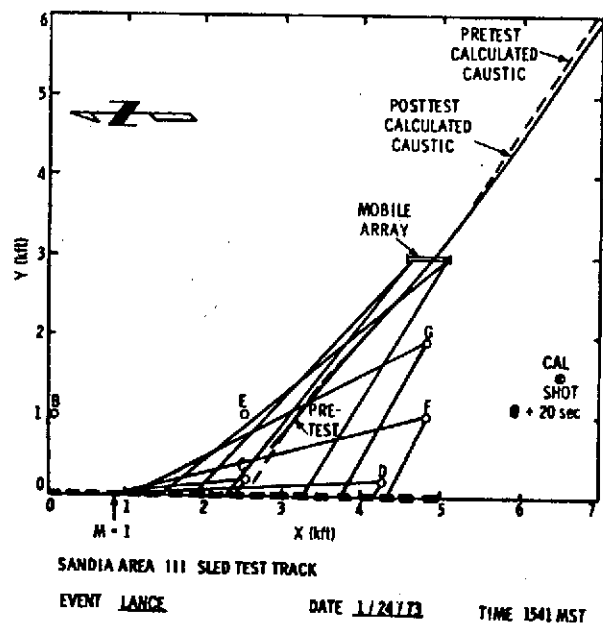


Figure A-41. Wave Propagation Paths

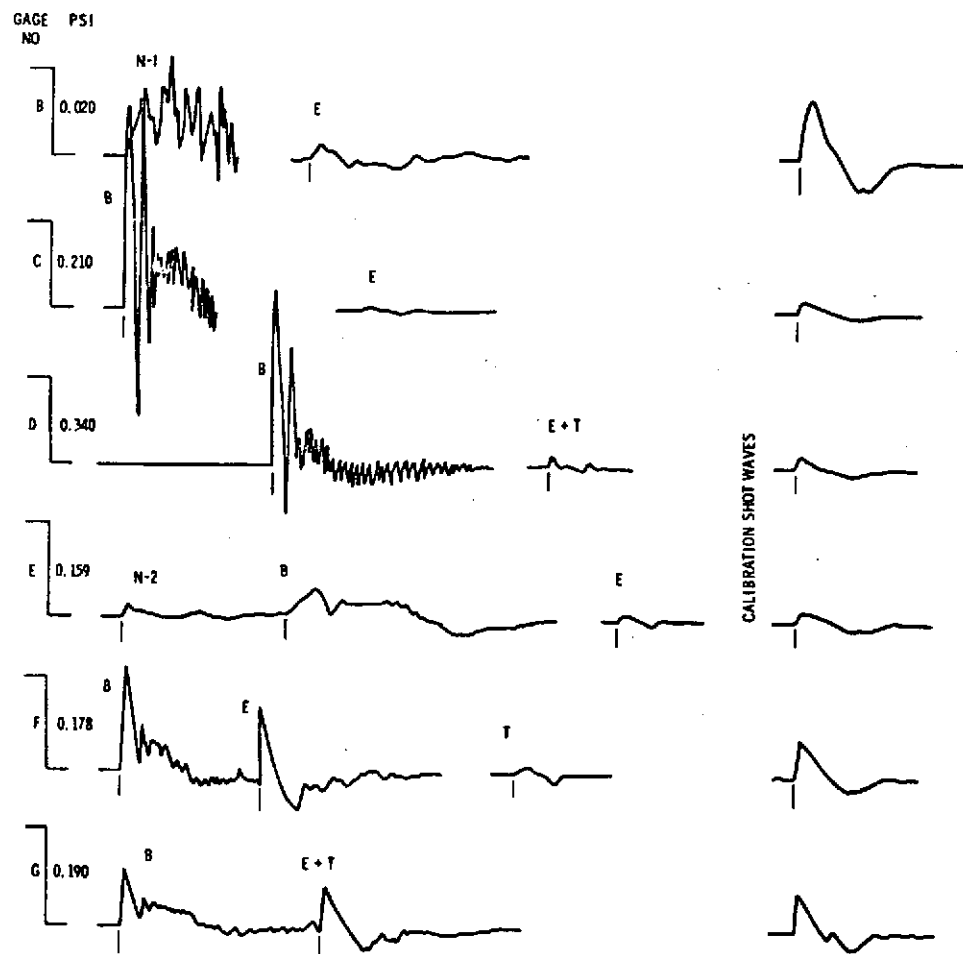


Figure A-42. Pressure Signatures, Fixed Array  
 1/24/73 Test

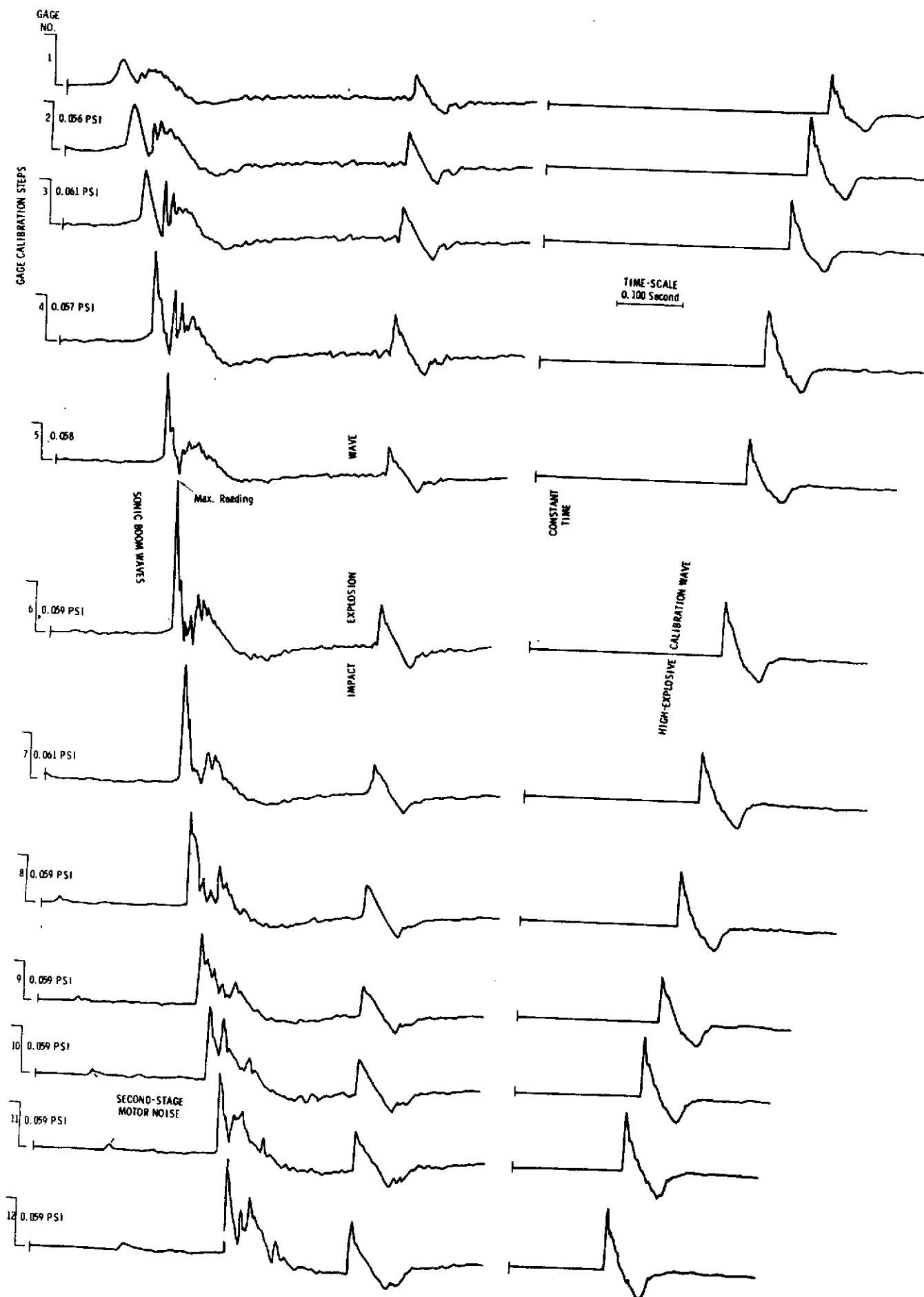


Figure A-43. Pressure Signatures, TM Array  
1/24/73 Test

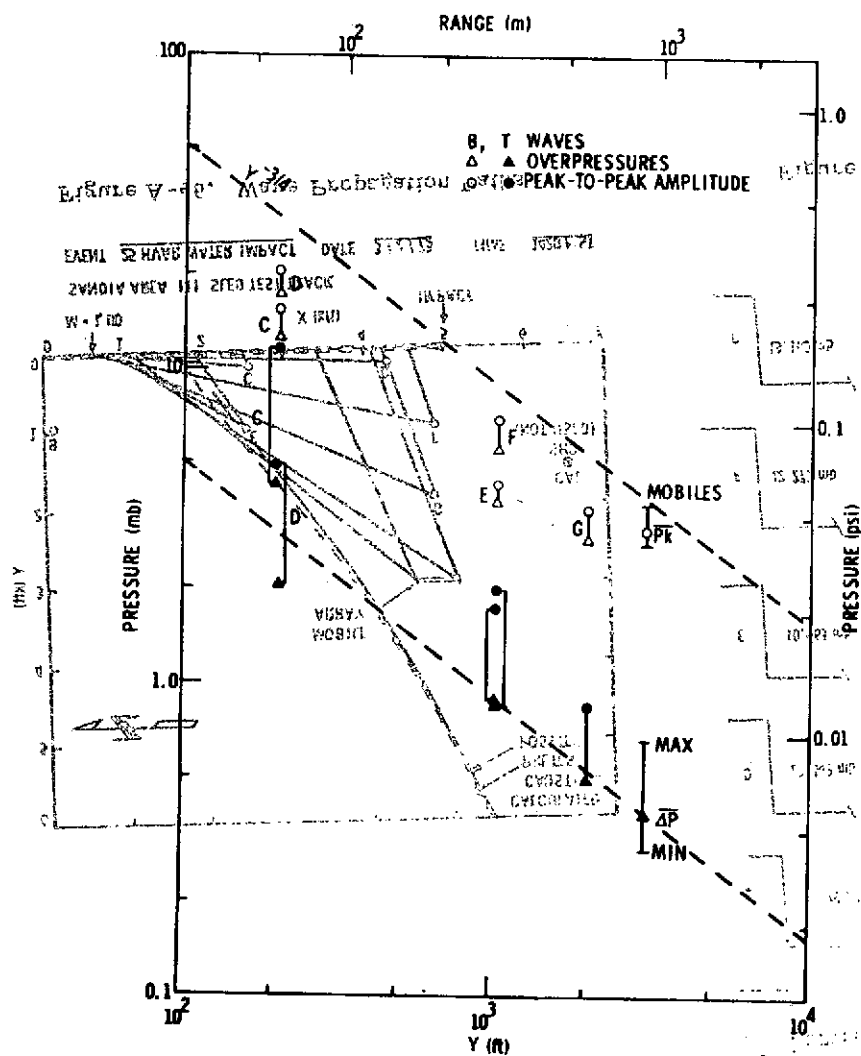


Figure A-44. Sonic Boom Pressures, 3/2/73 Sled Test

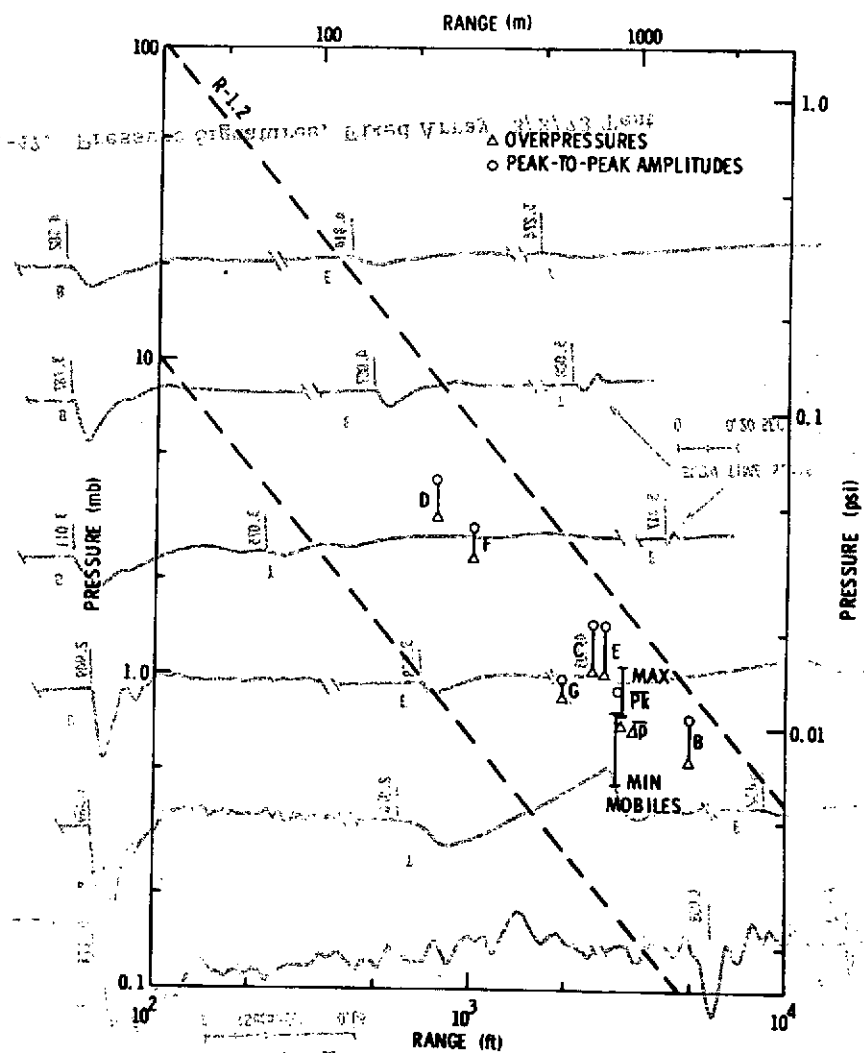


Figure A-45. Impact Explosion Pressure, 3/2/73 Sled Test

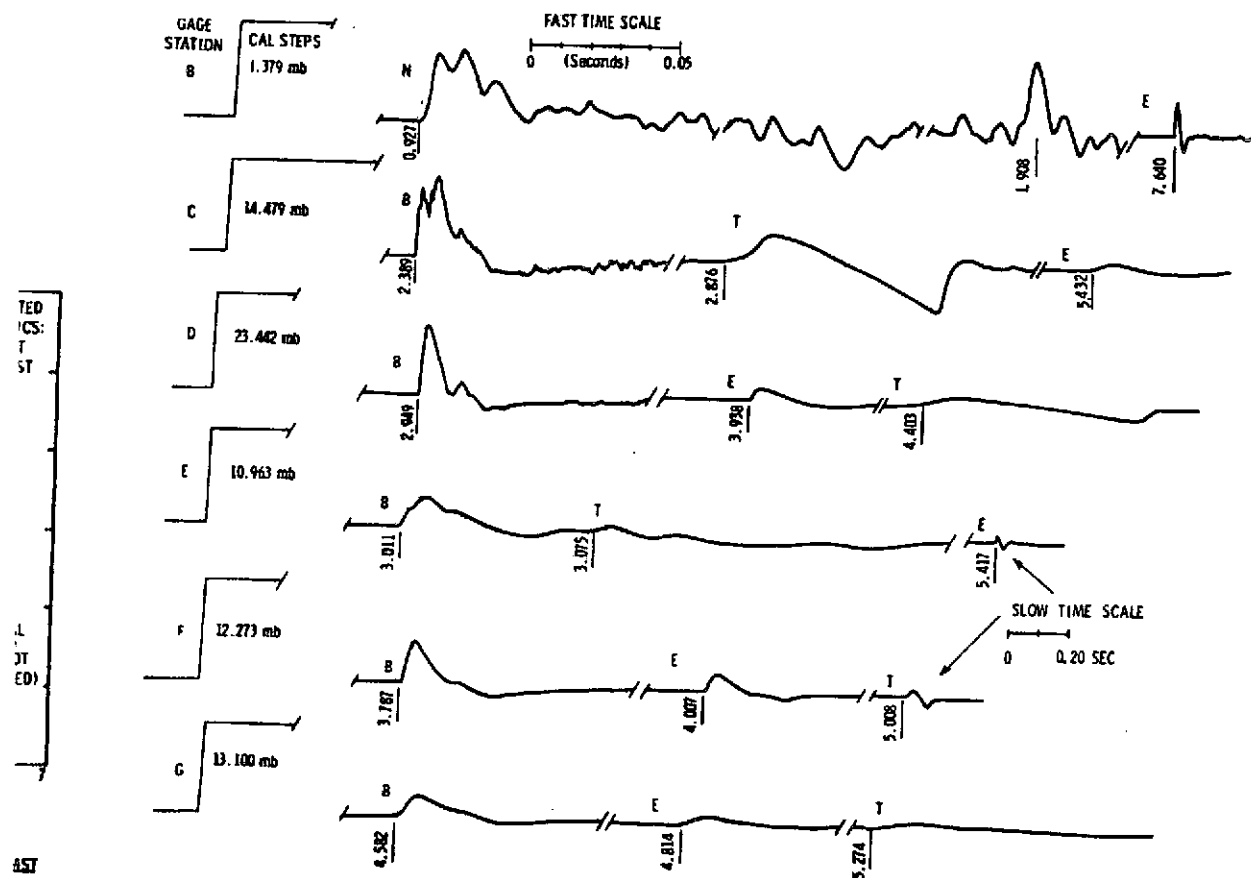


Figure A-47. Pressure Signatures, Fixed Array 3/2/73 Test

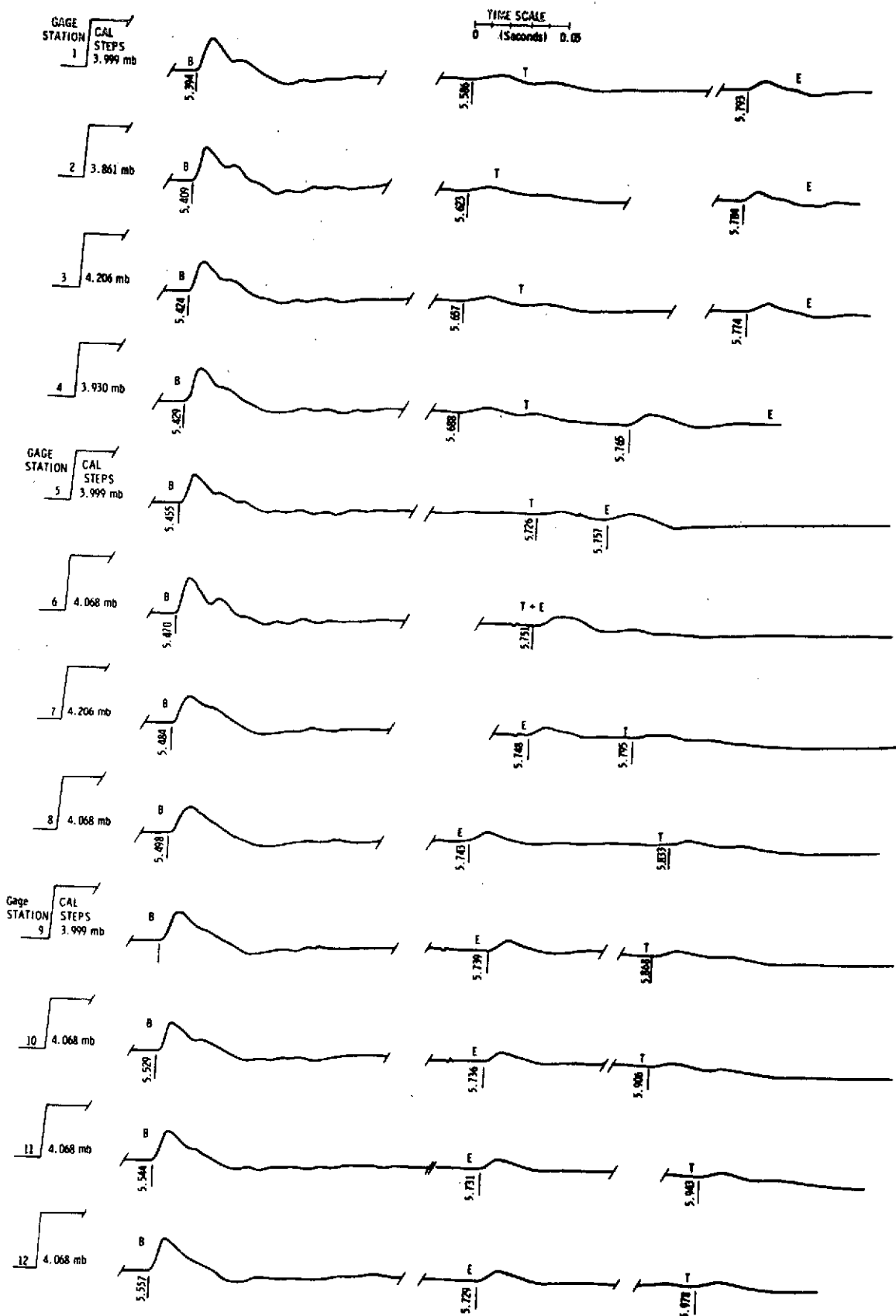


Figure A-48. Pressure Signatures Mobile Array,  
3/2/73 Test

C2

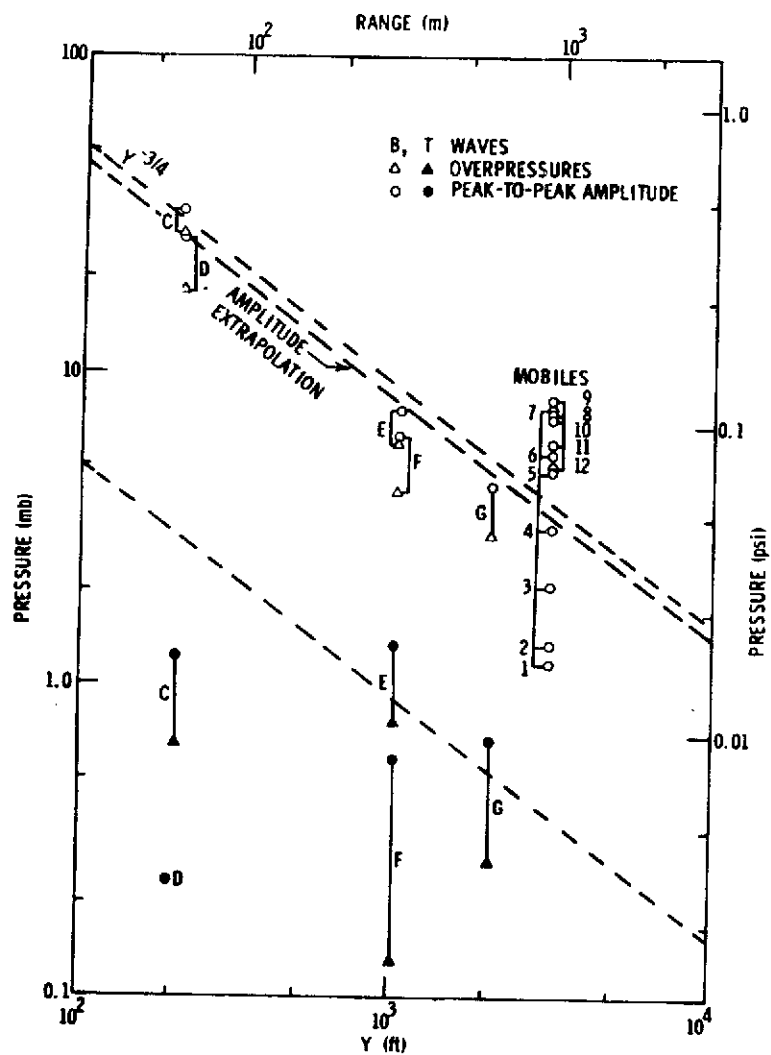


Figure A-49. Sonic Boom Pressures,  
5/8/73 (1) Sled Test

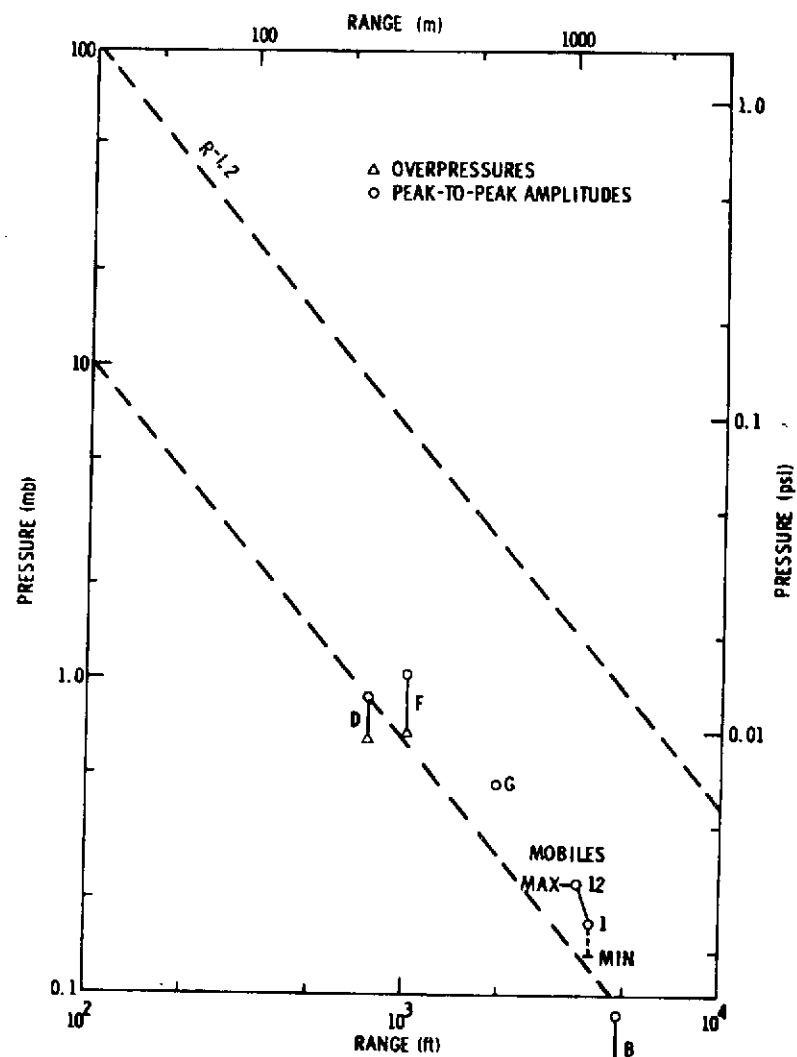


Figure A-50. Impact Explosion Pressures,  
5/8/73 (1) Sled Test

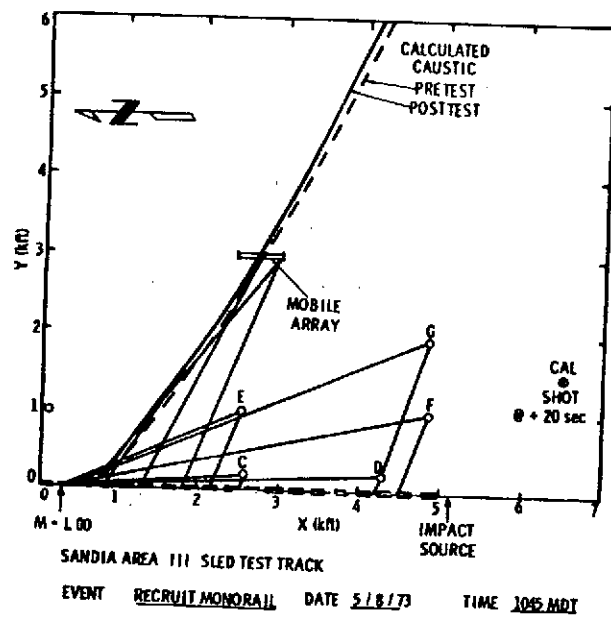


Figure A-51. Wave Propagation Paths

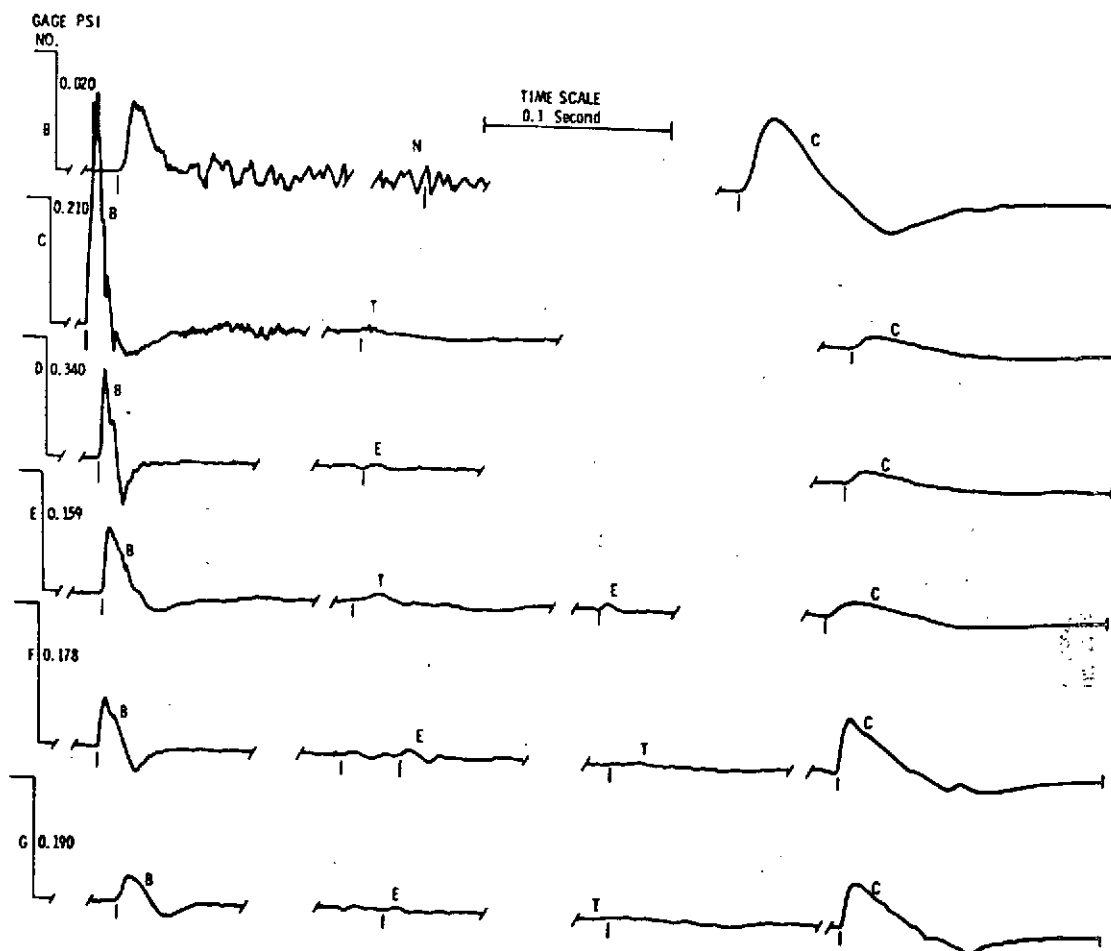


Figure A-52. Pressure Signatures, Fixed Array  
5/8/73 Test, Recruit Monorail



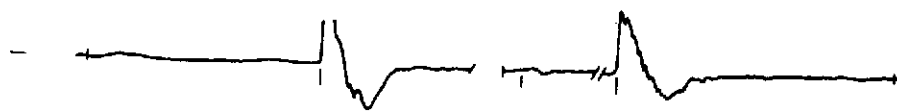


Figure A-53. Pressure Signatures, TM Array, 5/8/73 Test Recruit Monorail

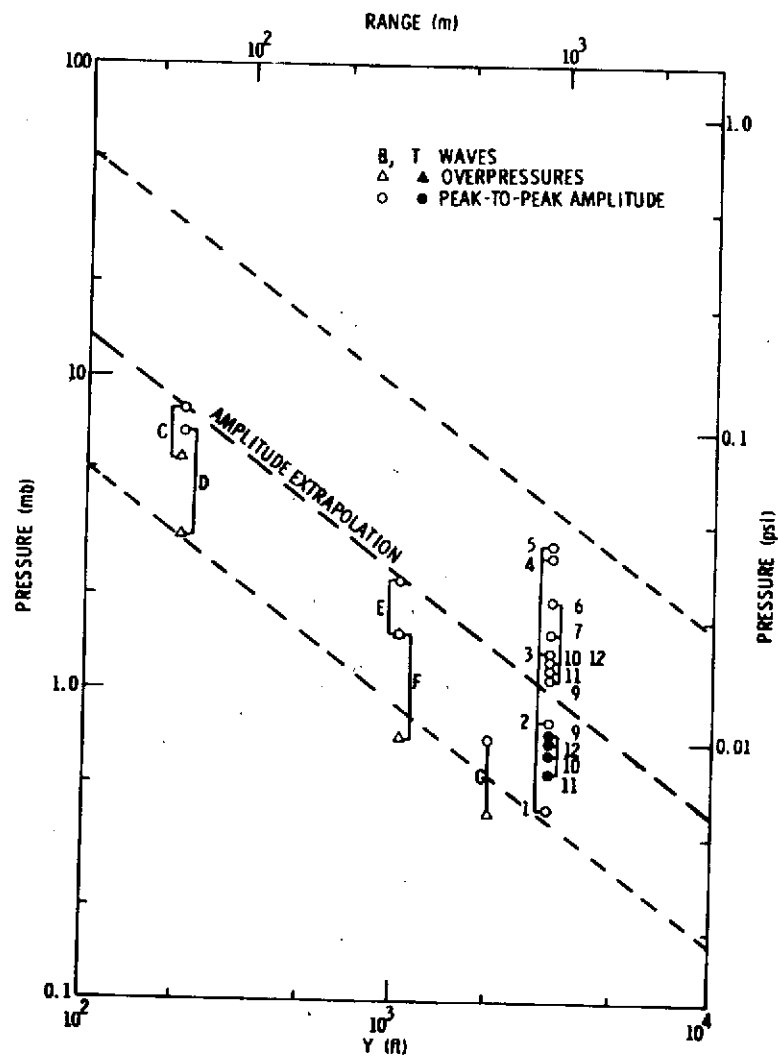


Figure A-54. Sonic Boom Pressures, 5/8/73 (11) Sled Test

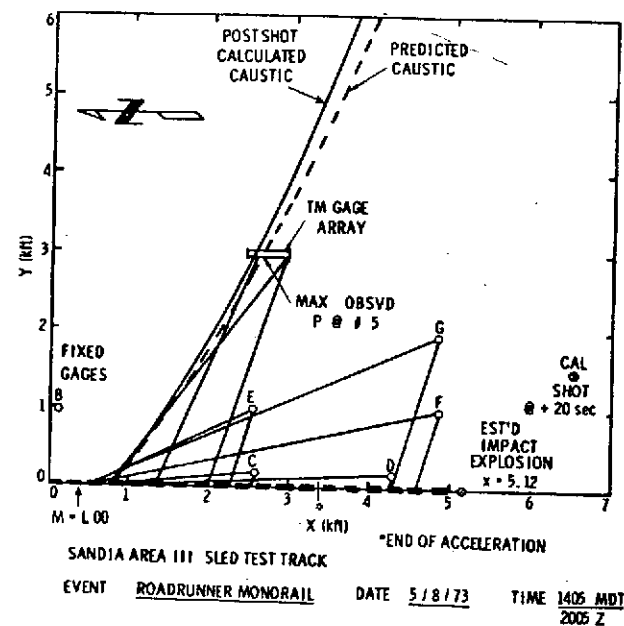


Figure A-55. Wave Propagation Paths

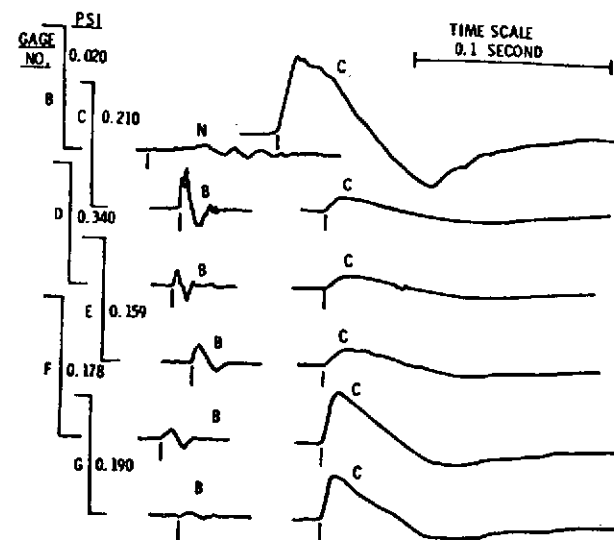


Figure A-56. Pressure Signatures Fixed Array, 5/8/73 Test, Roadrunner Monorail

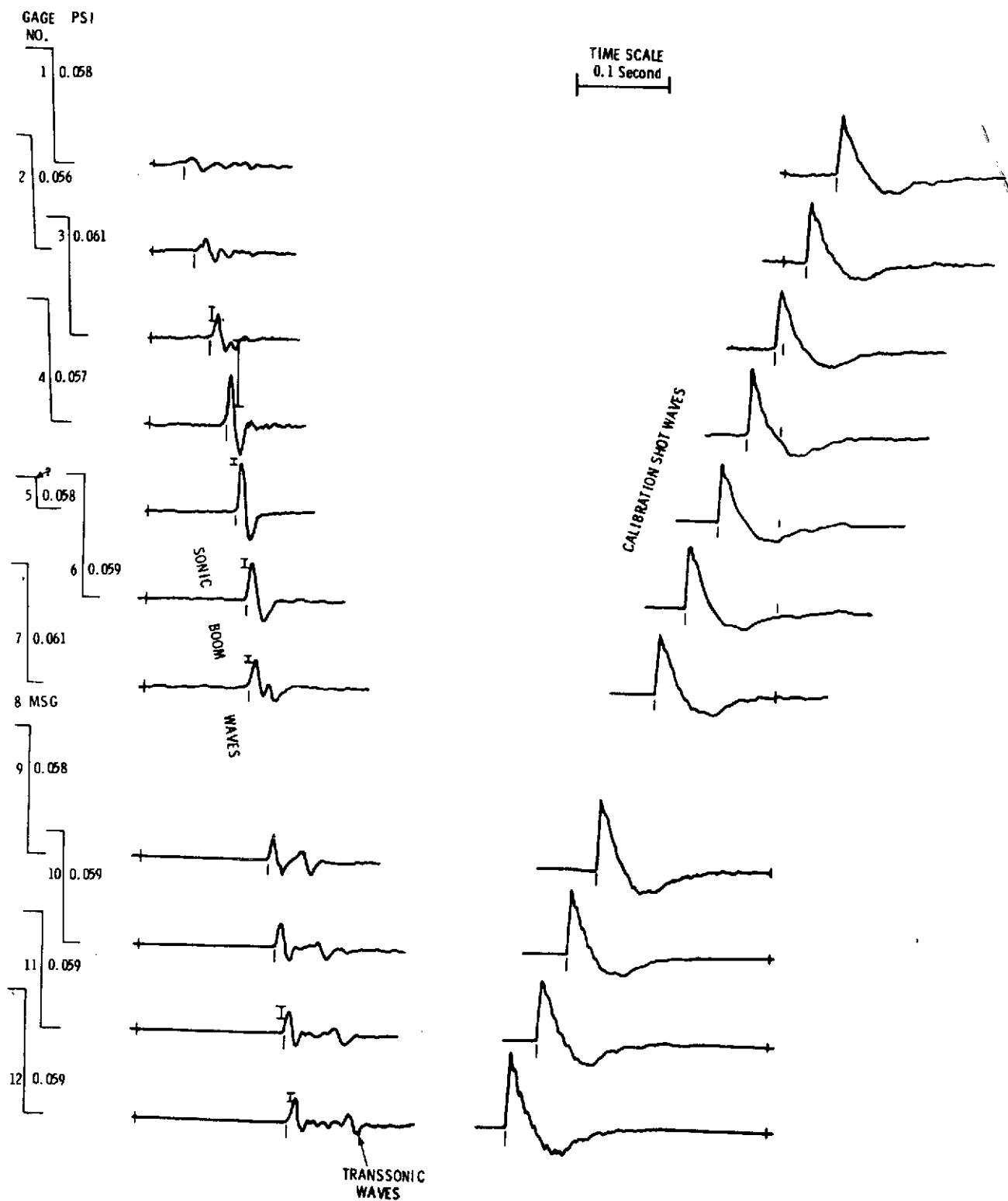


Figure A-57. Pressure Signatures, TM Array,  
5/8/73 Test, Roadrunner Monorail

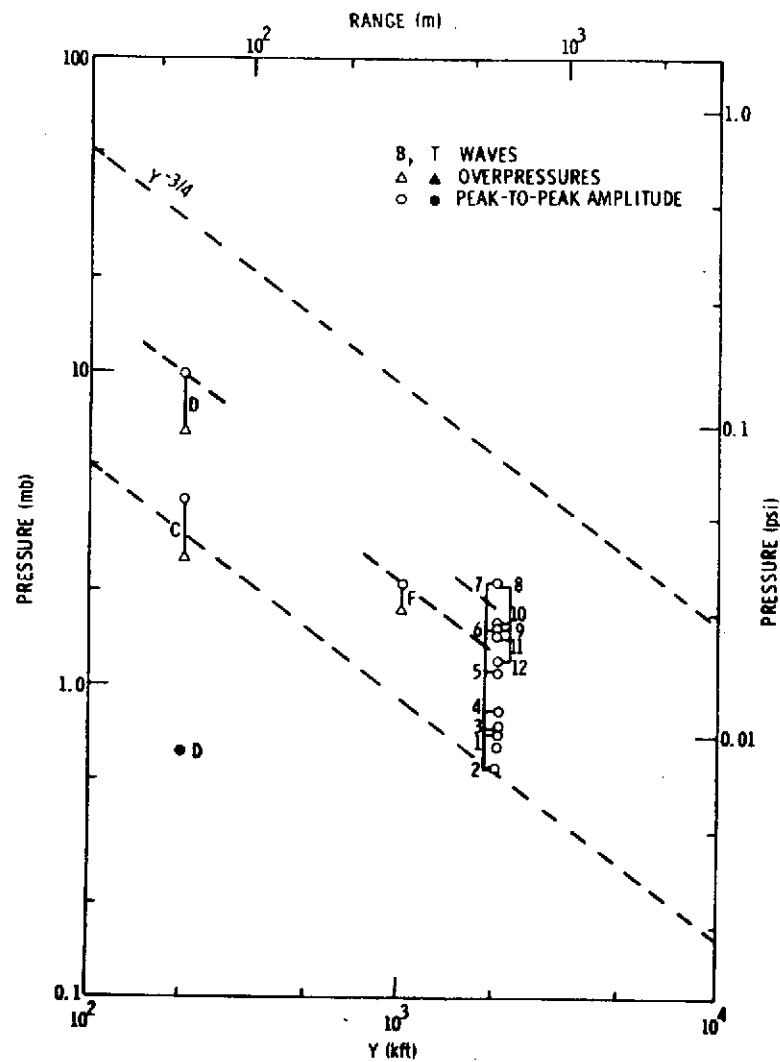


Figure A-58. Sonic Boom Pressures,  
5/15/73 Sled Test

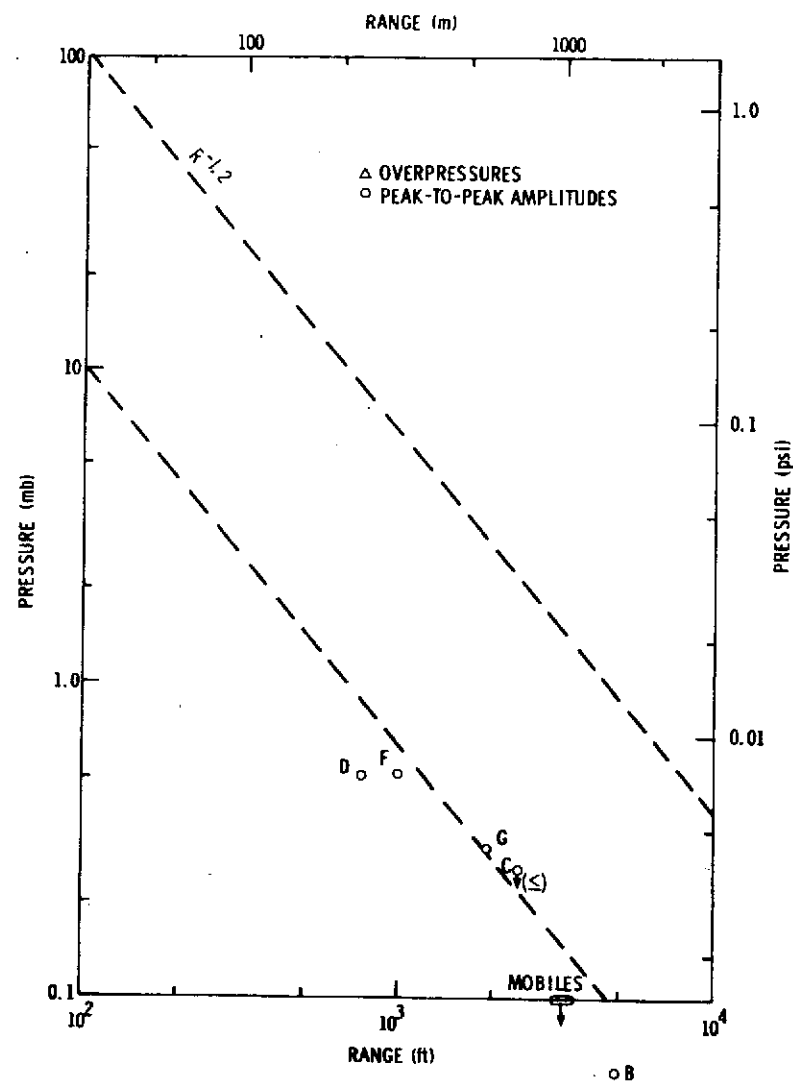
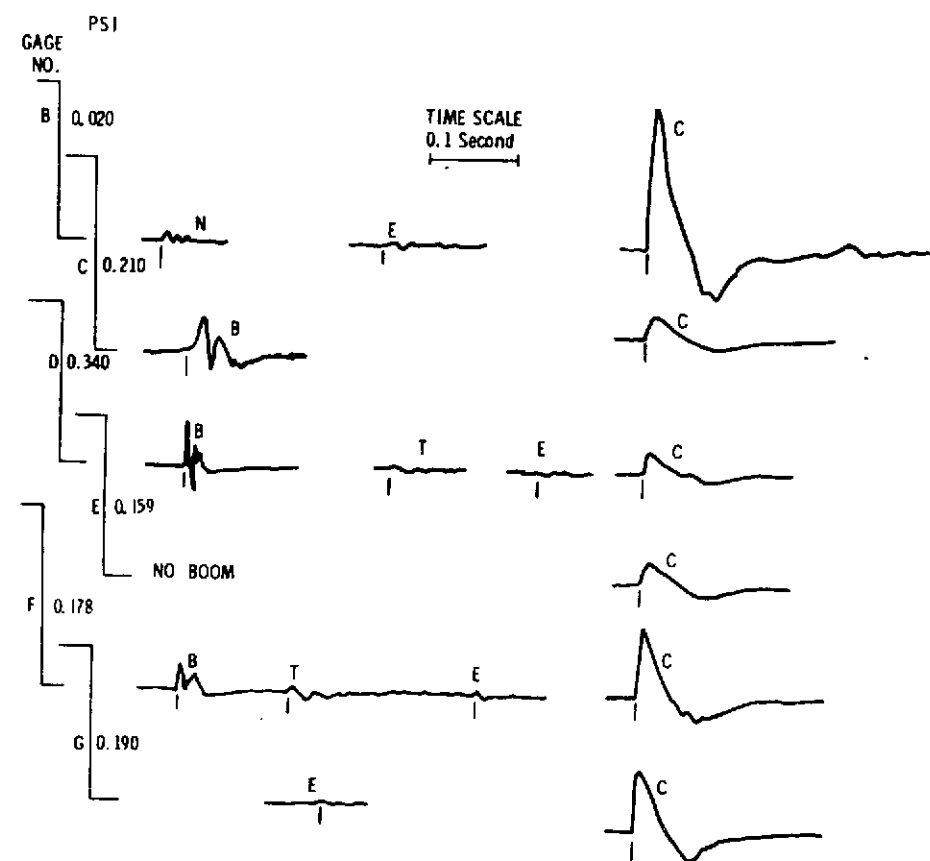


Figure A-59. Impact Explosion Pressures,  
5/15/73 Sled Test



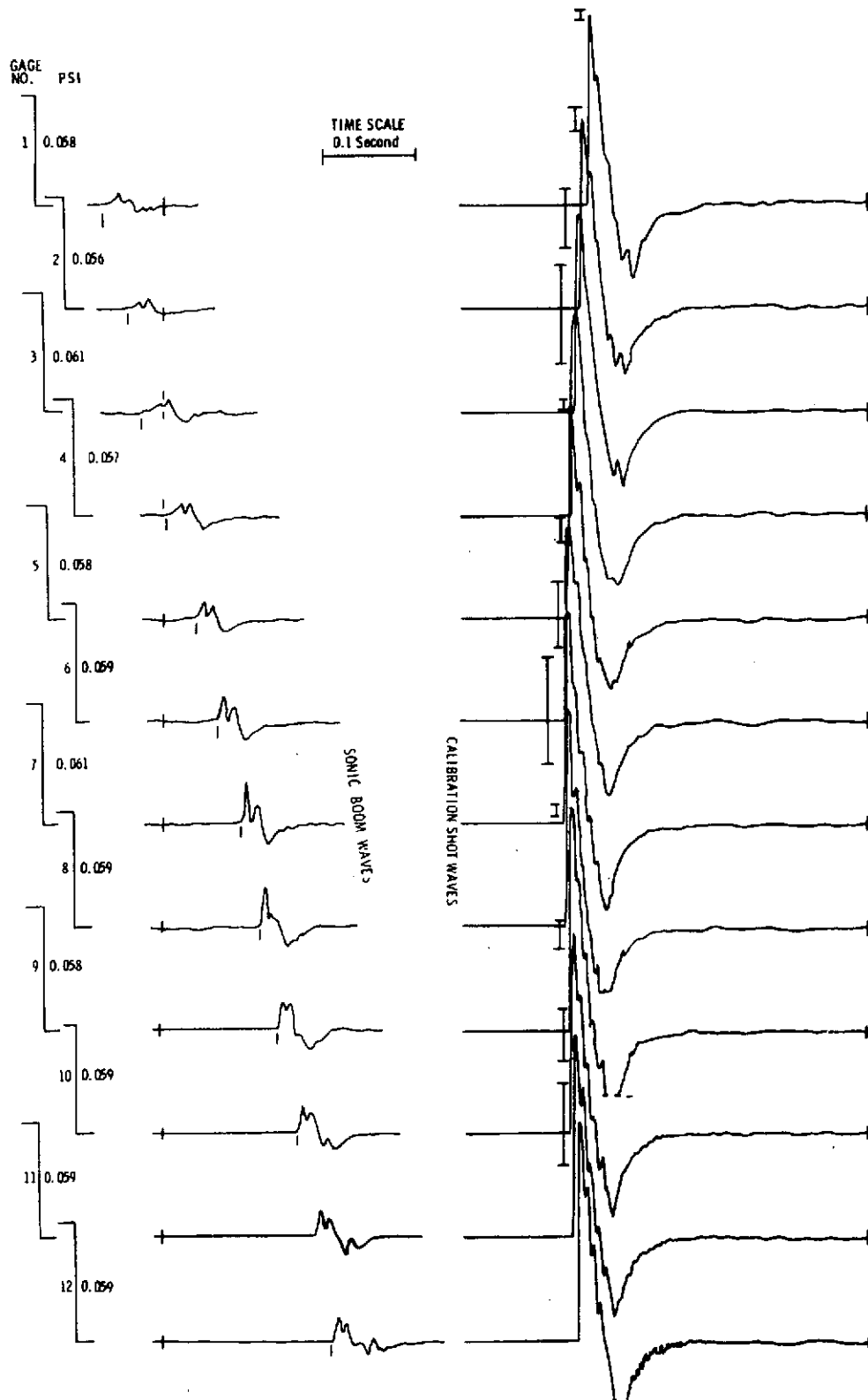


Figure A-62. Pressure Signatures, TM Array  
5/15/73 Test, Kiva-1 Monorail